UNIVERSIDADE FEDERAL DE MINAS GERAIS
Escola de Engenharia
Programa de Pós-graduação em Engenharia Elétrica

Tiago Coelho Magalhães

DEVELOPMENT AND VALIDATION OF A HIGH-CAPACITY FUNCTIONAL ELECTRICAL STIMULATION SYSTEM AND OF A REINFORCEMENT LEARNING ALGORITHM APPLIED TO THE FES-ASSISTED CYCLING MODALITY FOR A PARTICIPANT WITH PARAPLEGIA

Belo Horizonte
2022

Tiago Coelho Magalhães

DEVELOPMENT AND VALIDATION OF A HIGH-CAPACITY FUNCTIONAL ELECTRICAL STIMULATION SYSTEM AND OF A REINFORCEMENT LEARNING ALGORITHM APPLIED TO THE FES-ASSISTED CYCLING MODALITY FOR A PARTICIPANT WITH PARAPLEGIA

Tese apresentada ao Programa de Pós-Graduação em Engenharia Elétrica da Universidade Federal de Minas Gerais, como requisito parcial à obtenção do título de Doutor em Engenharia Elétrica.

Orientador: Prof. Dr. Henrique Resende Martins
Coorientadora: Profa. Dra. Andressa da Silva de Mello

Belo Horizonte

2022

Magalhães, Tiago Coelho.
M189d Development and validation of a high-capacity functional eletrical stimulation system and of a reinforcement learning algorithm applied to the FES-assisted cycling modality for a participant with paraplegia [recurso eletrônico] / Tiago Coelho Magalhães. - 2022.
1 recurso online (114 f. : il., color.) : pdf.

Orientador: Henrique Resende Martins.
Coorientadora: Andressa da Silva de Melo.

Tese (doutorado) - Universidade Federal de Minas Gerais, Escola de Engenharia.

Apêndices: f. 109 -113.
Bibliografia: f.92-99.
Exigências do sistema: Adobe Acrobat Reader.

1. Engenharia elétrica - Teses. 2. Aprendizado por reforço – Teses. 3. Estimulação Elétrica Funcional – Teses. I. Martins, Henrique Resende. II. Melo, Andressa da Silva de. III. Universidade Federal de Minas Gerais. Escola de Engenharia. IV. Título.

CDU: 621.3(043)

Ficha catalográfica elaborada pela Bibliotecária Letícia Alves Vieira - CRB-6/2337
Biblioteca Prof. Mário Werneck - Escola de Engenharia da UFMG

UNIVERSIDADE FEDERAL DE MINAS GERAIS
ESCOLA DE ENGENHARIA
COLEGIADO DO CURSO DE PÓS-GRADUAÇÃO EM ENGENHARIA ELÉTRICA

FOLHA DE APROVAÇÃO

"Development And Validation Of A High-capacity Functional Electrical Stimulation System And Of A Reinforcement Learning Algorithm Applied To The Fes-assisted Cycling Modality For A Participant With Paraplegia"

Tiago Coelho Magalhães

Tese de Doutorado defendida e aprovada, no dia 24 de novembro de 2022, pela Banca Examinadora designada pelo Colegiado do Programa de Pós-Graduação em Engenharia Elétrica da Universidade Federal de Minas Gerais constituída pelos seguintes professores:

Prof. Dr. Henrique Resende Martins- DEE (UFMG) - Orientador

Prof. Dr. Andressa da Silva de Mello (UFMG)

Prof. Dr. Cristiano Leite de Castro (UFMG)

Prof. Dr. Emerson Fachin Martins - Fisioterapia (UnB)

Prof. Dr. Alcimar Barbosa Soares - Engenharia Elétrica (UFU)

Prof. Dr. Claysson Bruno Santos Vimieiro - DEMEC (UFMG)

Belo Horizonte, 24 de novembro de 2022.

Documento assinado eletronicamente por **Henrique Resende Martins**, **Professor do Magistério Superior**, em 25/11/2022, às 07:51, conforme horário oficial de Brasília, com fundamento no art. 5º do Decreto nº 10.543, de 13 de novembro de 2020.

Documento assinado eletronicamente por **Alcimar Barbosa Soares**, **Usuário Externo**, em 25/11/2022, às 11:34, conforme horário oficial de Brasília, com fundamento no art. 5º do Decreto nº 10.543, de 13 de novembro de 2020.

Documento assinado eletronicamente por **Andressa da Silva de Mello**, **Chefe de departamento**, em 30/11/2022, às 16:24, conforme horário oficial de Brasília, com fundamento no art. 5º do Decreto nº 10.543, de 13 de novembro de 2020.

Documento assinado eletronicamente por **Claysson Bruno Santos Vimieiro**, **Professor do Magistério Superior**, em 01/12/2022, às 07:51, conforme horário oficial de Brasília, com fundamento no art. 5º do Decreto nº 10.543, de 13 de novembro de 2020.

Documento assinado eletronicamente por **Cristiano Leite de Castro**, **Professor do Magistério Superior**, em 01/12/2022, às 11:27, conforme horário oficial de Brasília, com fundamento no art. 5º do Decreto nº 10.543, de 13 de novembro de 2020.

Documento assinado eletronicamente por **Emerson Fachin Martins**, **Usuário Externo**, em 03/12/2022, às 05:47, conforme horário oficial de Brasília, com fundamento no art. 5º do Decreto nº 10.543, de 13 de novembro de 2020.

A autenticidade deste documento pode ser conferida no site https://sei.ufmg.br/sei/controlador_externo.php?acao=documento_conferir&id_orgao_acesso_externo=0, informando o código verificador **1912863** e o código CRC **C749B287**.

Dedicado ao meu Espírito protetor, à minha esposa Nathalia e ao meu amigo Jonatas.

Acknowledgments/Agradecimentos

First I would like to write a few words in Portuguese.

Como pobre homem que somos, há muito nos perguntamos sobre a existência de Deus e por vezes buscamos entender a Sua natureza íntima. Até hoje, a melhor resposta que encontrei para entender onde encontrar a prova da existência de Deus é: "*Num axioma que aplicais às vossas ciências. Não há efeito sem causa. Procurai a causa de tudo o que não é obra do homem e a vossa razão responderá.*" - Allan Kardec.

Ao final deste trabalho - nada mais do que o fim de uma pequena etapa na minha trajetória -, rendo graças a Deus por sua infinita sabedoria e misericórdia para com a minha pequenez. Agradeço à Ele e a Jesus por me permitirem ter tido essa oportunidade tão enriquecedora, sob vários aspectos. Ainda, àqueles que me guiaram com os seus conselhos, que me intuiram por tantas e tantas vezes e me deram forças em momentos que não teria conseguido seguir sozinho, a minha mais profunda e eterna gratidão.

À minha esposa Nathalia, que esteve comigo durante os quatro anos deste doutorado, a minha gratidão por ser tão amorosa, paciente, compreensiva e companheira. No seu silêncio eu encontrei o apoio que precisei e no seu amor as lições que ainda necessito aprender.

À minha mãe por seu amor cujas raízes são invisíveis aos meus olhos.

Agradeço em especial o amigo Jonatas Scarano Moreira por sua dedicação, força de vontade, paciência e tolerância durante dois árduos anos desta pesquisa.

Ao Prof. Henrique pela oportunidade de realizar um trabalho que me permitiu descobrir os meus propósitos. Sou grato pela orientação, confiança e tolerância recebidas nos seis anos de trabalho juntos, divididos em um mestrado e um doutorado.

Agradeço a Dra. Christine Azevedo Coste pela orientação durante trabalhos críticos e que contribuiram com a minha evolução como pesquisador.

Vale lembrar que este trabalho se deu, na sua maior parte, durante a pandemia. Teria sido muito mais difícil se não fosse pelas amizades que se solidificaram nesse período. Em especial aos amigos William e Jéssica, Amanda e Marcos Tulio, o meu mais profundo reconhecimento por me aturarem tão bem!

À UFMG, ao PPGEE e ao Centro de Treinamento Esportivo da UFMG.

Now, some words in English.

This work would not be possible without the help from Iron Maiden (specially) and so many others (bands) so present during this period.

"O mundo é a oficina. O corpo é a ferramenta.
A existência é a oportunidade. O dever a executar é a missão a cumprir.
O pensamento escolhe. A ação realiza.
O homem conduz o barco da vida com os remos do desejo e a vida conduz o homem ao porto que ele aspira a chegar.
Eis porque, segundo as Leis que nos regem, “a cada um será dado pelas próprias obras”."

Emmanuel

Resumo

A lesão traumática da medula espinhal (LME) pode resultar em paralisia completa ou incompleta de todas as funções motoras e sensoriais abaixo do nível da lesão. A atividade física e a mobilidade reduzidas podem causar alterações nas funções metabólicas e na composição corporal. Para minimizar as consequências da inatividade, a Estimulação Elétrica Funcional (*Functional Electrical Stimulation*, FES) pode beneficiar esses indivíduos em programas de reabilitação ou como tecnologia assistiva, onde as contrações musculares evocadas eletricamente são utilizadas para realizar atividades funcionais. Por exemplo, o ciclismo assistido por FES (FES-*cycling*) permite que indivíduos com LME com pouco ou nenhum movimento voluntário das pernas pedalem um cicloergômetro ou um triciclo reclinado. Embora os benefícios desta tecnologia sejam bem conhecidos, esse recurso pode ser inacessível principalmente em países emergentes como o Brasil. Nesse sentido, seria vantajoso para nossa comunidade ter acesso a toda uma plataforma FES de código aberto que pudesse ser explorada em diferentes contextos de atividades funcionais. Este trabalho aborda o desenvolvimento de um dispositivo de estimulação elétrica de alta potência de código aberto e todos os aspectos necessários para a implementação de um sistema de FES-*cycling* para sujeitos com LME. O dispositivo possui uma topologia de corrente constante capaz de criar pulsos bifásicos com amplitude, largura e frequência de até 150mA, 1000μs e 100Hz, respectivamente. Um aplicativo celular foi desenvolvido para definir e modificar os parâmetros de estimulação de até oito canais diferentes. A maior contribuição deste trabalho, entretanto, é a introdução de um novo algoritmo de controle com Aprendizado por Reforço (*Reinforcement Learning*, RL) para a adaptação em tempo real dos padrões de estimulação empregados nas sessões de FES-*cycling*. O algoritmo implementado apresenta uma estratégia *decayed-epsilon-greedy* para ajustar a carga elétrica injetada necessária para evocar contrações musculares. Para rastrear e controlar a cadência de pedalada predefinida, um controlador Proportional-Integral (PI) foi usado em paralelo para modular a amplitude de corrente dos canais de estimulação. O desempenho do controlador global foi avaliado sob diferentes configurações do algoritmo RL e explorado em diferentes cenários de pedalagem. Sessões de FES-*cycling* estacionárias e não estacionárias foram realizadas por um voluntário com paraplegia completa (ASIA Impairment Scale (AIS) A, T8) que foi capaz de pedalar por distâncias superiores a 4,5km. Os resultados evidenciaram que o algoritmo foi capaz de aprender e modificar o padrão de estimulação de acordo com a política pré-definida ao mesmo tempo em que rastreou as cadências de pedaladas configuradas. Por fim, este trabalho avaliou os efeitos de diferentes treinamentos de ciclismo assistido na Densidade Mineral Óssea (DMO) e na composição corporal durante um período de 2 anos. Embora tenha sido observado um aumento de 9,8% na massa magra das pernas ao final do protocolo, o resultado não refletiu as mudanças encontradas ao longo do programa, pois diferentes protocolos de treinamento

foram acompanhados de resultados diferentes. Esses achados apoiam a ideia de que o ciclismo assistido por FES pode ajudar os indivíduos com LME a recuperar a massa magra e reduzir a massa gorda quando associado a programas adequados de treinamento e nutrição. Alterações positivas na DMO foram encontradas na região lombar. Entretanto, uma diminuição significativa foi observada na região de interesse do fêmur, sugerindo cautela em afirmar que a modalidade melhora a saúde óssea nos membros inferiores em indivíduos com LME.

Palavras-chave: Estimulação Elétrica Funcional, FES-cycling, Estimulação Elétrica Neuromuscular, Estudo de Caso, Aprendizado por Reforço.

Abstract

Traumatic Spinal Cord Injury (SCI) can result in complete or incomplete paralysis of all motor and sensory functions below the level of injury. Reduced physical activity and mobility can cause changes in metabolic functions and body composition. To minimize the consequences of inactivity, Functional Electrical Stimulation (FES) can benefit these individuals in rehabilitation programs or as assistive technology, where electrically-evoked muscle contractions are used to perform functional activities. For instance, FES-*cycling* allows SCI-individuals with little or no voluntary leg movement to pedal a stationary machine or a recumbent tricycle. Although the benefits of this technology are well known, this resource may be inaccessible mainly in emerging countries like Brazil. In this regard, it would be advantageous for our community to have access to an entire open-source FES platform that could be explored in different functional activities contexts. This work aims to address the development of an open-source high-power capacity electrical stimulation device and all the necessary aspects to implement a FES-*cycling* system for individuals with SCI. The device features a constant current topology able to create biphasic pulses with amplitude, width, and frequency up to 150mA, 1000µs, and 100Hz, respectively. A mobile application was developed to define and modify the stimulation parameters of up to eight different channels. The main contribution of this work, however, is the introduction of a novel Reinforcement Learning (RL) control algorithm for real-time adaptation of the FES-*cycling* stimulation patterns. The designed algorithm features a *decayed-epsilon-greedy* strategy to adjust the injected electrical charge necessary to evoke muscle contractions. To track and control the predefined pedaling cadence, a PI controller was used in parallel to modulate the current amplitude of the stimulation channels. The global controller performance was evaluated under different RL settings and explored in different cycling scenarios. Overground and stationary FES-*cycling* sessions were performed by a volunteer with complete paraplegia (AIS A, T8) which was able to cycle overground for distances of more than 4.5km. The results evidenced that the algorithm was able to learn and modify the stimulation pattern according to the predefined policy while being able to track predefined pedaling cadences. Finally, this work evaluated the effects of different assisted cycling training on Bone Mineral Density (BMD) and body composition over two years. Although a 9.8% increase in lean mass legs was observed at the end of the protocol, the result did not reflect changes found throughout the program, as different training protocols presented different results. These findings support the idea that FES-assisted cycling can assist SCI-individuals to regain lean mass and reduce fat mass when associated with adequate training and nutrition programs. Positive changes in BMD were found in the lumbar region. However, a significant decrease was observed in the femur region of interest, suggesting caution in stating that the modality improves bone health in the lower limbs.

Keywords: Functional Electrical Stimulation, FES-cycling, Neuromuscular Electrical Stimulation, Case Report, Reinforcement Learning

List of Figures

List of Tables

List of abbreviations and acronyms

AD Autonomic Dysreflexia

AIS ASIA Impairment Scale

AP action potential

ASIA American Spinal Injury Association

BC body composition

BMD Bone Mineral Density

BMI Bone Mass Index

CNS Central Nervous System

CU Communication Unit

DAC Digital to Analog Converter

DCU Digital Control Unit

DXA Dual-Energy X-Ray Absorptiometry

EIM Electrical Impedance Myography

EMG Electromyography

ES Electrical Stimulation

FES Functional Electrical Stimulation

FM Fat Mass

FN Femoral Neck

FSR Force Sensitive Resistors

FT Femur Total

HAM *hamstring*

HCFES High-Capacity Functional Electrical Stimulation

IC Intergrated Circuit

IDE Integrated Development Environment

ILC Iterative Learning Control

IMU Inertial Measurement Unit

ISCD International Society of Clinical Densitometry

ISNCSCI International Standards for Neurological Classification of Spinal Cord Injury

LM Lean Mass

LS Lumbar Spine

MCU Microcontroller Unit

MDP Markov Decision Process

MEC Maximal Evoked Contraction

MN motor neuron

MOSFET Metal Oxide Semiconductor Field Effect Transistor

MRC Medical Research Council

MRI Magnetic Resonance Imaging

MU Motor Unit

NMES Neuromuscular Electrical Stimulation

PCB Printed Circuit Board

PI Proportional-Integral

PID Proportional Integral Derivative

PNS Peripheral Nervous System

PSU Power Supply Unit

RDA Recommended Daily Allowance

RF *rectus femoris*

RL Reinforcement Learning

RLC Repetitive Learning Control

SCI Spinal Cord Injury

SD Standard Deviation

SIU Sensor Interface Unit

SPI Serial Peripheral Interface

SU Stimulation Unit

VL *vastus lateralis*

VM *vastus medialis*

WHO World Health Organization

Contents

1 Introduction

1.1 Context and Relevance

Spinal Cord Injury (SCI) refers to damage to the spinal cord resulting from trauma, disease or degeneration. SCI can result from a traumatic event in the spine that fractures, dislocates or compresses one or more vertebrae (Alizadeh; Dyck; Karimi-Abdolrezaee, 2019). Traumatic SCI can temporarily or permanently interrupt the neurological functions at the distal level of the injury (Varma et al., 2013).

In the United States, the incidence of traumatic SCI is approximately 40 cases per million individuals (approx. 12,500 new cases per year), which implies a substantial economic impact of more than US$4 billion annually (Gorgey et al., 2014; Varma et al., 2013). In Brazil, epidemiological studies report difficulty in obtaining data on SCI incidence. The estimate varies from 16-26 (Botelho et al., 2014) to 40-50 (Nascimento et al., 2017) new cases for every million inhabitants per year. Worldwide, between 250,000 and 500,000 people suffer a spinal cord injury annually. Trauma is the result of automobile collisions (38%), falls (30%), violence (13%), incidents in sports activities (9%), and surgical procedures (5%) (Bennett J, M Das J, Emmady PD, 2022; Nas, 2015).

In 1973, the American Spinal Injury Association (ASIA) was created to improve the treatment of SCI-individuals based on the facilitated exchange of research results, data, and best practices among professionals (Roberts; Leonard; Cepela, 2017). The ASIA International Standards for Neurological Classification of Spinal Cord Injury (ISNCSCI) exam can be used to score the motor and sensory impairment following SCI (Betz et al., 2019; Roberts; Leonard; Cepela, 2017). This classification relates motor, sensory and reflexive abilities to the neurological level of injury, in addition to being partial or complete. The ASIA Impairment Scale (AIS) classifies the individual's functional impairment as:

- **AIS A: Complete**. No sensory or motor functions are preserved in the sacral segments of S4-S5;
- **AIS B: Sensory incomplete**. There is a motor deficit without sensory loss below the neurological level, including the sacral segments of S4-S5 (light touch, pin sensation, or deep anal pressure at S4-S5); no motor function preserved from three levels below the motor level in each half of the body;
- **AIS C: Motor incomplete**. The motor function is preserved below the neurological level and more than half of its muscles have strength lower than 3/5 of the Medical Research Council (MRC) scale;

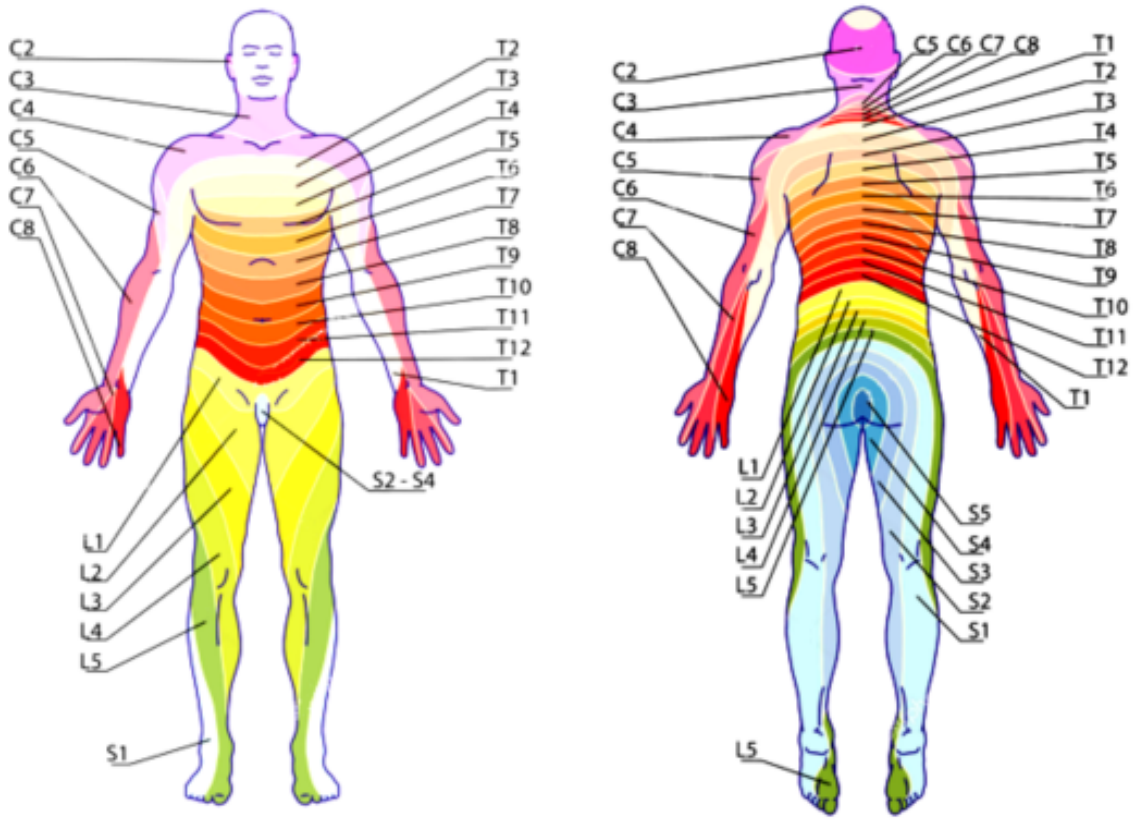

Figure 1 – Body motor and sensory regions with the respective neurological injury level. SCI can result in complete or partial loss of functions below the level of the injury.

- **AIS D: Motor incomplete**. Motor function is preserved below the neurological level and at least half of the muscles below the level have strength greater than 3/5 (MRC);
- **AIS E: Normal**. Sensory and motor functions in all segments are preserved.

Figure 1 illustrates the motor and sensory regions associated with their respective spinal cord segment.

Lesions that affect the cervical segment usually result in quadriplegia. Patients with C3 or higher lesions need ventilatory support and C4 can spontaneously control breathing. C5 injury results in some control of the shoulder and elbow flexion; however, there is no control in the hand or wrist. The transfer in these cases is totally dependent. People with a C6 lesion have some control of the wrist but not of the hands. Despite the need for support in the transfer, these patients have some independence in activities related to nutrition, care and hygiene, in addition to dressing their upper body. Elbow extension at the C7 level and finger flexor muscle strength at the C8 level are sufficient, which results in greater independence in daily and transfer activities.

Thoracic segment injuries result in paraplegia. At levels T1 to T8, despite hand control, trunk control is ineffective. T9 to T12 injuries allow greater control of the trunk and abdominal muscles, resulting in good balance in the sitting position. Injuries to the lumbar and sacral regions result in paralysis and loss of sensation in the lower extremities, in addition to the possibility of loss of bowel and bladder control and sexual dysfunction. The sensory-motor functional capacity of individuals affected by SCI is, therefore, strongly influenced by the level of the lesion and is aggravated if the lesion is complete (Nas, 2015).

Events after SCI are divided into immediate (first 2 hours), acute (2 to 48 hours), sub-acute (48 hours to 14 days), intermediate (14 days to 6 months) and chronic (from the 6^{th} month) (Ahuja et al., 2017). Some therapeutic goals are beneficial in certain phases of SCI, as they target the events that occur in this phase. For instance, early rehabilitation in the acute and subacute phases can prevent joint contractures, minimize the loss of muscle strength, maintain functional capacity and relieve pain. The primary objective in this case is to minimize long-term complications. Passive and isometric exercises must be performed intensively. It is also essential to maintain BMD and the normal functioning of the respiratory and digestive systems. To avoid pressure ulcers, the patient's position should be changed every 2 to 3 hours (Siddiqui; Khazaei; Fehlings, 2015).

In the chronic phase, independence may be the primary objective to be attained by patients with SCI, regardless of whether the injury is partial or complete. However, this ability depends on numerous factors such as the level of injury, degree of spinal cord impairment, age, weight, motivation, spasticity and functional capacity of the patient. Rehabilitation composed of functional exercises, occupational therapy and the use of orthoses are suggested to restore or improve the abilities needed for daily living according to the potential of each individual (Varma et al., 2013).

Moreover, within one year after the trauma, more than fifty percent of patients with complete SCI develop osteoporosis and the long-term follow-up indicates an increase in the prevalence rate to more than eighty percent (Varacallo M, Davis DD, Pizzutillo P, 2022). The decline in BMD increases the occurrence of fractures and leads to severe consequences, from skin lesions to lower limb amputation and premature death (Morse et al., 2019; Champs et al., 2019). The risk for various complications is aggravated by the neurological level and extent of the injury, in addition to the lifetime costs of care and the impact on psychological and social behaviors (Fattal et al., 2017).

Due to functional impairment and a sedentary lifestyle, the metabolic functions and body composition are altered, leading to a significant loss of lean mass and accumulation of fat mass (Sezer, 2015). Long-term problems also include respiratory, cardiovascular, urinary and intestinal complications (including neurogenic bladder or neurogenic bowel and urinary tract infections), spasticity, pain syndromes, autonomic dysreflexia, deep vein thrombosis and pressure ulcers. This scenario favors the increase in morbidity and

mortality (Bennett J, M Das J, Emmady PD, 2022).

Therefore, rehabilitation and other treatment approaches are encouraged to improve the patient's functional level and reduce the consequences of SCI. Neuromuscular Electrical Stimulation (NMES) and Functional Electrical Stimulation (FES) may also be considered to evoke muscle contractions and overcome the lack of volitional limb motor activity. These technologies use surface or implanted electrodes to apply low-current Electrical Stimulation (ES) pulses over a muscle belly or nerve trunk to evoke muscle contractions. NMES aims to restore nerve and muscle metabolism that are dysfunctional (Maffiuletti, 2010). FES induces coordinated muscle contractions to assist in the reproduction of functional movements both independent or associated with body-machine devices to be explored in rehabilitation, sports and leisure (Scheer et al., 2021; Peckham; Knutson, 2005).

Cycling is one of the most researched modalities among the different assisted exercises. In general terms, FES-*cycling* coordinates the electrically-evoked contraction of specific muscles within limited ranges of the pedaling cycle that allows individuals with impaired voluntary leg movement to pedal a recumbent tricycle or ergometer. FES associated with the pedaling activity triggers metabolically active muscle contractions in a coordinated manner and in association with eventual natural (within the preservation zone) and artificial (electrically-evoked contractions of the paralyzed muscles in the loss zone) controls, which can be used in rehabilitation and also as assistive technology.

The difference to a conventional exercise or therapy is the possibility for the individual to perform the task independently if a system adapted for the modality is available (Bo et al., 2017; Fattal et al., 2021). Furthermore, compared to other activities such as standing and walking, FES-*cycling* can minimize the risk of falls and bone fractures - especially for individuals with SCI - as the exercise can be performed in a recumbent position. Furthermore, it can be accomplished early in the rehabilitation process by individuals with high levels of impairment.

The modality has evidenced several physiological and psychological benefits, including positive impacts on pain, cardio-respiratory function, body composition and bone metabolism (Gorgey et al., 2014; Scheer et al., 2021). FES-*cycling* is therefore a powerful tool to maintain the health of the musculoskeletal system below the level of injury which is an essential characteristic to prevent comorbidities and complications resulting from muscle atrophy.

1.2 Purpose and Contributions

1.2.1 Motivations

In the FES-*cycling* modality, a fixed baseline stimulation pattern is usually defined from which pulse amplitude, width, frequency or even a combination of these parameters are modified by a controller to track cadence, torque and power (Cousin; Duenas; Dixon, 2021; Sijobert et al., 2019). In addition to evaluating the performance of closed-loop controller architectures and the cycling outcomes, these investigations reveal that the choice of the strategy to be developed reflects a trade-off between what is expected from the rehabilitation goals and the level of complexity from a technological point of view.

For instance, it can be argued that the first assesses whether the use of the technology is aimed at therapeutic applications (cardiovascular conditioning and prevention of atrophy through exercises) that may opt for greater simplicity of implementation in the clinic; or related to more complex functional goals, including assistance in activities such as walking, standing, cycling, etc. The second considers the development of technology itself, which includes various sensors, the Electrical Stimulation (ES) unit itself, the implementation of elaborate electronic instrumentation and, mainly, the time-consuming development of complex control strategies and algorithms to deal with non-linearity and temporal variability of muscle response.

On the one hand, simplifying the methods associated with the FES-*cycling* modality can lead to a drastic reduction in the implementation time and reduce the complexity of the stimulation pattern adjustment, which seems to be a common objective in recent research. On the other hand, the complexity while developing the technology can increase in the background. In any case, however, research possibilities are created to study of novel methodologies that encourage the use of this technology.

In a recent work published by Sijobert et al. (2019), researchers introduced a novel algorithm for the automatic detection of stimulation events in FES-*cycling* regardless of alterations in the pilot seating position, which suggests a reduced time to optimize the stimulation patterns. The study simplified the definition of the ES parameters while providing a method that could be adapted to different users and devices. They used Inertial Measurement Units (IMUs) to automatically detect the start and stop events of muscle stimulation through a simple *if-then* algorithm and a relatively simple assembly was employed for time optimization. Even though some adjustments of offset parameters were necessary before the start of stimulation, the algorithm was successfully tested and the participant was able to pedal in both stationary and non-stationary conditions.

The same research group proposed another approach using torque feedback to automatically determine the optimal stimulation intervals for the muscles to be activated during FES-*cycling* (Schmoll et al., 2021). By analyzing the difference between active (with

stimulation) and passive (without stimulation) torques over a complete pedaling cycle, the researchers demonstrated that it was possible to differentiate between the contribution and resistance phases for a given muscle group. The algorithm automatically identified the stimulation intervals for the participant's left and right quadriceps and hamstring muscles. Despite excellent results and reducing the system complexity, the stimulation pattern obtained from the torque analysis was validated on a home trainer without any cycling load during short periods. As this approach is based on net-torque produced on pedals, it is expected that different load resistances may affect the cycling dynamics, which was not validated in the experiment.

Learning control techniques such as Iterative Learning Control (ILC) and Repetitive Learning Control (RLC) have also been suggested to automatically adapt the stimulation pattern and improve the performance of tracking repetitive or periodic activities through the use of knowledge obtained in previous interactions between the controller and the system environment (Duenas et al., 2020; Duenas et al., 2020). Even though applied to nonlinear systems, ILC is frequently designed assuming linear models and uses the observed error from previous trials as information to modify the input signal for the subsequent iterations to anticipate for repeated disturbances. However, it cannot perfectly track the required action to be executed (Bristow; Tharayil; Alleyne, 2006).

ILC differs from RLC as the first is intended for discontinuous operation. The use of the RLC technique for cadence tracking during stationary FES-*cycling* was investigated by Duenas et al. (2016) and Duenas et al. (2020). The researchers explored the switching of the stimulation pattern across different muscle groups based on the joint effectiveness to produce torque while being assisted by an electrical motor in regions of the crank cycle with low torque efficiency. Besides being designed to exploit the periodicity of the desired cadence trajectory by learning from previous control inputs for each muscle group and the electric motor, the controller used nonlinear models with parametric uncertainties in the system and was implemented by a personal computer due to its complexity. However, an essential feature of the ILC and RLC techniques is that the algorithm cannot exempt itself from a mathematical model of the uncertainties that affect the system which, in turn, could facilitate its implementation.

In this sense, Reinforcement Learning (RL) emerges as a reward-based machine learning training method that may overcome the need for complex mathematical models of the environment and its disturbances while being able to track repetitive activities. The concept relies on a learner, a decision maker and a so-called agent, which assesses the state of the environment by mapping it into actions and then evaluates a numerical reward obtained from it as training information. In other words, the agent perceives the current state of the environment and learn an optimal policy i.e., a stochastic rule by which the agent selects actions as a function of states.

A distinguishing feature of RL is to formalize the idea of a goal through a reward signal sent from the environment to the agent as a response to the selected action at a specific time. The objective is to maximize the notion of cumulative reward over a particular period and not the immediate reward, which requires the creation of rules for the agent to balance between exploring new actions and exploiting already known actions (Sutton; Barto, 2018).

A recent study introduced a method using RL for real-time optimization of stimulation patterns while monitoring the average cadence error during simulated FES-*cycling* sessions (Wannawas; Subramanian; Faisal, 2021). The performance outcome obtained with a musculoskeletal model simulation was compared to other controllers, such as PID and Fuzzy Logic. Despite not being clear about how the controller would act on the pulse parameters in real scenarios, a control algorithm was suggested to learn how to adapt the electrical pulses of different leg muscles by evaluating the interactions with the system. It was also proposed that the method could compensate for muscle fatigue and track desired cadences. A considered drawback, however, was the large number of interactions and data needed for training the agent. For example, the preliminary results reported the need for an additional ten minutes to train the algorithm before obtaining satisfactory tracking performance, limiting the investigation to be conducted in real-world cycling sessions.

Considering the aforementioned investigations, to reduce the FES-*cycling* implementation time by simplifying the design of electrical stimulation patterns and reducing the complexity of control techniques, it seems advantageous to use learning methods that reward desired behaviors of a particular agent that is capable of exploring different manners to interact with the cycling environment aiming to improve the stimulation pattern and consequently the cycling performance.

1.2.2 Contributions

In recent decades, a global effort has been witnessed on the development of novel rehabilitation technologies to reproduce functional activities assisted by electrical stimulation, including walking, grasping, rowing, transferring, standing and cycling (Schauer, 2017; Ho et al., 2014). For instance, the FES-*cycling* modality, which allows individuals with SCI to practice physical activities in the clinic or in a recreational way, has been extensively researched. As a result, positive effects on health and fitness-related outcomes have been demonstrated and a set of technical notes and research consolidated the potential behind Functional Electrical Stimulation (Scheer et al., 2021). However, this technology is still inaccessible to a large part of the population with SCI as the general price ranges from $\$16,000$ to $\$30,000$ USD[1].

[1] https://www.anatomicalconcepts.com/articles/2017/03/28/2017-3-28-fes-cycling-system-cost

Given the high cost of these systems, especially for emerging countries, a relevant question is how to democratize access to this technology, whether through direct access to the final product or the development itself. Considering the first a public health issue, this work was encouraged to offer an alternative through the latter, which is concerned with creating an open-source FES platform. In addition to the benefit for individuals with SCI, access to a whole Electrical Stimulation project would allow researchers, engineers and even clinicians to develop their own applications not limited to commercial devices, which can be fully modified according to their interests.

Regarding the application of FES-*cycling*, one of the major drawbacks of the modality is the need for modifying the stimulation pattern (i.e., the stimulation intervals within the pedaling cycle and the pulse parameters for each stimulation channel) and the mechanical aspects of the tricycle or ergometer for each individual. The complexity and time-consuming process of defining these parameters can discourage the use of this technology for clinical or research purposes.

In this sense, it is hypothesized that the use of learning methods for the automatic adjustment of stimulation parameters by the system itself would overcome the actual limitations regarding the FES-*cycling* realization. Furthermore, by creating a method for the modulation of the stimulation parameters based on previous interactions between the system and the environment, interesting research possibilities are created, such as optimizing the injection of electrical charge to delay the muscle fatigue process - a limitation of the Electrical Stimulation technique - and to advance in new strategies in computer-assisted technologies for individuals with SCI and other neurological impairments.

1.2.3 Objectives

The following objectives will be addressed in this work:

1. the development of an entire FES system and its validation with a SCI volunteer during FES-*cycling* sessions;
2. the creation of a methodology to improve and simplify the definition process of the stimulation parameters for the FES-*cycling* based on machine learning concepts;
3. the realization of a case report to document changes in Bone Mineral Density (BMD) and body composition in a 38-year-old man with complete paraplegia during two years of FES-cycling.

Regarding the validation of FES-*cycling* with a participant with SCI, the following contributions are targeted:

- validate the system capacity to track different pedaling cadences during FES-*cycling* sessions;
- evaluate physiological aspects in response to two different intensity FES-*cycling* training programs;
- evaluate the pedaling performance of FES-cycling, including distance, pedaling time, average and maximum speed, and average and maximum power;

1.3 Organization of this D.Sc. Dissertation

This dissertation is organized into 6 chapters, following the structure presented in Figure 2. Chapter 1 introduces the motivations and primary objectives of this D.Sc. dissertation. Chapter 2 discusses the physiological aspects and mechanisms of Functional Electrical Stimulation. Chapter 3 presents the HCFES device and cycling system projects. Chapter 4 introduces a novel algorithm based on RL concepts designed to optimize the stimulation pattern online during the cycling sessions. Chapter 5 details the 2-year FES-*cycling* intervention protocol and the results obtained on Bone Mineral Density (BMD) and body composition for a single participant with paraplegia. Finally, Chapter 6 summarizes the main findings and the future developments of this work.

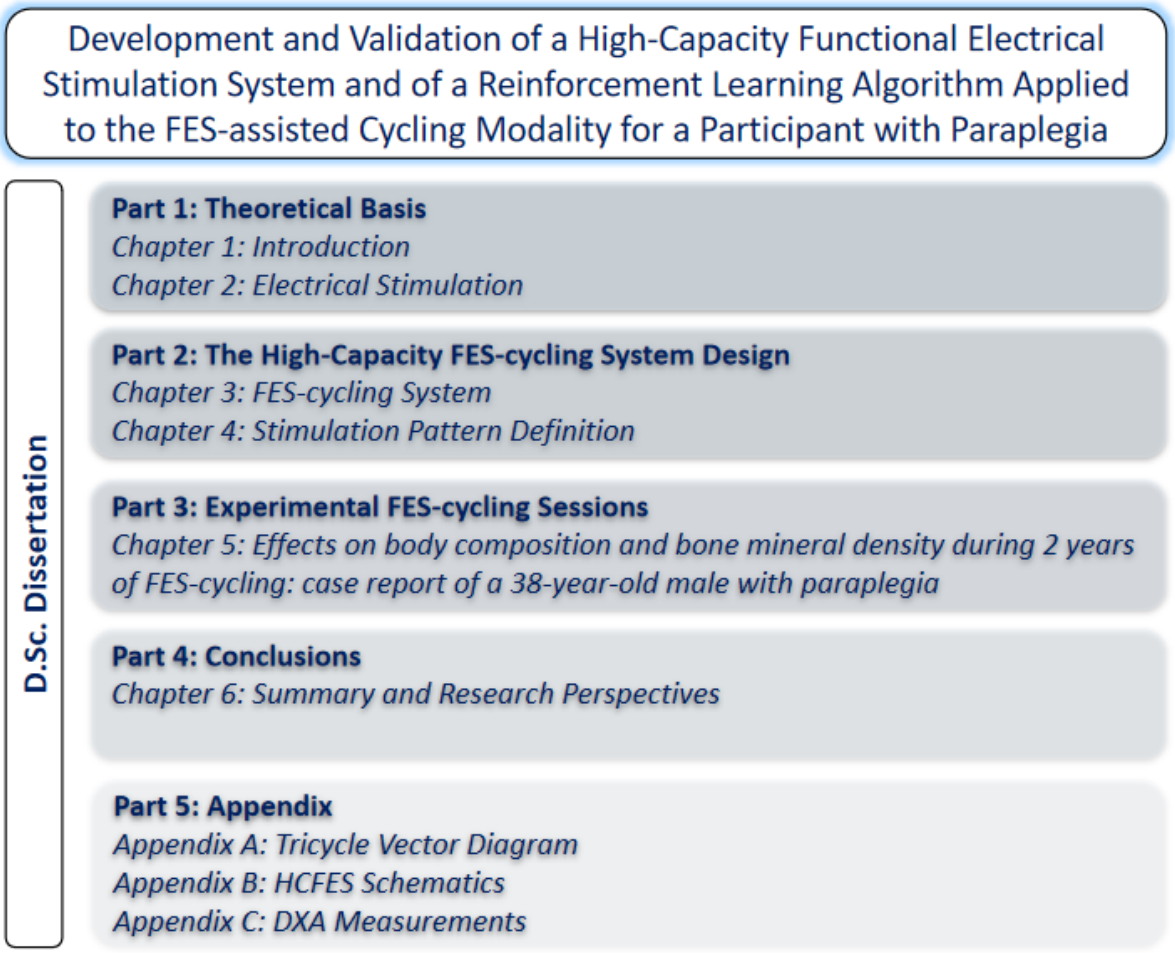

Figure 2 – Structure of the D.Sc. dissertation.

1.4 List of Publications

The findings of this research have resulted in the publication of 2 journal papers, one conference paper which became a book chapter and a Case Report has been submitted. These publications are presented as follows:

1. Coelho-Magalhães, T.; Coste, C. A.; Resende-Martins, H. A Novel Functional Electrical Stimulation-Induced Cycling Controller Using Reinforcement Learning to Optimize Online Muscle Activation Pattern. **Sensors**, v. 22, n. 23, 2022. ISSN 1424-8220. https://www.mdpi.com/1424-8220/22/23/9126.

2. Coelho-Magalhães, T.; Fachin-Martins, E.; Silva, A.; Coste, C. A.; Resende-Martins, H. Development of a High-Power Capacity Open Source Electrical Stimulation System to Enhance Research into FES-Assisted Devices: Validation of FES Cycling. **Sensors**, v. 22, n. 2, 2022. ISSN 1424-8220. https://www.mdpi.com/1424-8220/22/2/531.

3. Coelho-Magalhães, T.; Vilaça-Martins, A. F.; Araújo, P. A.; Resende-Martins, H. Programmable Multichannel Neuromuscular Electrostimulation System: A Universal

Platform for Functional Electrical Stimulation. In: Bastos-Filho, T. F.; Caldeira, E. M. de O.; Frizera-Neto, A. (Ed.). **XXVII Brazilian Congress on Biomedical Engineering**. Cham: Springer International Publishing, 2022. p. 1371–1377. ISBN 978-3-030-70601-2.

4. Coelho-Magalhães, T.; Amaral, G. M.; Silva, P. E.; Resende-Martins, H. Effects on Bone Mineral Density and Body Composition During 24 months of FES-assisted Cycling: Case Report of a 38-year-old Male with Paraplegia. **Case Report Submitted**, 2022.

1.5 Supplementary materials

Experimental results and datasets are available as following:

- FES-*cycling* videos available at the project's YouTube Channel
- HCFES project can be downloaded at: https://osf.io/pf3ru/
- Reinforcement Learning (RL) Project Files can be downloaded at: https://osf.io/fb87w/
- BMD and body composition (BC) data can be assessed at: https://osf.io/95xbs/
- MATLAB App to evaluate the tricycle configurations: GitHub link

2 Electrical Stimulation

One of the main objectives of this work is to evaluate the implications of FES-assisted cycling on the physical condition of a participant with SCI under different intensity training programs. Therefore, it is necessary to study the mechanisms associated to the Electrical Stimulation, the nervous system structures and the physiology related to the musculoskeletal system.

This subsection presents a brief review of neuromuscular physiology and the mechanisms required for muscle contraction. However, the specific structure of the muscle fiber and the molecular basis of muscle contraction will not be addressed. The detailed aspects were discussed in the author's master's dissertation (Coelho-Magalhães, Tiago, 2018). Unless otherwise noted, this section is based on the following references: (Bear; Connors; Paradiso, 2015; Hall, 2015; Magee; Zachazewski; Quillen, 2007).

2.1 Neuromuscular Physiology

The nervous system is divided into the Central Nervous System (CNS), consisting primarily of the brain and spinal cord; and Peripheral Nervous System (PNS), which includes nerves, ganglia and nerve endings. The neuron is the primary functional unit of this system and its structure is divided into the following fractions: soma, dendrites and axon. The latter contains an excitable membrane that allows the transfer of action potential (AP) throughout the nervous system.

More specifically, the resting potential of the axon membrane is negatively charged in relation to the extracellular fluid (typically at -65mV); however, in response to commands from the nervous system itself or to external stimuli (electrical, thermal or mechanical), an influx of Na^+ ions initiates the membrane depolarization. If this potential is raised beyond a triggering threshold, an action potential is created. The spatially propagation of the action potential along the axon is due to the influx of positive charges that depolarize the membrane of adjacent segments to generate new action potentials. These are directed to the CNS (afferent signals) and PNS (efferent signals).

The transfer of pulses throughout the nervous system occurs in electrical or chemical synaptic transmissions. The later uses neurotransmitters to exchange information and there is no physical contact between the presynaptic axon and the postsynaptic cells, including other neurons and muscle, glandular and sensory cells. In relation to muscle fibers, the region where the synapse occurs is called the neuromuscular junction, considered very effective due to the high concentration of neurotransmitter receptors (also known as

neuroreceptors) in the motor end plate.

The association between the skeletal muscle and the parts of the nervous system that command it constitutes the somatic motor system, which is responsible for controlling functions that are consciously influenced. Each muscle fiber is innervated by a branch of lower motor neurons contained within the ventral horn of the spinal cord. The alpha motor neuron innervates extrafusal muscle fibers to generate force; and gamma motor neuron innervates intrafusal muscle fibers responsible for proprioception. The combined motor neurons and all muscle fibers it innervates constitute a Motor Unit (MU).

The motor neurons (MNs) are further organized according to the spinal segment to which they are associated, which are grouped according to the spinal roots: cervical (C, 1 to 8); thoracic (T, 1 to 12); lumbar (L, 1 to 5); and sacral (S, 1 to 5). Somatic motor neurons are not evenly distributed throughout the spinal cord. The ventral horns of the C3-T1 and L1-S3 segments are relatively larger, as they act on a larger set of muscle groups. The muscles that control the movement of the shoulder, elbow, pelvis, and knee joints are called **proximal muscles**; of the hands, feet and digits are controlled by the **distal muscles**; finally, muscles controlling the trunk movements are called **axial muscles**.

The motor units can be classified according to the muscle fibers that compose them, depending on their metabolism and corresponding action: (1) *slow-twitch* (type I) fibers, which can sustain long contraction duration and are more fatigue resistant; and (2) *fast-twitch* (type II) fibers, which creates powerful forces for shorter duration and fatigue quickly. Type II fibers can be further subdivided into *fast-twitch fatigue-resistant*, *fast-twitch fatigue-intermediate*, and *fast-twitch fatigable fibers*. It is important to mention, however, that neuronal innervation is a determining factor in the muscular phenotype, since the propagation speed of the action potential is related to the diameter and axon type (whether myelinated and unmyelinated axons).

For an individual without neurological impairments to perform a voluntary muscle contraction, the recruitment order of motor units follows the Henneman's size principle, where type I fibers (smaller), more fatigue-resistant, are recruited first than type II (larger) fibers, which are more fatigable (Mendell, 2005). As adjacent fibers are recruited in synergy during a muscle contraction - a phenomenon called spatial summation -, the force achieved is influenced by the fibers activated. However, fast fibers, which fatigue more quickly, exert more force when compared to slow ones. Thus, a compromise between the required muscle force to be produced and duration of activity must be considered.

Furthermore, other limiting factors to the amount of force produced by a muscle includes its initial length, which is related to the overlap of actin and myosin bridges; the temporal summation phenomenon, which achieves sustained contractions (tetanic) by increasing the stimulus frequency not to allow the tension in the muscle to relax between

successive twitches; and, finally, the force-velocity relationship, which is also influenced by fibers that constitute the musculature, which, in turn, impacts the performance achieved during physical activities, since the force is decreased as the speed of the movement increases. Therefore, in addition to the type of fiber to be recruited, the number of motor units recruited, the length of the skeletal muscle, and the nature of the muscle contraction are factors that affect the ability of an individual to perform a physical activity.

As will be discussed later in this chapter, the distribution of fast and slow fibers is extremely relevant for the FES-*cycling* modality studied in this work, since the proportion of fibers in SCI-individuals is altered as a result of muscle atrophy secondary to the injury and greatly limits their capacity to perform the activity for a certain time, with greater or lesser speed and under different load contexts. Physical training, therefore, must be well defined and in accordance with the objectives to be achieved for a given volunteer. Still, the performance of the activity is impacted by other factors, such as cardiopulmonary, biomechanical, psychological, etc.

2.2 Electrical Stimulation

Neuromuscular Electrical Stimulation (NMES) is characterized by the use of electrical pulses to artificially evoke the contraction of paretic or paralyzed muscles in order to restore nerve and muscle metabolism that are dysfunctional. Functional Electrical Stimulation (FES) induces electrically evoked muscle contractions in a coordinated manner to assist in the reproduction of functional movements both independent or associated with body-machine devices. In this case, to reproduce a functional movement, the electrically evoked contractions of different muscles must be performed in synergy and synchronised with the functional activity (Hamid; Hayek, 2008).

FES-*cycling* is a commonly researched technique which allows individuals with little or no voluntary leg movement to pedal a stationary bicycle or tricycle (*trike*), usually stationary (Scheer et al., 2021). Other activities and modalities are also studied, such as rowing (Gibbons; Beaupre; Kazakia, 2016), walking (Coelho-Magalhães, Tiago, 2018), standing balance (Rouhani et al., 2017) etc.

2.2.1 Functional Electrical Stimulation Mechanisms

An important feature regarding nerves and muscle fibers is their responsiveness to electrical stimulation. Muscle contraction can be artificially evoked through electrical pulses that are preferable applied over the motor point of the muscle of interest. This location presents the muscle's greatest excitability that is observed with the minimum electrical stimulation intensity necessary to evoke a contraction (Moon et al., 2012), and where the branch of the intramuscular motor nerve is connected to the muscle (Ragnarsson,

2008). However, muscle contractions can be achieved in denervated muscles by applying electrical pulses with much higher intensities, which may limit the application of the electrical stimulation for rehabilitation purposes or as assistive technology (Boncompagni, 2012). In this work, the application of Functional Electrical Stimulation was addressed only in situations where the peripheral nervous system remained intact.

To electrically evoke muscle contractions with this technology, electrical pulses momentarily concentrate negative charges on one of the electrodes while the other is deficient. As a result of the electric potential difference created, an ionic current is induced under the surface electrodes positioned over the muscle of interest. Eventually, the induced ionic current reach the excitable membrane of the peripheral nerve and action potentials along the axons are triggered (Robinson; Robinson; Snyder-Mackler, 2008).

However, as the membrane depolarization process depends on the intensity of the induced current, some factors greatly impact the efficiency of electrical stimulation, namely: (1) the impedance of body tissues and the thickness of the subcutaneous fat layer, since tissue conductivity is influenced by the water and ion content; (2) the stimulation pulses parameters, including amplitude, pulse width and stimulation frequency; (3) the size and electrodes positioning, in which the current density is related to the intensity of the electric current per unit area of the electrode.

The influence of subcutaneous fat thickness during the application of NMES has also been evaluated in combination with different configurations of surface electrodes, suggesting that the current intensity required to reach the muscle activation threshold is increased when larger surface electrode are used; when the distance between the stimulation electrodes increases; and as the thickness of the adipose tissue increases due to its high resistivity (Doheny et al., 2010). Nevertheless, the effect of the dimensions and distance between electrodes is reduced as the fat layer becomes denser.

The electrical pulse parameters also have a great impact on the effectiveness of the muscle contraction, in which it is of interest to reduce discomfort and maximize the spatial recruitment of muscle fibers. To raise the depolarization level of the membrane cell to the triggering threshold, a combination between the current amplitude and the pulse duration is required to achieve the excitability response of a given tissue (Gorgey et al., 2014). Furthermore, as the electrical pulses are repeated at a certain frequency, a tetanic contraction is eventually developed.

In this case, a restriction imposed by the application of electrical stimulation is related to the spatial recruitment of muscle fibers that are located closer to the electrodes. If the pulse intensity is held constant, contractile activity is imposed on the same group of motor units. As the intensity increases, deeper fibers can be recruited; however, a transmission-propagation fault is observed in the surface fibers. Still, this pattern of recruitment can cause an exaggerated metabolic cost that can anticipate muscle fatigue.

2.2.2 Methodological Considerations

Maffiuletti (2010) described some important physiological and methodological considerations for the use of Neuromuscular Electrical Stimulation (NMES). For instance, the effectiveness of NMES is suggested to depend less on controllable external factors, such as pulse parameters or electrode characteristics, but rather on the individual's intrinsic anatomical properties, which determine the muscle's response to electrical stimuli. In fact, there is no consensus on pulse parameterization to be used during NMES or FES sessions, and the use of different format of electrodes have been reported (Ibitoye et al., 2016; Scheer et al., 2021). Manipulating the intensity, frequency and waveform of the electrical pulse can optimize the muscle tension produced and indirectly assess the effectiveness of electrical stimulation, however (Rabello et al., 2020). Even so, such characteristics must be observed individually, which supports the considerations described previously.

Anyway, it is necessary to find a set of parameters that are commonly associated with the effects sought by the application of electrical stimulation aimed at neuromuscular activity. Typically, to improve functional capacity or increase muscle size, NMES parameters include relatively short biphasic pulses ($0.2 - 0.6$ms) delivered at a frequency of 30-50Hz at the current amplitude tolerated by the volunteer. Even when the intensity is the maximum tolerable, the force generated as a result of the contraction evoked by electrical stimulation is generally low when compared to the maximum force generating capacity of the muscle (<50%), and decreases rapidly as muscle fatigue occurs (Blazevich et al., 2021).

Specifically, for the FES-assisted cycling modality, the most recent review evaluated 92 studies and summarized the characteristics of stimulation pulses mentioned in recent intervention protocols, such as amplitude 140(0-180)mA, frequency of 35(20-60)Hz, and pulse width of 300(200-500)μs; where the parameter is reported as the median and interquartile range in parentheses (Scheer et al., 2021). The fact that there is no agreement between the stimulation parameters may be associated with the different protocols and different objectives of the studies. In any case, a common interest is maximizing the efficiency of stimuli and promoting the delay of muscle fatigue.

Several approaches to offset the rapid muscle fatigue during FES exercises for individuals with SCI have been investigated and were summarized in a recent systematic review (Ibitoye et al., 2016). Methods included the modification of stimulation patterns, the optimization of electrode positioning, improvement of exercise protocols and the development of biofeedback-controlled stimulation. The researchers concluded that, despite the numerous possibilities and potential results, the effective management of fatigue during FES-evoked muscle contractions is still limited, since most studies have not demonstrated clinical relevance because they have not been sufficiently researched to support definitive conclusions. Furthermore, it seems to exist a lack of consensus regarding the results of the

proposed techniques.

For instance, in the mentioned review, eighteen studies investigated the effectiveness of the optimization of stimulation patterns suggesting that the modification of the frequency of different stimulation trains delays the effect of muscle fatigue. Some of these studies reported that alternating constant frequency trains with closely spaced doublet stimulation pulse trains indicated greater improvements in fatigue. Other works, however, found no significant results unless the patterns were used along with other techniques. One of the studies evaluated the effect of modulating the pulse width during FES-*cycling* sessions and also reported not to be able to significantly influence the muscle fatigability if the frequency is kept constant (Gorgey et al., 2014).

Regarding the electrode placement, the adequate positioning over the motor points of the muscle of interest is necessary for the ideal recruitment of muscle fibers. It was suggested to use electrode arrays to recruit motor units more selectively and obtain more efficient motor control, which would also impact the muscle fatigue. However, the use of arrays or systems that multiplex electrodes is almost not used outside of an experimental environment and some studies have not identified significant differences in fatigue resistance for configurations different from those used in conventional stimulation (Schmoll et al., 2021).

Another ES characteristic while evoking muscle contractions considers the waveform and the balance of charges between the phases of the pulse. Greater stimulation efficiency can be achieved with symmetrical pulses compared to asymmetrical pulses (Rabello et al., 2020). The symmetrical rectangular shape is suggested as ideal, as it overcomes the problem of nerve fiber membrane accommodation; in addition, the pulse must evenly distribute the charges at the electrode locations during the stimulation period, in order to avoid any damage to body tissues as a result of electrochemical imbalance.

Finally, it is possible to avoid sudden contractions through a trapezoidal stimulation profile, where the pulses gradually increase the amplitude value until reaching the nominal value (ramping up), remain activated for the period of interest, and subsequently decrease in amplitude until total deactivation (ramping down) (Melo et al., 2015).

2.2.3 Limitations

Although FES-*cycling* has been studied for decades and its positive outcomes amply demonstrated, the application of this exercise modality is limited due to reduced efficiency in terms of output power and endurance, as the non-selective responsiveness of electrically evoked contractions favors the early onset of muscle fatigue.

An important characteristic during voluntary contractions refers to the MUs being activated asynchronously and under different frequency patterns, making it possible to

develop controlled contractions at relatively low frequencies. Also, during sustained contractions, a switching process of MUs allows motor units that were not activated previously to be recruited in replacement of those already activated. These characteristics ensure the reduction of muscle fatigue and promote greater efficiency in performing routine activities (Hamid; Hayek, 2008). However, unlike the voluntary contraction process, neuromuscular or functional electrical stimulation does not respect the Henneman's size principle and activates motor neurons in a non-selective, spatially fixed and temporally synchronous pattern, leading to a reverse recruitment order process that fatigues muscles more rapidly (Jubeau et al., 2007; Gregory; Bickel, 2005).

In addition to the non-physiological aspects of MU recruitment, the excitability of motor neurons decreases as they are electrically stimulated and the failure of excitation-contraction coupling results in reduced torque when performing functional activities (Peckham; Knutson, 2005). Furthermore, muscle atrophy due to chronic diseases, paralysis and inactivity can alter the proportion of *slow-twitch* type I to *fast-twitch* type II fibers, which leads to greater muscle fatigue (Ibitoye et al., 2016). These characteristics accelerate the muscle fatigue process and reduce the time of physical exercise, restricting the health benefits to these individuals and reducing the interest in the practice of this modality for outdoor leisure.

Specifically for the FES-*cycling* modality, other aspects can limit the effectiveness of electrical stimulation, which can be translated into the power produced during exercise. In addition to the eventual inefficiency of neuromuscular muscle activation, factors such as muscle atrophy due to chronic diseases, paralysis and disuse, in addition to the degree of spasticity, can result in greater muscle fatigue and reduced exercise session duration. Consequently, the benefits offered by the modality are limited and the use of this modality for leisure activities outside the clinic is restricted (Ragnarsson et al., 2008).

Another inherent characteristic inherent to the electrical stimulation application during the assisted activity is the non-linearity and time-variability of the muscle response that highlights the need for modifying the pulse parameters to adjust the stimulation intensity in order to improve the evoked response in the face of the excitation-contraction coupling failure and muscle fatigue. Regarding the FES-*cycling* modality, in addition to correctly determine the intervals within the pedaling cycle in which each muscle is recruited, it is therefore necessary to dynamically modulate the pulse parameters (amplitude, width and frequency) to create a synergistic contraction between the different muscle groups, in such a way as to maximize the torque efficiency exerted on the pedals and delay muscle fatigue. In this scenario, the use of open-loop architectures is very limited and the need for closed-loop control strategies emerges (Melo et al., 2015).

In response to these restrictions and in addition to promoting synchronicity with functional activities, electrical stimulation systems are therefore encouraged to be designed

with a closed-loop architecture, which improves stimulus efficiency, as pulse parameters (frequency, pulse width and intensity) can be dynamically changed (Melo et al., 2015; Cousin; Duenas; Dixon, 2021). Furthermore, given the need for higher energy pulses, as deeper fibers are required for contraction, the stimulation system must have a high power capacity in order to develop functional activities for longer periods and allow less responsive individuals to stimulation to initiate functional activities assisted by FES (Guimarães et al., 2016; Bellman et al., 2017).

3 FES-cycling System

3.1 Introduction

The literature suggests Functional Electrical Stimulation (FES) systems to have their pulse parameters (frequency, width and amplitude) undergoing changes dynamically, especially the reduce the rapid muscle fatigue and maximize muscle tension during FES-assisted exercises (Ibitoye et al., 2016; Fattal et al., 2018; Maffiuletti, 2010). Furthermore, many functional activities require distinct muscle groups to be activated synergistically to assist in the reproduction of the functional movement. For FES-*cycling*, different combinations of muscle groups can be electrically evoked to perform the pedaling activity. Among these strategies, stimulation of the *quadriceps*, *hamstrings*, *tibialis anterior*, *gastrocnemius* and *gluteus* muscles is considered (Guimarães et al., 2016; Coste; Wolf, 2018; Galea et al., 2013; Ibitoye et al., 2016). These characteristics emphasize the need for the ES systems to have multiple channels and to able to modulate the electrical stimulation pulses according to the physiological and functional needs (Bellman et al., 2016).

Considering the need for the technological development of FES-assisted devices, a miniaturized *Programmable Electrical Stimulation System* was conceptualized during the author's master's studies aiming to create a device to be explored in FES-assisted activities and for Neuromuscular Electrical Stimulation (NMES) purposes (Coelho-Magalhães, Tiago, 2018). The device was designed to be connected to various sensors and to perform different stimulation strategies to meet the current research needs on FES-assisted activities, including cycling and walking. During the course of that research, a constant-current ES topology for a prototype with a 3-channel architecture was first developed. Later, in the current work, the topology was improved and the ES evolved into an 8-channel system, which was validated in FES-assisted cycling sessions with a person with paraplegia.

Even though the theoretical detailing of the system is necessary and of great scientific value, one of the main contributions of this work is not restricted to presenting the system's topology and architectures itself, but making the entire FES-*cycling* system an open-source project, including hardware, firmware, software and mechanical designs that will allow other researchers to study and modify the design for any purpose. Information on how to download the project files are available in Appendix B.

This section aims to present the proprietary 8-channel *High-Capacity Functional Electrical Stimulation* (HCFES) system developed and discuss its validation during FES-*cycling* sessions with a participant with complete paraplegia. A discussion on the cadence tracking algorithm is explored. Some mechanical aspects of the tricycle (*trike*) used during

the experiments are also documented.

To facilitate the documentation of the intervention protocol and to better discuss the impact on BMD and body composition (BC) obtained with the volunteer as result of 2 years of cycling sessions, the case report will be addressed separately in Chapter 5.

3.2 Material and methods

3.2.1 Proprietary Electrical Stimulation System

3.2.1.1 Hardware

Figure 3 illustrates the proposed architecture for the 8-channel HCFES system.

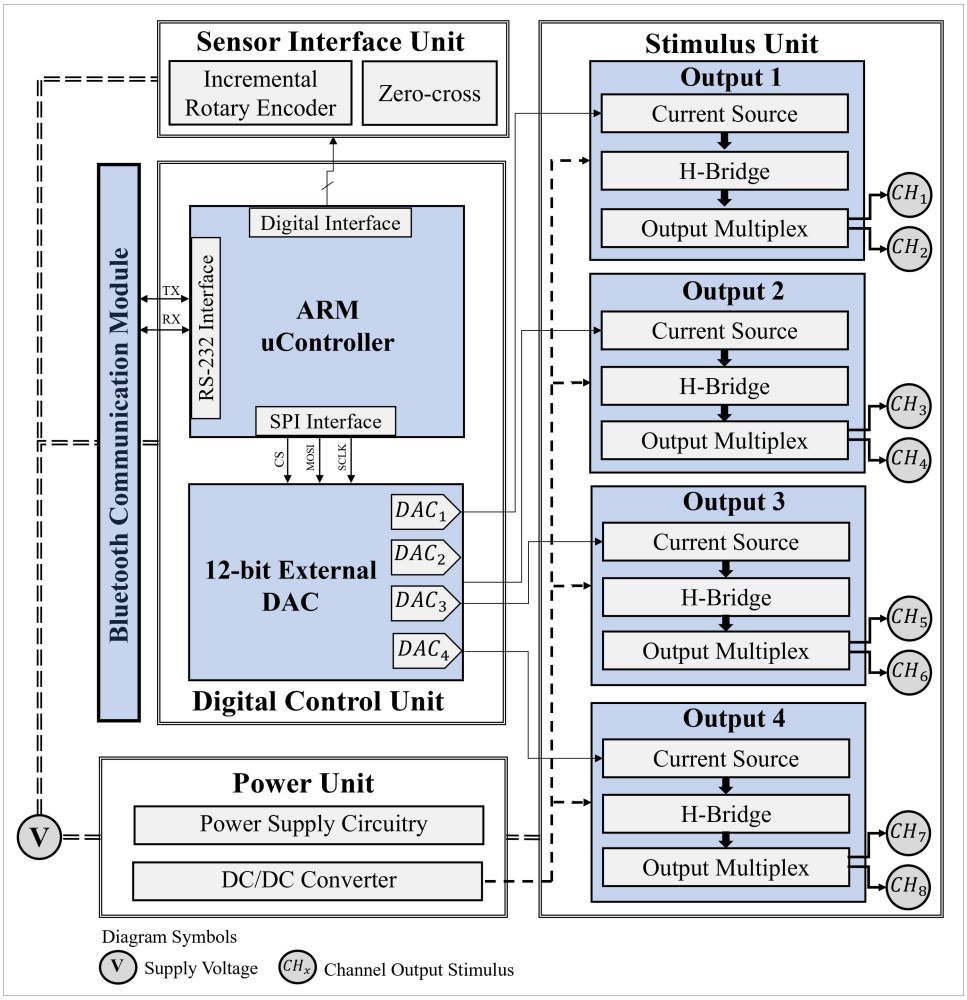

Figure 3 – Proprietary 8-channel HCFES system architecture consisted by a Digital Control Unit (DCU), a Communication Unit (CU), Power Supply Unit (PSU), Sensor Interface Unit (SIU) and Stimulation Unit (SU)

The *Digital Control Unit* (DCU) is responsible for the HCFES system resource management and is based on an ARM®Cortex-M7 Microcontroller Unit (MCU) that features high processing capacity and low power consumption. These characteristics

meet the requirements for data processing, sensor interfacing, communication and power consumption of the proposed ES system.

The MCU communicates with an external 12-bit Digital to Analog Converter (DAC) through a Serial Peripheral Interface (SPI). The DAC Intergrated Circuit (IC) can output four independent analog voltage signals (see DAC_x in Figure 3) which are used as reference for the current source ES output circuit. By varying the DAC output signals over time for each of the output channels, the amplitude of the stimulation pulses can therefore be modulated. Furthermore, different pulse waveform can be created if needed.

The DCU can also be connected to different type of sensors, including encoders and IMUs. Finally, data can be sent to an external platform through the *Bluetooth* communication interface for online and offline data processing.

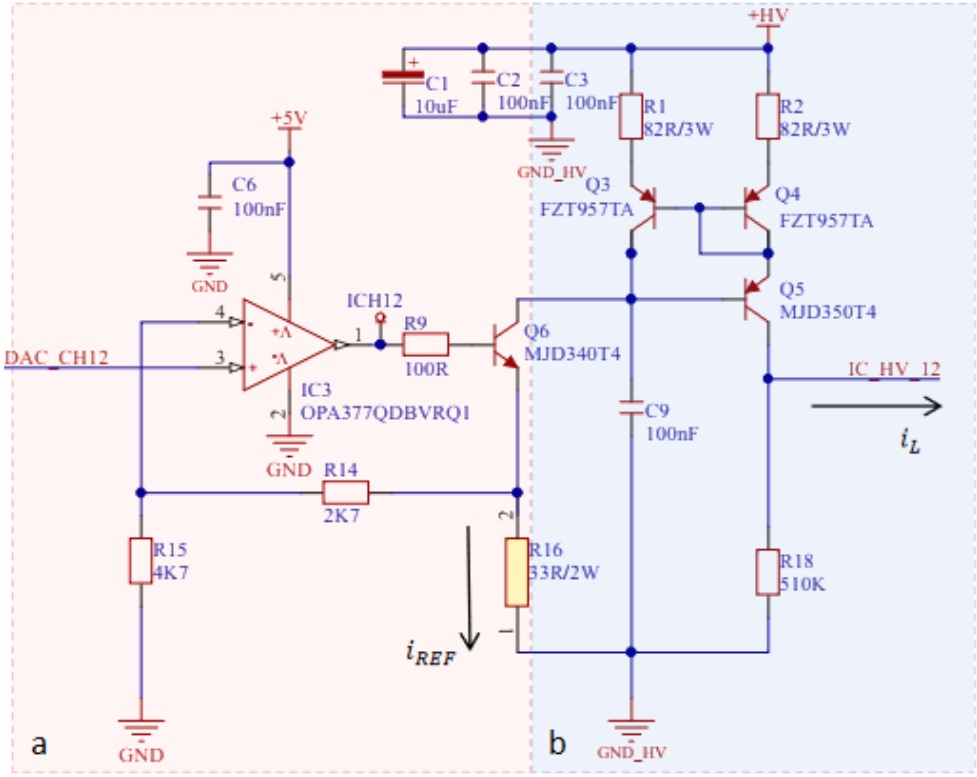

Figure 4 – (a) Voltage-current converter with controlled gain and (b) Wilson current-mirror. The operational amplifier (**IC3**) in association with **Q6** and **R16** converts the external DAC output voltage signal (**DAC_CH12**) into a current signal (i_{REF}); the Wilson current mirror controls the i_L current amplitude to remain constant regardless of impedance variations.

The *Stimulation Unit* (SU) presents distributed power flow through independent constant-current sources associated with the different stimulation channels. Each stimulation output consists of a voltage-current converter, a Wilson current mirror and an *H-bridge* circuit (Figure 4). The output signals generated from the external DAC feed the SU and are converted into reference currents (i_{REF}) for the Wilson current mirror, which

in turn guarantees the maintenance of the amplitude of the electrical stimulation pulse current (i_L) against the expected load variations during ES application.

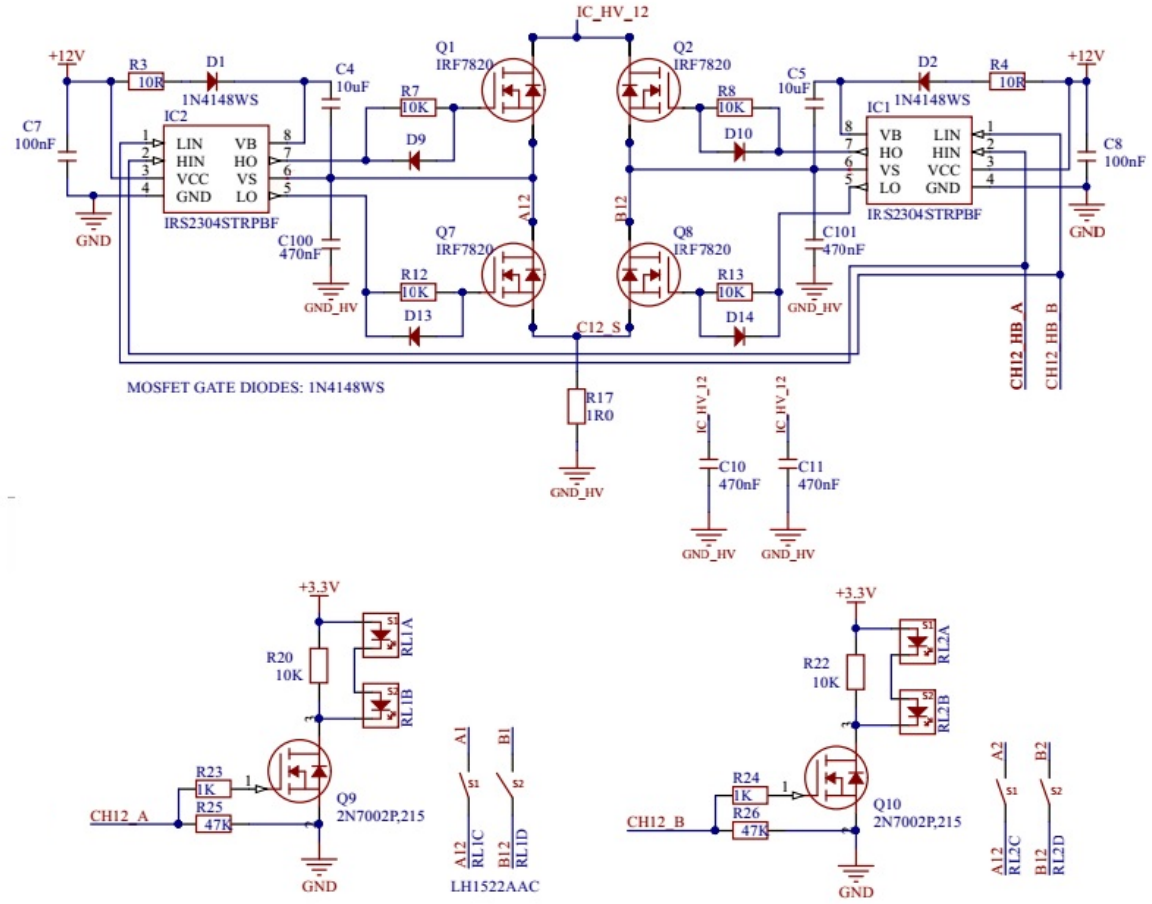

Figure 5 – H-bridge circuit and circuitry for activating channels A and B of one of the four independent output channels. The net **IC_HV_12** corresponds to the output current signal of the Wilson current-mirror (see Figure 4). Two independent solid-state relays can be activated but not simultaneously. Capacitors C10, C11, C100 and C101 are optional.

Figure 5 presents the H-bridge and output circuitry of channel one. The output circuit of the other channels are equivalent. The proposed topology employs four power MOSFETs controlled by high performance half-bridge driver integrated circuits that allows the pulse current to flow through the load in both directions to generate biphasic pulses. It is important to highlight that there are four multiplexed stimulation outputs which allow eight channels to be created (see Figure 3). The multiplexing feature is performed by independent solid-state relays ($LH1522AAC$) and its associated circuitry. The two multiplexed channels of each output circuit cannot be activated simultaneously, however.

The *Power Supply Unit* (PSU) DC/DC converter provides the high-output voltage necessary to achieve pulse amplitudes up to 150mA. A 50W DC/DC module A50-120Y (American Power Design®, Windham, NH, USA)[2] was employed in the latest ES system

project. The small size, wide input, and excellent regulation of this converter suited the project high performance requirements.

The *Sensor Interface Unit* (SIU) can be programmed to process data from open-closed mechanical switches, Force Sensitive Resistors (FSR), Inertial Measurement Unit (IMU), Electrical Impedance Myography (EIM) and Electromyography (EMG) modules. In regard to FES-assisted cycling, IMUs can be employed as an alternative to the encoders as they can describe body orientation and detect events associated to joint angles. This feature facilitates installation and eliminates mechanical modifications required for systems using encoders (Sijobert et al., 2019).

Finally, the electrical schematics and the Printed Circuit Board (PCB) lay-out of the HCFES project was developed using the Altium Designer software v18.1.3 (Altium Limited, San Diego, CA, USA).

3.2.1.2 Firmware and Software Interface

The firmware architecture was designed to meet the real-time requirements and to make the most of hardware resources. Firmware libraries were created for the ES management and for the functions of the peripheral units, which can also be used in future applications. For this experiment, a custom firmware was developed in the STM32Cube Integrated Development Environment (IDE) v1.8.0 (STMicroelectronics, Geneva, Switzerland).

An Android mobile application (*app*) was developed in the Android Studio software platform (v4.1.3) to set and modify the pulse parameters of the stimulation channels during cycling sessions. The *app* was designed to collect and save data for offline processing which includes the configuration for each channel (ON/OFF, start angle, finish angle, frequency, pulse width and amplitude); also, timestamp, cadence reference value, actual angle and actual speed.

The HCFES can operate in three different modes which are selected through the *app*: (1) *Manual*, (2) *Automatic* and (3) *Control*. In the *Manual* mode, the ES pulses are fired with the predefined parameters (amplitude, width and frequency) only and are independent of the configured stimulation range. The pulse parameters can be manually updated at any time, however. This operation mode is mainly for NMES purposes. For *Automatic* operation, pulses are triggered according to the stimulation range of each channel and no automatic modulation of parameters is performed unless changed manually. This operating mode is suitable for cycling sessions where a manual control of the stimulation pulse parameters is preffered. The third mode (*Control*) is intended for FES-*cycling* for applications in which the cadence-tracking feature is activated and the ES are modulated

[2] A50 Series 50.0 Watt: https://www.apowerdesign.com/products/A/A50/

by a controller.

The *app* was also designed to exchange data with the HCFES system via *Bluetooth* (@10Hz) during cycling sessions. The collected information is saved in a local database for posterior processing.

3.2.1.3 Cadence Tracking Control Strategy

In the *Control* operating mode, the current amplitude was modulated by a Proportional-Integral (PI) controller with the intention of tracking a predefined cadence. The amplitude was limited to 100mA. Its diagram is illustrated in Figure 6. The cadence error was calculated as the difference between the desired crank angular velocity (reference value) and the measured crank angular velocity.

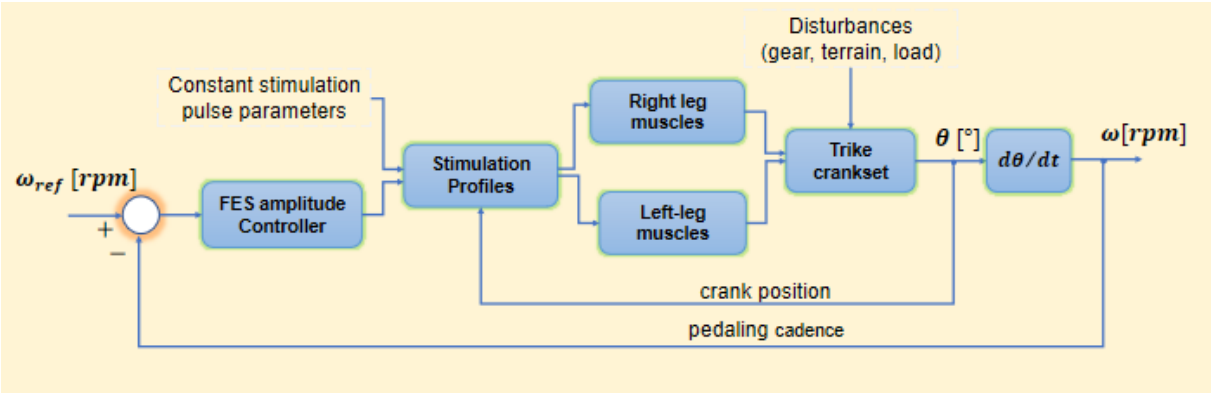

Figure 6 – The control strategy implemented for FES-*cycling* cadence tracking.

The control algorithm increases or decreases the pulse amplitude simultaneously for all channels starting from initial preset values and was executed by the MCU at 10Hz. This approach was defined to maintain a constant relationship between the activation parameters of each channel/muscle. Although frequency and pulse width are held constant by the controller algorithm, it is possible to change these parameters manually and for each channel individually through the mobile application even during operation.

Even though the FES-*cycling* is a nonlinear time-varying system due to the physiological aspects of the rider, a PI controller was employed and the parameters were heuristic defined. The proportional gain was empirically adjusted to $K_p = 0.45k_1$, where k_1 was set to a constant value corresponding to 1mA at the controller output. The integral gain was adjusted to reach a minimum error in the steady state and was finally defined as $K_i = 0.34k_1$.

The stimulation control output signal (pulse amplitude) is composed of a portion proportional ($m_p(n)$) to the sampled cadence error $e(n)$ and another proportional to the integral ($m_i(n)$) of the sampled cadence error as defined in Equation 3.1:

$$u_x(n) = p_x(\theta) \cdot [m_p(n) + m_i(n)], n \in \mathbb{Z} \tag{3.1}$$

where $u_x(n)$ is the control signal for muscle $x = \{VL + RF, VM, HAM\}$; θ is the crankset position; and $p_x(\theta)$ represents the phase control defined as:

$$p_x(\theta) = \begin{cases} 1, \ \theta_x^{start} \leqslant \theta \leqslant \theta_x^{end} \\ 0, \ otherwise \end{cases} \tag{3.2}$$

where $\theta_x^{end} - \theta_x^{start}$ correspond to the stimulation interval of muscle x. The portion proportional to the cadence error can be written as:

$$m_p(n) = K_p \cdot e(n), n \in \mathbb{Z} \tag{3.3}$$

and the portion proportional to the integral of the cadence error can be approximately written as

$$m_i(n) = m_i(n-1) + K_i \cdot e(n-1), n \in \mathbb{Z} \tag{3.4}$$

In order to evaluate the controller performance, a methodology for cadence tracking was proposed. A predefined cadence sequence was set starting at 25rpm for 60 seconds, then rising to 38rpm for 30 seconds, rising again to 42rpm and maintaining for 60 seconds. Then, down to 38rpm for 30 seconds and finishing at 25rpm for 60 additional seconds. A one-sample Wilcoxon signed-rank test was performed to determine whether the median of the whole pedaling cycle was equal to each of the cadences defined in the protocol.

3.2.1.4 Bench Tests

Detailed bench tests to assess the capacity and performance of the 3-channel system have been discussed in the author's master's dissertation (Coelho-Magalhães, Tiago, 2018). As the topology was already validated, the author understood there was no need for repeat the following bench tests: load variation, linearity and waveform variation. Still, the maximum current intensity, channel independence and ES triggering tests were performed. The pulse measurement was obtained as the potential difference over a 500Ω load using the oscilloscope's mathematical subtraction operation ($M = ch_1 - ch_2$).

In addition, a typical trapezoidal waveform with a ramping up and ramping down pattern was implemented via firmware to prevent sudden contractions and to achieve more physiological evoked responses. Both the rise and fall ramps represent fixed (but adjustable) percentages of the configured stimulation range. The pulse pattern was measured and validated using the Logic Pro 16 logic analyzer (Saleae, San Francisco, CA, US) at $1.56MS/s$ (samples per second).

3.2.2 Trike and Biomechanical Aspects

Recent research has discussed the methodology and stimulation protocols required for FES-assisted cycling, including the mechanical specifications of the tricycle (*trike*)

(Guimarães et al., 2016; Fattal et al., 2018; Metani et al., 2017). Based on these works, a recumbent tadpole tricycle (Trike Full Suspension, *Arttrike*, Porto Alegre, RS, Brazil) with two front wheel and one rear wheels was selected for the project. Tadpole *trikes* offer greater stability when compared to delta-shaped tricycles (one front wheel and two rear wheels). To support the legs, a pedal with calf support was used that maintains the ankle joint at 90° (HASE® Bikers, Waltrop, Germany) and restrict the leg movement to the sagittal plane. A foam layer protected the legs from calf support direct contact. The tricycle and its main components are shown in Figure 7.

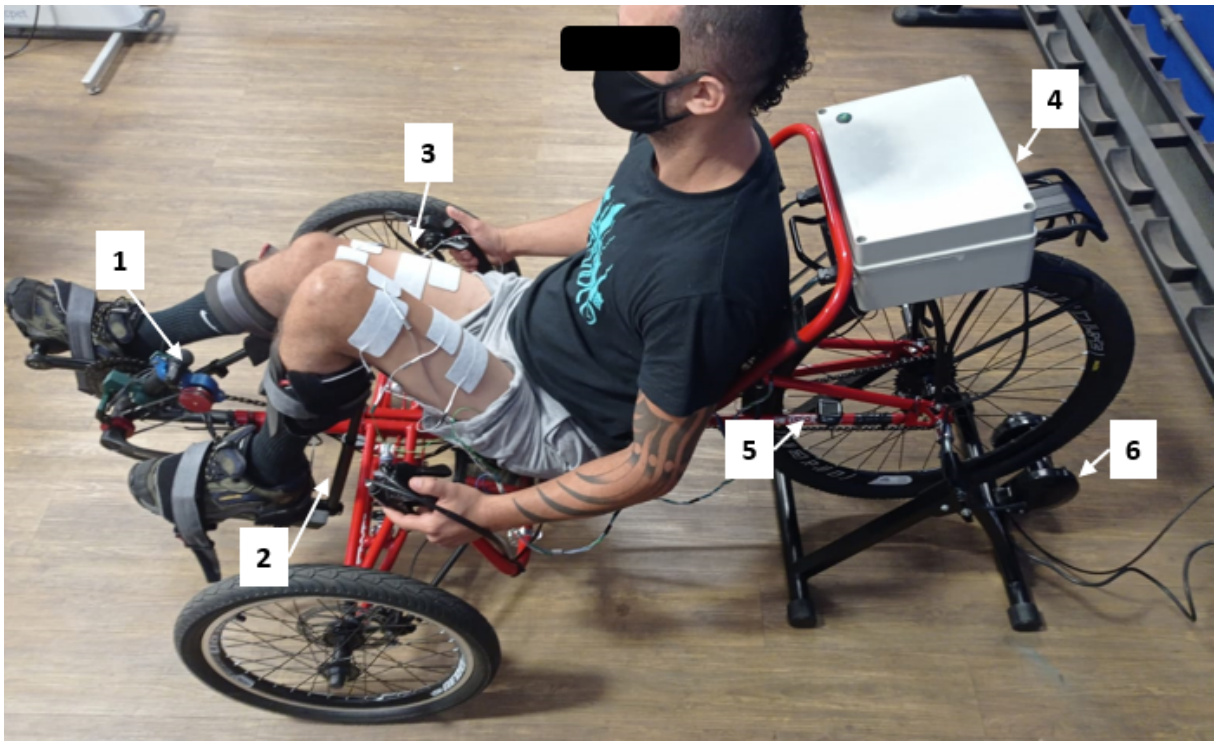

Figure 7 – *Trike* and its main components: (1) encoder, (2) calf support, (3) surface electrodes, (4) proprietary pacing system, (5) speed sensor, (6) training roller.

The cycling sessions were supposed to happen fixed on a passive cycling trainer (GTSM1, São Paulo, SP, Brazil) or overground. When stationary, a passive magnetic training stand allowed the configuration of different cycling loads to adjust the pedaling resistance to the incremental training program. Also, the gear ratio of the *trike* was empolyed for the same purposes. The disturbance brought by the load variation and gear ratio variations is a condition of fundamental importance for the study of control techniques, which would require the modulation of the ES pulse parameters to overcome the muscle fatigue and track desired cadences in different scenarios.

Although a specific application for FES-*cycling* is addressed in this work, the system can be connected to different sensors, such as the Inertial Measurement Unit (IMU), which would allow the development of other studies, such as the identification of events for the gait (Coelho-Magalhães, Tiago, 2018). In this work, despite the possibility of using IMUs,

which would allow the identification of events in the FES-*cycling* modality (Guillou et al., 2021; Sijobert et al., 2019) an encoder was used to determine the cycling angle and a belt transmission technique was employed to measure the crank angle. Figure 8 illustrates the designed mechanism, including the mechanical drawings of each part. Two pulleys of the same size (Figure 8.3 and Figure 8.4) were connected by a timing belt (model Schneider 2048 MXL-80256 06) where a driver pulley was associated with the trike crank and a driven pulley was integrated into a rotary incremental encoder (model LPD3806-360BM-G5-24C). The driver pulley had a rectangular span for zero-crossing detection (Figure 8.2).

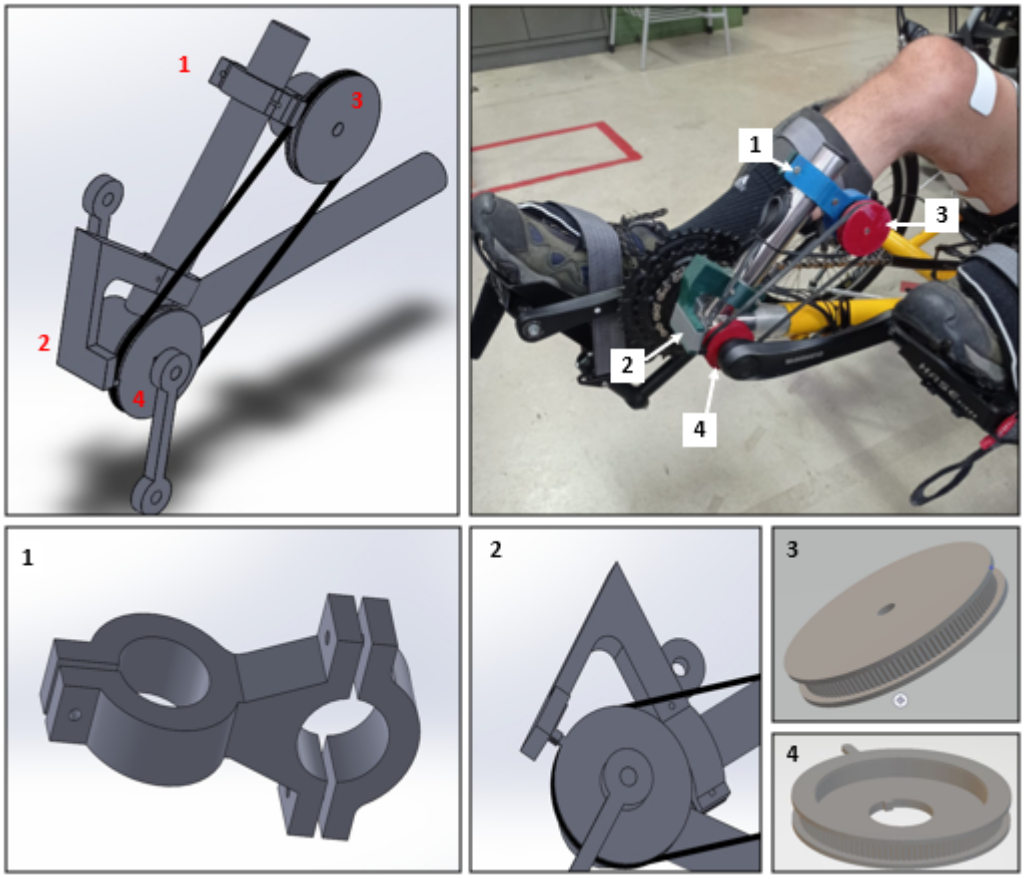

Figure 8 – Belt drive technique to measure crank angle. Crankset positioned at 0°. (1) Encoder support part; (2) 0° detector module; (3) driven pulley associated with the encoder; (4) drive pulley associated with the main shaft.

The stimulation phase for each of the muscles selected in the pedaling cycle is defined based on the individual's biomechanics in relation to the crank. The mechanical optimization of the trike is, therefore, essential for obtaining an adequate cadence and for maximizing the power produced by the muscular contraction, and this procedure must be performed for each individual individually. If the biomechanical settings are not in agreement, the coordination of leg extension and flexion will not result in an efficient pedaling, which is suggested as one of the factors that most impact the low power production during the FES-*cycling* exercises for SCI-individuals (Ragnarsson et al., 2008).

The tricycle used in the project allows the modification of the distance between the crank and the cyclist. In this sense, it was of interest to evaluate the most appropriate distance for the volunteer in respect to his biomechanical characteristics, i.e., extension and flexion limits, which may be limited due to spasticity.

Raven and Freudenstein methods were used to determine the equations of a four-bar mechanism and assess the amplitude of the variables of interest (Mata et al., 2016). Knee (θ_{knee}) and hip (θ_{hip}) angle variations were calculated according to volunteer's biomechanics settings and to determine the most suitable length between the crank and the hip of the volunteer. The procedure used to determine the respective angles is presented in Appendix A and a MATLAB application using the App Designer (MATLAB R2016a) was created for a dynamical analysis of the possible mechanical configurations of the tryke in respect to the volunteer biomechanics.

3.2.3 Experimental Setup

One participant (38 years, male) with complete Spinal Cord Injury (AIS A, T8) was recruited for this study and signed a written informed consent. Patient history and physical assessment data are detailed in Chapter 5. The research was approved by the UFMG local Ethical Committee (CAAE: 30989620.6.0000.5149, Ethical Approval number 4.190.128) in agreement with the Declaration of Helsinki.

Vastus medialis (VM), vastus lateralis and rectus femoris (VL+RF), and hamstrings (HAM) muscles were stimulated during pedaling sessions. Rectangular self-adhesive surface electrodes (9x5cm, Arktus®, Santa Tereza do Oeste, PR, Brazil) were used as following settings: (1) an electrode positioned 3cm above the upper edge of the patella on the distal motor point of the VM muscle; and another electrode on the proximal motor point of the same muscle; (2) an electrode positioned 3cm above the upper edge of the patella on the distal motor point of the VL muscle and another electrode on the proximal motor point of the RF muscle; (3) one electrode placed 5cm above the popliteal fossa and the other 15-20cm above the popliteal fossa for the HAM stimulation. For a illustrated view of the electrode positioning, refer to Figure 9.

Rectangular and symmetrical biphasic pulses with amplitude limited to 100mA, pulse width of 500μs-600μs, and frequency at 35Hz were employed during the sessions. In order to evaluate the cycling performance, the initial pulse amplitude parameters were defined for the left side as RF+VL=50mA, VM=30mA, and HAM=40mA; for the right side: acRF+VL=45mA, acVM=25mA, and acHAM=35mA.

The stimulation pattern for muscle activation is presented in Figure 10. Right and left *hamstring* (HAM) are shown as the blue grids; right and left *vastus medialis* (VM) as the horizontal and vertical blue lines respectively; and *vastus lateralis* (VL) + *rectus*

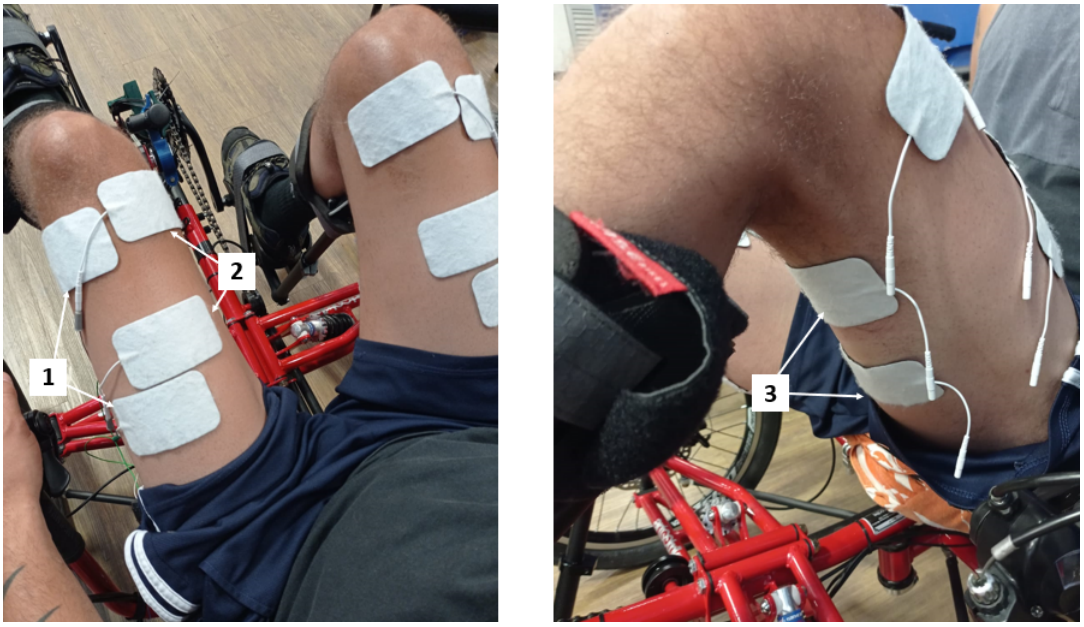

Figure 9 – Electrode positioning: (1) *vastus lateralis* (VL) + *rectus femoris* (RF); (2) *vastus medialis* (VM); (3) *hamstring* (HAM).

femoris (RF) as the dotted squares. Zero angle is when the crank arm is positioned horizontally, the right leg extended.

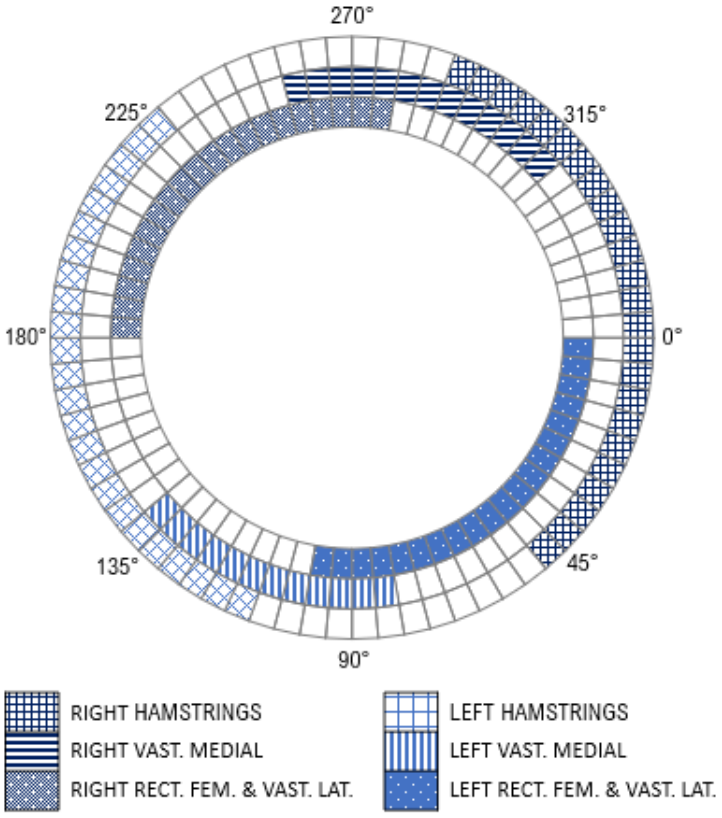

Figure 10 – Final stimulation profiles showing the start and end angles for each muscle within a pedaling cycle.

3.3 Results

3.3.1 Hardware

This subsection presents the 4-layer layout of the PCB (Figure 11) and the 3D visualization (Figure 12) of the *High-Capacity Functional Electrical Stimulation* (HCFES) system that was developed in this work. Board dimensions are 10.6x18.5cm.

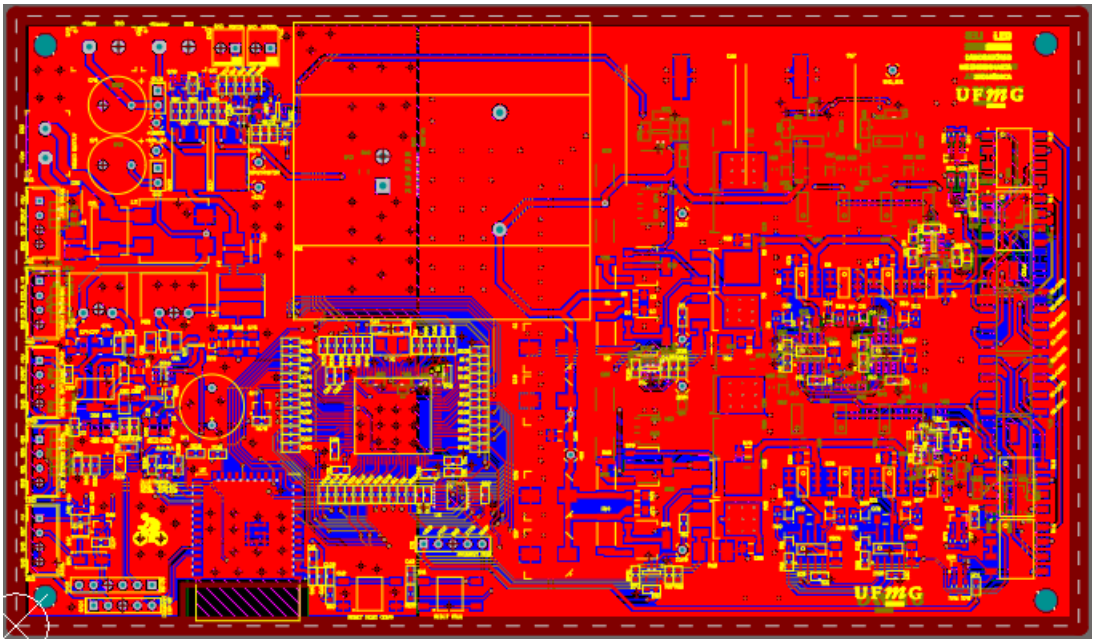

Figure 11 – Top view of the developed Printed Circuit Board.

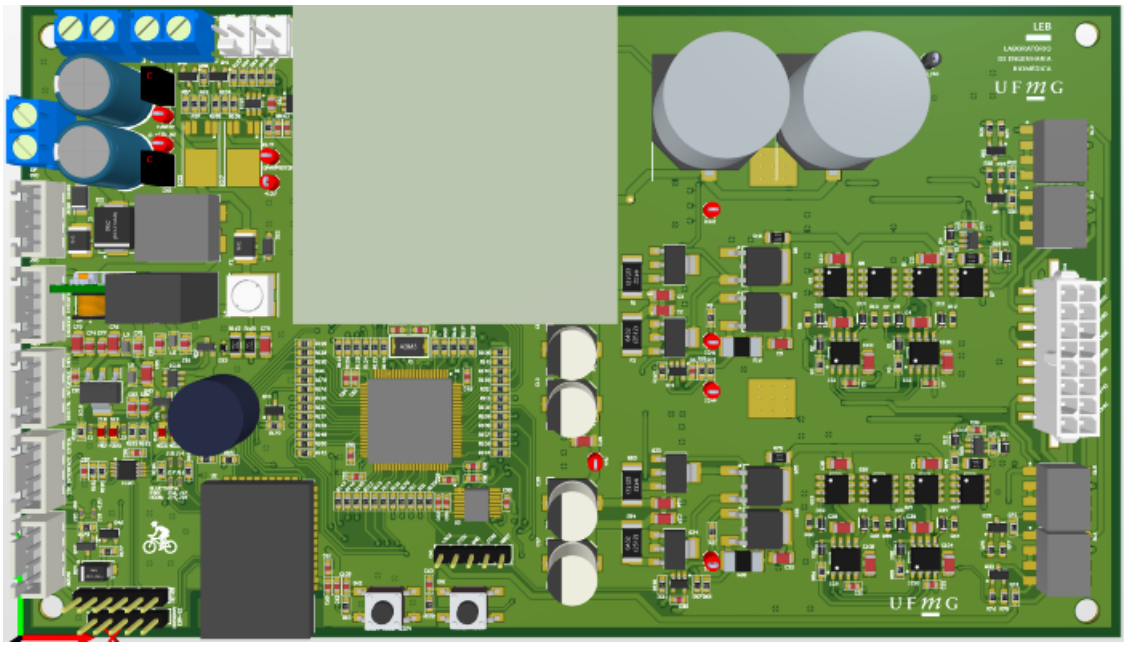

Figure 12 – 3D visualization of the developed Printed Circuit Board.

The scheme for measuring the biphasic ES pulses generated by the HCFES is

demonstrated in Figure 12. The oscilloscope is configured for the MATH mode (*ch1* - *ch2*).

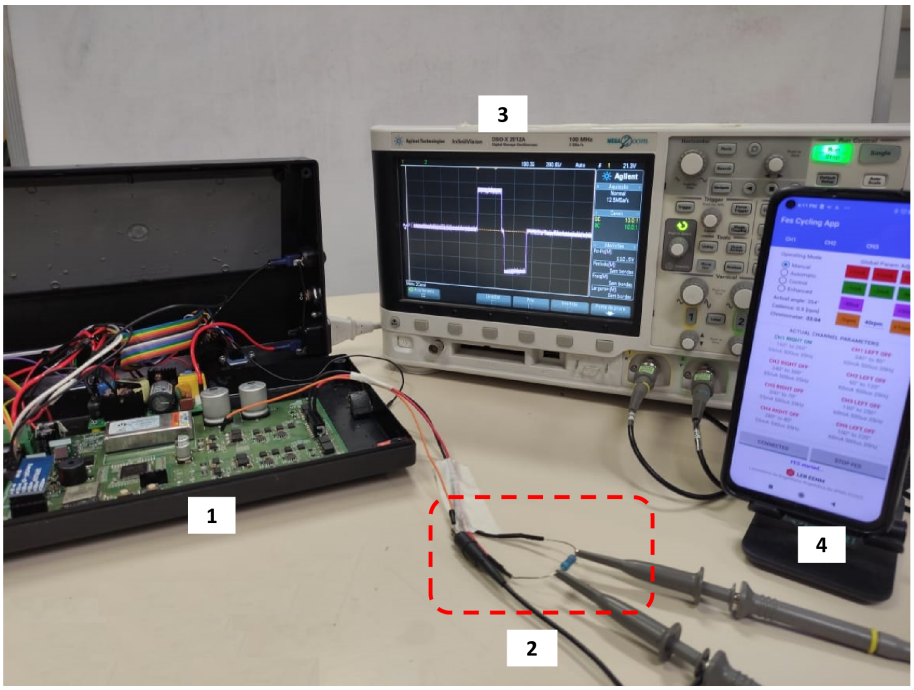

(a) Biphasic rectangular pulse at 500μs and 55mA

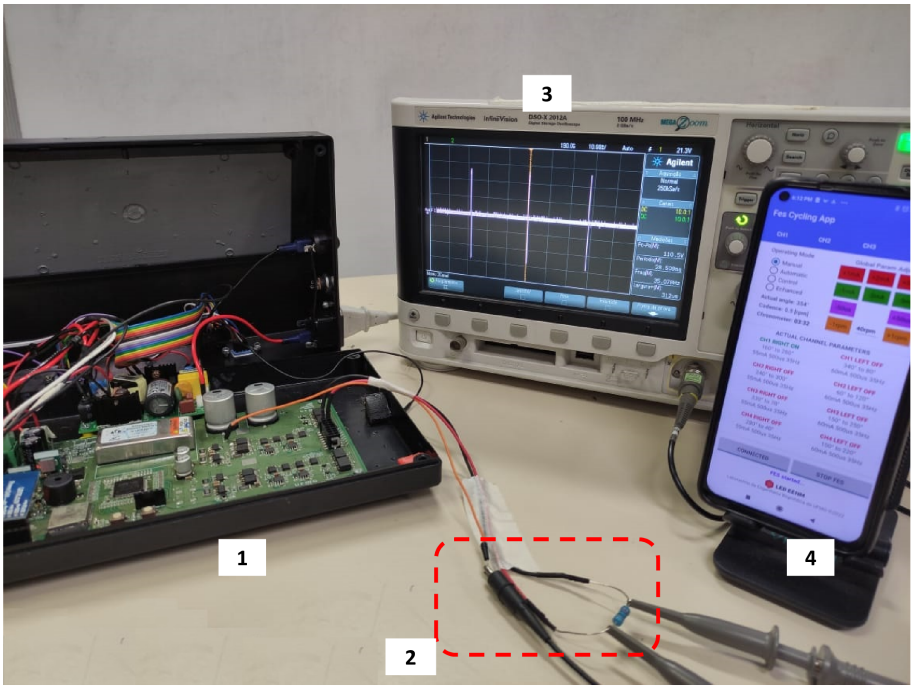

(b) Pulses @35Hz and 55mA.

Figure 12 – HCFES in manual mode generating biphasic ES pulses. 1) HCFES system; 2) differential measurement over a 500Ω load; 3) Oscilloscope screen; 4) Android app.

Figure 13 shows the power capacity of the HCFES device to reach pulse amplitudes of up to 150mA, pulse widths of up to 1000μ, at frequencies of up to 100Hz.

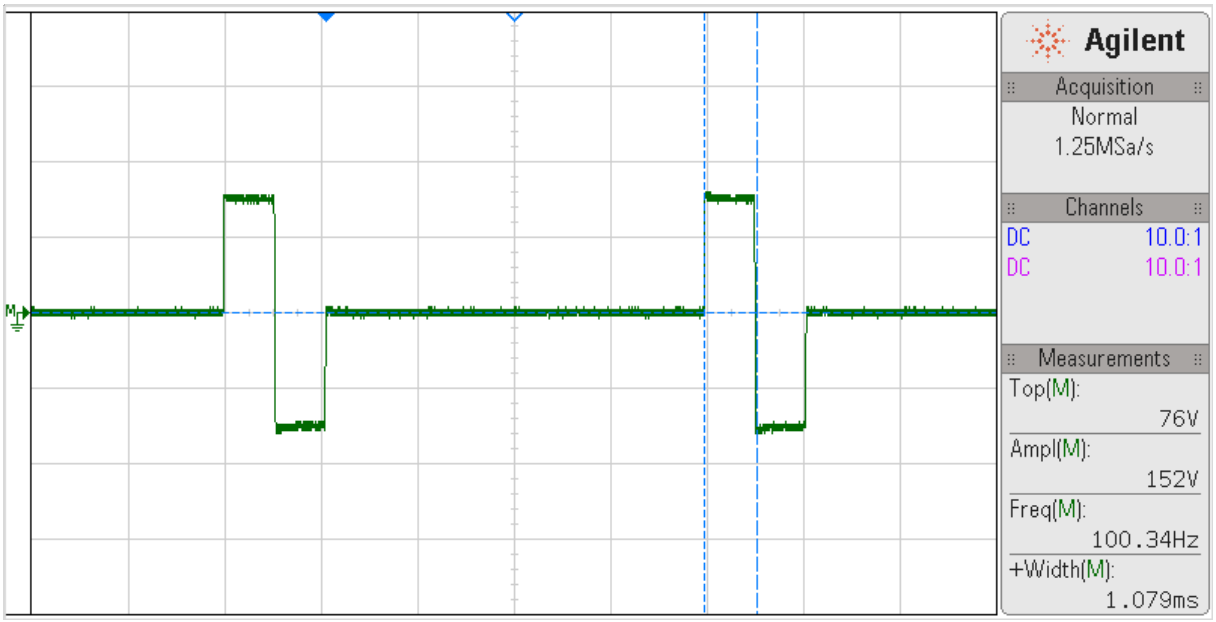

Figure 13 – Biphasic pulse waveform at a frequency of 100Hz, width of 1000μ and current amplitude of 150mA for a load of 500Ω. The mark on the right highlights the amplitude and frequency measurements and the mark below, in the center, the oscilloscope's time/div setting.

Figure 14 illustrates the pulses being triggered in synchronism with the cycling activity for three different channels simultaneously and at different frequencies. The ramping up/down stimulation pattern is also demonstrated.

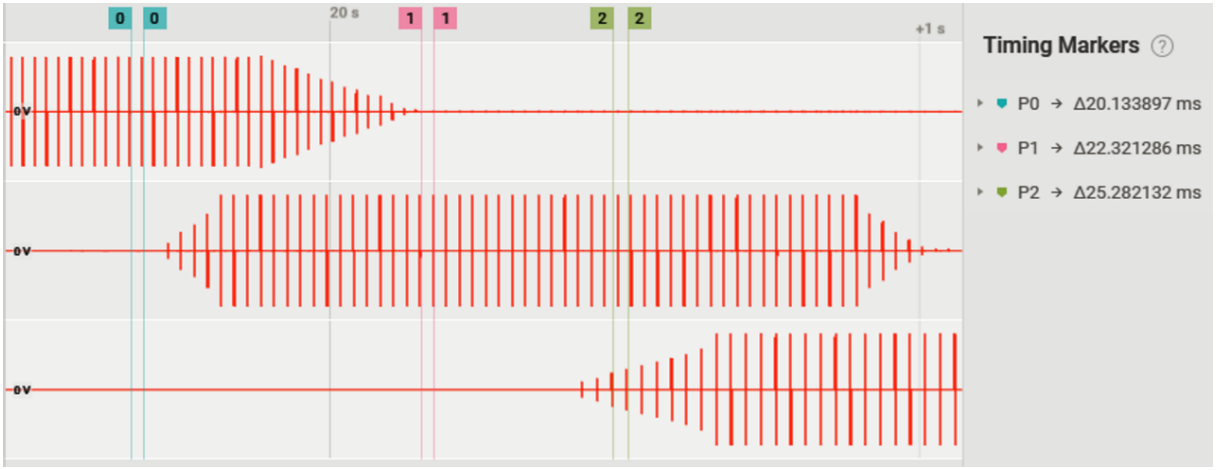

Figure 14 – Triggering of biphasic and rectangular pulses in different segments of the pedaling cycle. Channel 1 (upper) is at a frequency of 50Hz; channel 2 (middle) at 45Hz; channel 3 (lower) at 40Hz. The ascent and descent ramps were implemented via firmware to promote a contraction with more physiological and less sudden characteristics.

The measurements performed in Figure 14 evidences that the specified DC/DC converter supported the demand for the three channels stimulating simultaneously configured with different parameters of frequency, current intensity and pulse width.

3.3.2 Mobile Application

The mobile application (Android) developed to interface the HCFES is shown in Figure 15.

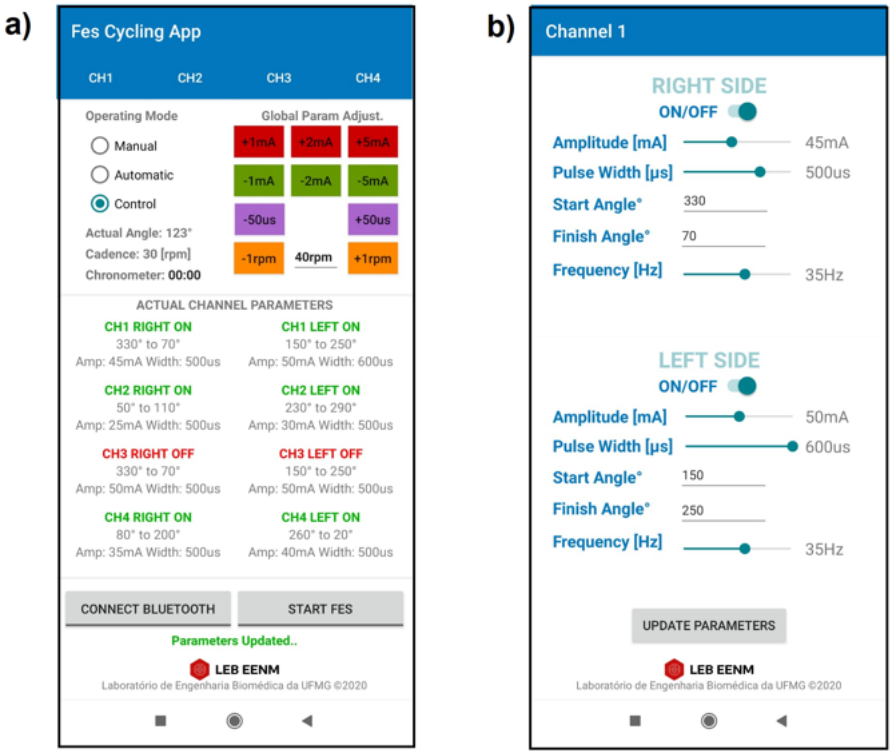

Figure 15 – Proprietary mobile application developed for system configuration. (a) Main screen displaying real-time data and parameters for Manual, Automatic and Control modes; (b) Channel screen for parameter configuration (channel 1).

The main interface gives the option to select the muscle groups needed for cycling along with the start and end angles at which they are activated, i.e., the stimulation interval. The *app* allows the pulse parameters to be set and modified online during cycling sessions. There are buttons available for global parameters adjustment in the main screen to increase or decrease current amplitude, pulse width and reference cadence (Figure 15.a). Individual channel interfaces configures the parameters for right and left sides (Figure 15.b). Three different modes of operation can be selected through the application (see *Operating Mode* in Figure 15.a): (1) *Manual*, for NMES; (2) *Automatic*, for FES-assisted cycling with automatic triggering of stimulation pulses but without any automatic modulation of parameters unless changed manually; (3) *Control*, for FES-*cycling* with cadence-tracking feature activated.

When using automatic mode, parameters are changed manually by adjusting the global parameters (increase/decrease in amplitude and pulse width) or individually, as each channel has an individual screen to set parameters for the right and left sides. In control mode, parameters are automatically adjusted so that the pedaling cadence tracks the set reference value (setpoint). The main interface allows instant adjustment of pulse parameters manually during the session and, if the control mode is selected, the reference cadence can be set and changed.

Figure 16 illustrates the database created which includes time, reference cadence (*setpoint*), current angle (*angle*), current cadence (*speed*), the state of each channel ($ch_{XY}state$) , start ($ch_{XY}startangle$) and end ($ch_{XY}finishangle$) angle of stimulation, trigger frequency ($ch_{XY}freq$), pulse width ($ch_{XY}pw$) and amplitude ($ch_{XY}amp$). In the parameter nomenclature, "X" corresponds to the channel number, where $X = \{1, 2, 3, 4\}$; and "Y" indicates whether the leg is left or right, where $Y = \{l, r\}$.

3.3.3 Cadence Tracking and Performance Results

Cadence tracking results are illustrated in Figure 17. A moving-average filter with a window size of 20 was used for a better visual inspection. The cadence control strategy evidenced that the system was able to follow the predefined cadences. For 25rpm, the measured reference was 24.84 ± 2.5 ($p = 0.060$); for 38rpm, the measured reference was 37.86 ± 2.23 ($p = 0.002$); and for 42rpm, the measured reference was 41.93 ± 2.34 ($p = 0.208$). An online video is available for demonstration[3].

Regarding functional outcomes, the volunteer's pedaling performance increased from approximately 20 seconds to 45 minutes after the 5^{th} month on the cycling trainer. In this period, in his best performance, he covered 5,349m with an average speed of 7.1Km/h and a maximum speed of 8.0km/h. Since the experiments were started, pedaling time and distance were evaluated as primary functional parameters which are related to the load imposed on the pedaling. An improvement in distance and pedaling duration was observed after the cadence control was implemented. The functional and performance results, however, will be better addressed in Chapter 5.

[3] Cadence-tracking protocol: https://youtu.be/6cgDhPWPzII

	time	setpoint	angle	speed	ch1rstate	ch1rstartangle	ch1rfinishangle	ch1rfreq	ch1rpw	ch1ramp	ch1lstate	ch1lstartangle	ch1lf
	Filtro	Filtro	Filtro	Filtro	Filtro	Filtro	Filtro	Filtro	Filtro	Filtro	Filtro	Filtro	Filtro
13885	Tue Aug 31 08:41:04 ...	38	17	35.59	1	200	300	35	600	70	1	20	120
13886	Tue Aug 31 08:41:05 ...	38	40	37.95	1	200	300	35	600	69	1	20	120
13887	Tue Aug 31 08:41:05 ...	38	63	38.19	1	200	300	35	600	68	1	20	120
13888	Tue Aug 31 08:41:05 ...	38	86	38.46	1	200	300	35	600	68	1	20	120
13889	Tue Aug 31 08:41:05 ...	38	109	38.33	1	200	300	35	600	68	1	20	120
13890	Tue Aug 31 08:41:05 ...	38	133	39.51	1	200	300	35	600	68	1	20	120
13891	Tue Aug 31 08:41:05 ...	38	156	38.83	1	200	300	35	600	68	1	20	120
13892	Tue Aug 31 08:41:05 ...	38	179	38.72	1	200	300	35	600	68	1	20	120
13893	Tue Aug 31 08:41:05 ...	38	202	38.33	1	200	300	35	600	68	1	20	120
13894	Tue Aug 31 08:41:05 ...	38	224	37.41	1	200	300	35	600	69	1	20	120
13895	Tue Aug 31 08:41:05 ...	38	247	37.58	1	200	300	35	600	69	1	20	120
13896	Tue Aug 31 08:41:06 ...	38	269	37.03	1	200	300	35	600	69	1	20	120
13897	Tue Aug 31 08:41:06 ...	38	292	37.58	1	200	300	35	600	69	1	20	120
13898	Tue Aug 31 08:41:06 ...	38	315	37.58	1	200	300	35	600	69	1	20	120
13899	Tue Aug 31 08:41:06 ...	38	338	38.19	1	200	300	35	600	68	1	20	120
13900	Tue Aug 31 08:41:06 ...	38	1	37.41	1	200	300	35	600	69	1	20	120
13901	Tue Aug 31 08:41:06 ...	38	24	36.85	1	200	300	35	600	69	1	20	120

13885 - 13902 de 38158 Ir para: 1

Figure 16 – Database from a FES-*cycling* session.

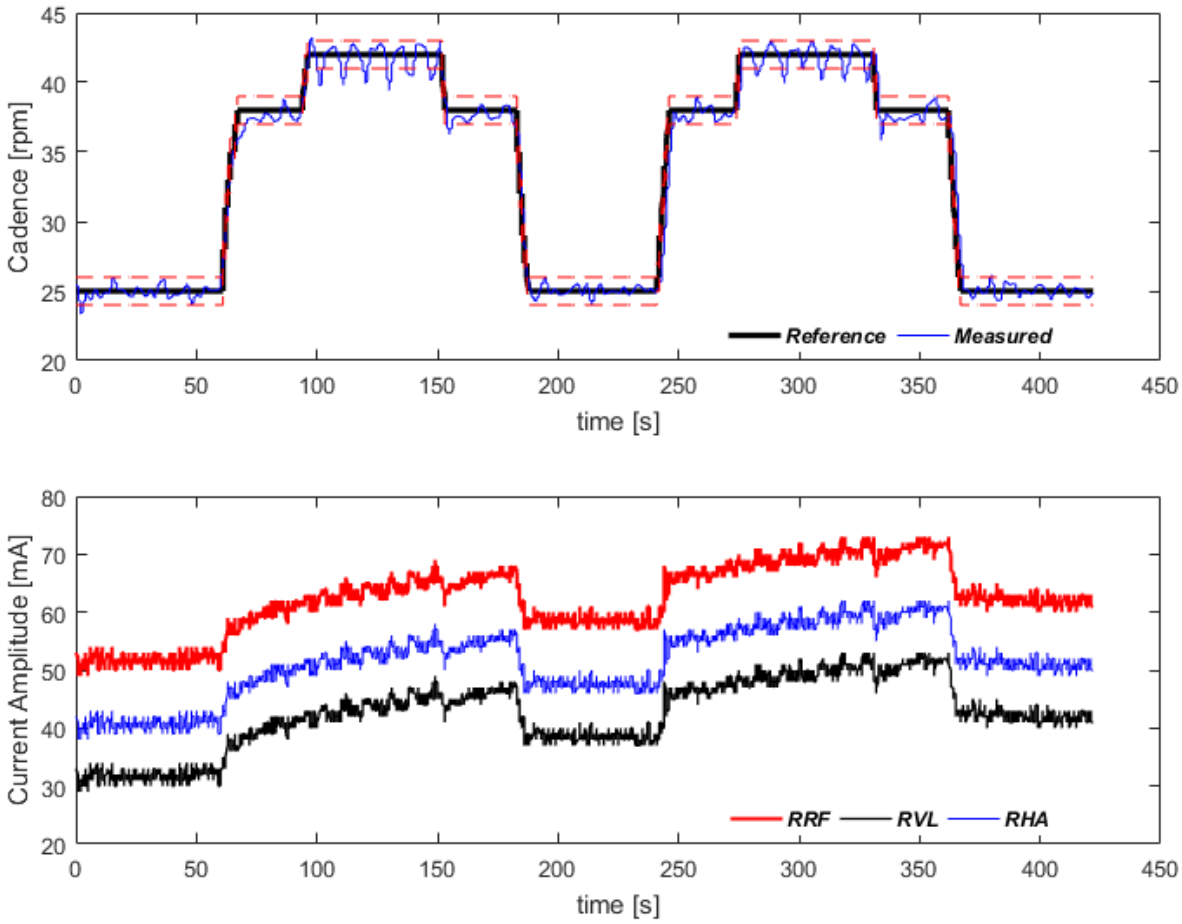

Figure 17 – Cadence tracking protocol. In the first graph, the dashed lines around the reference cadence correspond to ±1rpm. Variation in pulse amplitude for the three muscles of the right lower limb are shown in the second graph.

3.4 Discussion

Engineering research needs instrumented devices to support new developments and allow an accurate assessment of the functional modalities being performed. For the different researches that make use of FES, it is necessary devices with high power capacity and that allow the study and development of new functionalities. Often, however, researchers struggle to develop their own FES systems or find it difficult to implement their systems using commercial devices, which can limit the implementation of advanced control strategies and the possibility of connecting different types of sensors. In this sense, the results obtained from the development of the HCFES presented, including hardware, firmware and software, make it possible to overcome limitations imposed on the implementation of advanced control strategies, the possibility of connecting different types of sensors, and assisting actions that require greater power from the stimulation devices.

In addition to the electrical capabilities of the system, one of the objectives of this work is the creation of a methodology to improve the definition of stimulation parameters for the FES-*cycling* activity through Reinforcement Learning (RL) techniques. As will be presented in Chapter 4, this was only possible because of the high processing capacity of the Digital Control Unit (DCU) which was able to embed relatively-complex algorithms, including machine learning techniques.

Regarding the physiological and methodological aspects of the use of electrical stimulation, it is well known that its effectiveness depends less on controllable external factors, such as pulse parameters or the characteristics of the electrodes, and more on the individual's intrinsic anatomical and physiological properties, which determine the muscle response to electrical stimuli (Maffiuletti, 2010). As the FES cycling system was evaluated with only one volunteer, it is necessary to apply this methodology to other individuals to address which factors lead to a longer pedaling time: whether in fact they are technical aspects or whether they are more related to the responsiveness of the participant. Nevertheless, the proprietary FES cycling system and the methodologies implemented to improve functional electrical stimulation efficiency evidenced the possibility of maximizing pedaling duration for a given individual through control techniques.

The presented methodology proposed the variation of the pulse amplitude while keeping the frequency and pulse width constant. Another study addressed a similar strategy of cadence tracking using pulse width modulation instead but evidenced larger cadence oscillation and cadence error compared to our findings (Fonseca et al., 2017). It is unclear, however, whether the results obtained were better due to the way the parameters were varied or whether this was due to other factors, such as trike mechanics, stimulation system performance, individual responsiveness, or the implementation of system control.

A limitation of this study is that the training roller did not allow the consistent

setting of the resistance to the pedaling. However, the protocol took place incrementally; that is, as the volunteer managed to pedal at a certain difficulty level, the roller resistance (or the gear ratio) was increased manually through mechanical adjustments to improve the functional aspects (distance) and encourage improvement for the volunteer. Thus, it would be difficult for other researchers to compare the results with the results obtained in this study.

Another constraint is related to the adjustments of the mechanical parameters of the tricycle, which were made for one person only. It was necessary to adapt a commercial trike for the project and it was not possible to modify the seat inclination and crank height. This condition restricted the achievement of the best biomechanical configuration. If other volunteers had participated in the experiment, the mechanical adjustments would have to be carried out individually, which would have demanded a relative effort to define the best FES pulse parametrization (i.e., the stimulation range of each angle).

3.5 Conclusion

This chapter presented all necessary aspects to implement an adaptive FES-cycling system and brought more information about the high-capacity stimulation system previously addressed in another context (Coelho-Magalhães, Tiago, 2018). The *High-Capacity Functional Electrical Stimulation* (HCFES) system was able to generate biphasic electrical pulses with amplitude, width and frequency up to 150mA, 1000μs, and 100Hz, respectively. The system was able to implement controlling strategies and allowed a participant with complete paraplegia to pedal both stationary and non-stationary.

4 Stimulation Pattern Definition

4.1 Introduction

In the FES-cycling modality, whereas a fixed baseline stimulation pattern is usually defined so that a controller can modulate the pulse parameters, this chapter introduces a new algorithm in which a Reinforcement Learning (RL) agent was designed to continuously learn through its interaction with the cycling environment how to optimize the stimulation parameters according to pre-programmed policies while tracking a reference cadence.

Through an online quantitative analysis of the cycling cadence error and its relationship with the electrical charge injected to maintain the pedaling movement, the agent modifies the baseline stimulation pattern while a Proportional-Integral (PI) controller modulates the current amplitude to track a pedaling cadence. For the agent to act in the environment and to balance between exploring novel actions and exploiting the most rewarding actions, the proposed RL algorithm is based on a *decayed-epsilon-greedy* strategy associated with a finite Markov Decision Process (MDP), which is used for modeling sequential decision problems.

It was hypothesized that a non-stationary baseline stimulation pattern would be more efficient in adjusting the amount of injected electrical charge to the time-varying characteristics of the musculature, greatly influencing *stimulation cost* during the assisted session. Therefore, from a quick definition of the initial configuration of the stimulation pattern, it is of interest to assess if the agent would be able to learn to act in the environment aiming to increase the accumulated reward received over time based on a user-defined policy and simultaneously being capable of tracking a preset pedaling cadence.

The performance of the global control strategy proposed was evaluated in two different RL settings and explored in different cycling scenarios. Overground FES-assisted cycling sessions were performed by a participant with SCI (AIS A, T8).

4.2 Materials and Methods

4.2.1 Participant

One participant (38 years, male) with complete Spinal Cord Injury (AIS A, T8) was recruited for this study and signed a written informed consent. Patient history and physical assessment data are detailed in Chapter 5. The research was approved by the UFMG local Ethical Committee (CAAE: 30989620.6.0000.5149, Ethical Approval number

4.190.128) in agreement with the Declaration of Helsinki.

4.2.2 Trike Settings

Non-stationary FES-cycling sessions were performed overground on a recumbent tadpole tricycle (Arttrike, Porto Alegre, RS, Brazil). The original crankset was replaced by a power-meter crank (2INPOWER, Rotor Bike Components, Madrid, Spain). Orthotic calf support (HASE® Bikes, Waltrop, Germany) was fixed to the pedals to keep the ankle joint at 90° and restrict the leg movement to the sagittal plane. Crank angle was evaluated through an incremental encoder (model LPD3806-360BM-G5-24C). Data processing and statistical analysis were performed in MATLAB R2021a (MathWorks, Natick, MA, USA).

4.2.3 Electrical Stimulation

Vastus medialis (VM), vastus lateralis and rectus femoris (VL+RF), and hamstrings (HAM) muscles were stimulated during pedaling sessions.

Rectangular self-adhesive surface electrodes (9x5cm, Arktus®, Brazil) were used as following settings: (1) an electrode positioned 3cm above the upper edge of the patella on the distal motor point of the VM muscle; and another electrode on the proximal motor point of the same muscle; (2) an electrode positioned 3cm above the upper edge of the patella on the distal motor point of the VL muscle and another electrode on the proximal motor point of the RF muscle; (3) one electrode placed 5cm above the popliteal fossa and the other 15-20cm above the popliteal fossa for the HAM stimulation. For an illustrated view of the electrode positioning, refer to Figure 24 in Chapter 5.

Rectangular and symmetrical biphasic pulses with amplitude limited to 100mA, pulse width of 450μs-600μs, and frequency at 35Hz were employed during the sessions. A PI controller modulated the pulse amplitude to track a cadence of 35rpm chosen to allow the volunteer to cycle for a minimum of 30 minutes and produce an average power greater than 10W.

4.2.4 Data acquisition

The mobile application (Android *app*) presented in Chapter 3 was modified to include the *Enhanced* mode, which enables the RL algorithm during FES-*cycling* sessions (Figure 18). All *app* functionalities previously described were maintained. Crank-angle, cadence and power were also measured by the power meter. Data was transmitted via Bluetooth to a personal computer at a sample rate of 50Hz and processed by the software ROTOR INpower Software 2.5 (Madrid, Spain).

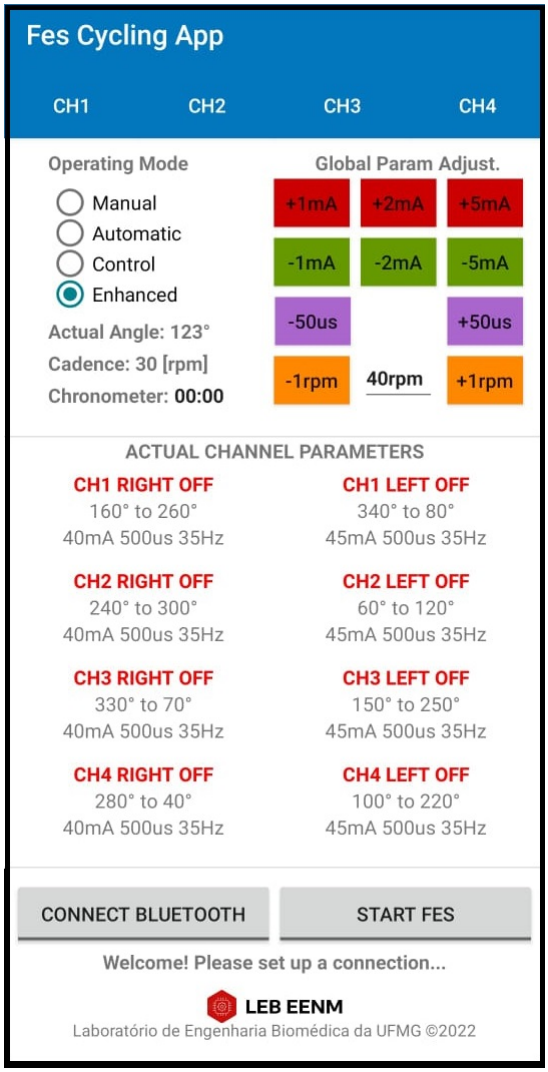

Figure 18 – Proprietary mobile application developed for system configuration with the *Enhanced* mode selected.

4.2.5 Reinforcement Learning Algorithm

In a particular state, the agent acts on the environment for a limited period and expects to receive a numerical reward. At the beginning of every interaction, the agent may choose a different action at a predefined exploratory percentage rate (ϵ, epsilon). These actions have an impact on the environment, which observation, in turn, leads to a new state. The algorithm was implemented in such a way that, at a given state, the RL agent may execute a random action to change the baseline stimulation pattern. The selected action may increase or decrease the amplitude and/or pulse width parameters by a predefined value. In this work, however, the pulse frequency and the start and stop angles at which the muscles are stimulated were kept constant.

Within a predefined number of interactions, that is, a sub-sequence of the whole interaction process named episodes, the agent randomly chooses between exploring new actions (increasing/decreasing current amplitude and/or pulse width) or exploiting past

actions that have given the highest reward, called *greedy actions*, to change the stimulation pattern temporarily. The agent then evaluates the rewards received by the temporary implementation of the modifying action on the cycling environment. At the end of every episode, the amplitude and pulse width parameters of each channel is maintained or updated (increased/decreased) according to the greedy action that the agent has learned to be the most rewarding and a new episode starts from this new baseline setting. At this point, to eventually decrease the exploration rate, the epsilon parameter is then multiplied by a decay factor, justifying the *decayed-epsilon-greedy* strategy.

Let $D_3 = \{-0.5, 0, +1\}$ be a predefined numerical set and the pulse parameters width and amplitude be the variables ω and α respectively. Let also be the set of six stimulation channels used in the pedaling cycle (VL+RF, VM and HAM; left and right limbs). The set from which the agent can select one possible action is $A = \{(\alpha, \omega) : \alpha, \omega \in D_3\}$, i.e., the set of all the possible combinations between the two stimulation parameters the agent could modify, totaling nine different actions available independently for each channel. To learn which is the most rewarding action within a specific period, the need for exploring different *non-greedy* actions is created.

In this sense, the ϵ-greedy with a decaying rate $dr \in [0, 1]$ method was implemented to balance exploration and exploitation. As mentioned earlier, at the end of each episode, the ϵ parameter, which represents the percentage of time the agent will choose to explore new actions, is multiplied by a decaying factor (dr), suggesting that, over time, the agent would be able to find the optimal pattern and the need for exploring changes in these pulse parameters would decrease. These settings depend on how often it is wanted the agent to change the stimulation pattern to improve it.

Finally, a set of rules was defined as action selection criteria for the agent to follow, including: 1) not exceeding a predefined range of values for the pulse parameters; and 2) not reducing the pulse width when the current amplitude, the variable on which the PI controller acts, is at its maximum value. Increasing the pulse width was allowed in this scenario, however. The process of tuning parameters in the proposed algorithm depends on the project objectives. They can be modified to explore different RL approaches associated with FES-assisted activities and different strategies for policy and reward implementation.

Figure 19 presents the global control strategy with the agent–environment interaction scheme and the PI-controller. The possible actions for the agent for modifying independently both the amplitude and pulse width of the individual channels are also evidenced by the following representation: 0, no change; +1, increase in one step the pulse parameter; -0.5, decrease in one-half step. The steps were defined in the firmware. At a state S_t, the RL agent selects one of the possible actions for each channel, respecting the predefined rules. The chosen action may change a particular channel's pulse amplitude and/or width. In parallel, the control contribution from the PI controller for cadence

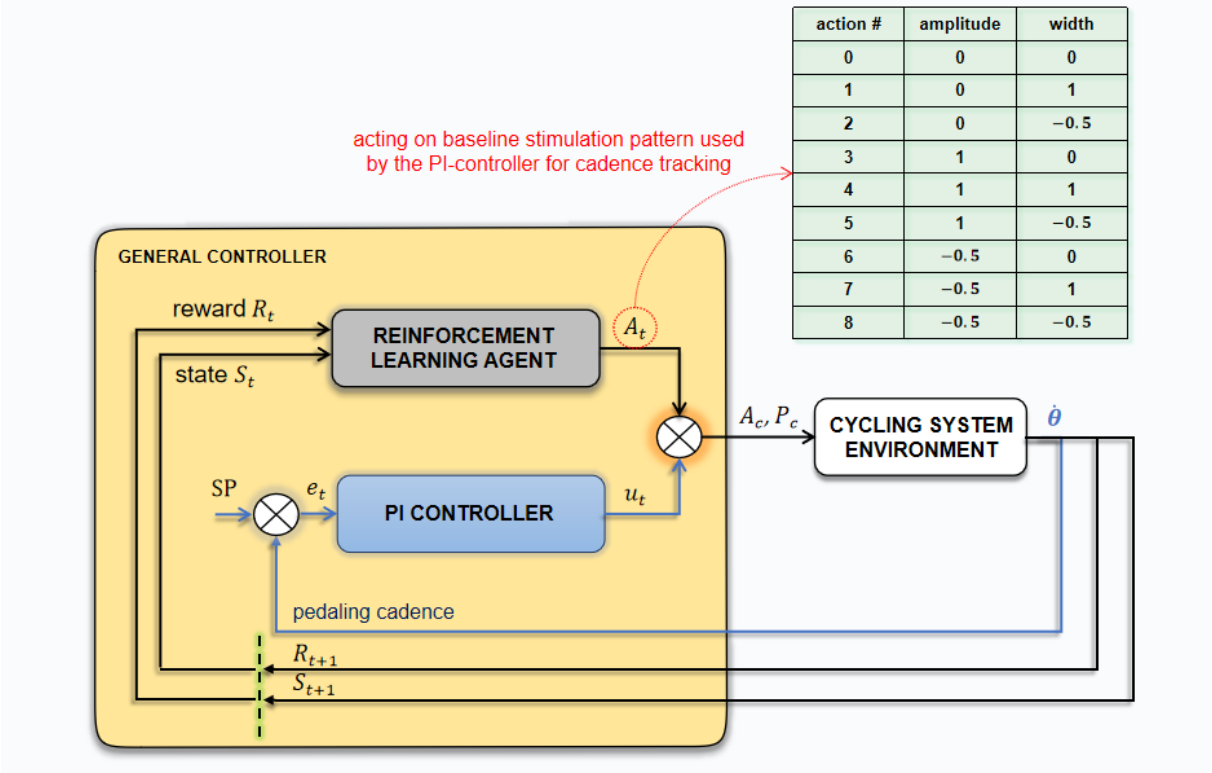

Figure 19 – The global control strategy with the agent–environment interaction scheme and the PI-controller.

tracking. Signals A_c and P_c represent the amplitude and pulse width output of the general controller. The interaction dynamics is based on the following description:

1. The agent interacts with the environment at a sequence of discrete time steps, $t = 0, 1, 2, ...$ for each of the enabled stimulation channels simultaneously. For a specific time-step t, the agent perceives a state vector $S_t \in \mathbb{R}^2$ consisting of crank angle θ, and average pedaling cadence error $\overline{e}(\dot{\theta})$; and chooses one action for each channel, $A_{t,c} \in A$, which is multiplied by the predefined constants k_a and k_w. For instance, suppose at time-step t channel 2 has the baseline parameters: $a_2 = 45mA$, $w_2 = 500\mu s$ and $f_2 = 35Hz$. Let's consider the constants $k_a = 1(mA)$ and $k_w = 20(\mu s)$. If the agent randomly selects the action #5 ({1, -0.5), see Figure 19), in the subsequent interaction, the channel 2 parameters would be set to $46mA$ $(45mA + 1 \cdot 1mA)$ and $490\mu s$ $(500\mu s - 0.5 \cdot 20\mu s)$. Notice that, even if it was not used here, the frequency could also have been included in the algorithm. In this case, considering three variables to be changed $(n = 3)$, the set of possible actions (3^n) would be 27. Also, it would be possible to choose the frequency parameter instead of amplitude or width. These possibilities, among the possible inclusion of other parameters (for instance, the stimulation ranges), make the algorithm flexible to suit the purposes defined in many research and application contexts.

2. The algorithm features a set of rules to which the agent must obey when choosing

actions. In this case, limit values have been set for each of the parameters (α, ω) and were defined in the firmware. For example, for the pulse width starting from the baseline at $500\mu s$ and throughout the cycling session, if the default limiting for the width parameter was set to $+100\mu s$ and $-50\mu s$, any chosen action that exceeds $600\mu s$ or is below $450\mu s$ would be refused and the agent would have to select another one. It is important to emphasize that the agent performs this whole procedure for each channel independently and at every time step.

3. Each interaction impacts the cycling environment and, from its observation, it is possible to compute a predefined expected reward. In this work, the expected reward was proposed to be defined as described in equation Equation 4.1.

$$R_{t+1,c}(\dot{\theta}, \theta) = \begin{cases} \mid P_c^2\sqrt{A_c} - \overline{P_c}^2\sqrt{M_a - A_c} \mid \overline{e}(\dot{\theta})^{-1}, \ \theta_c^{start} \leqslant \theta \leqslant \theta_c^{end} \\ 0, \ otherwise \end{cases} \tag{4.1}$$

where $P_c = (\, w_c + \omega_c \cdot k_w) \cdot 10^4$; $A_c = (\, a_c + \alpha_c \cdot k_a + u_c) \cdot 10^3$; $\overline{P_c} = P_{c,max} + P_{c,min} - P_c - P_k$ (the maximum and minimum values are defined by firmware and P_k was set to 100 in the experiment, which was tuned observing the cycling performance); M_a is the maximum amplitude defined at $100mA$; θ is the actual angle within the pedaling cycle and $\dot{\theta}$ is the pedaling cadence; $\overline{e}(\dot{\theta})$ is defined as the result of a simple moving average cadence error with window size set to 10; and θ_c^{start} and θ_c^{end} correspond to the stimulation interval for the stimulation of channel c. Notice that the rewards are inversely proportional to the cadence error as the agent was designed to exploit actions that promote the lowest cadence error. The reward dynamics which relate

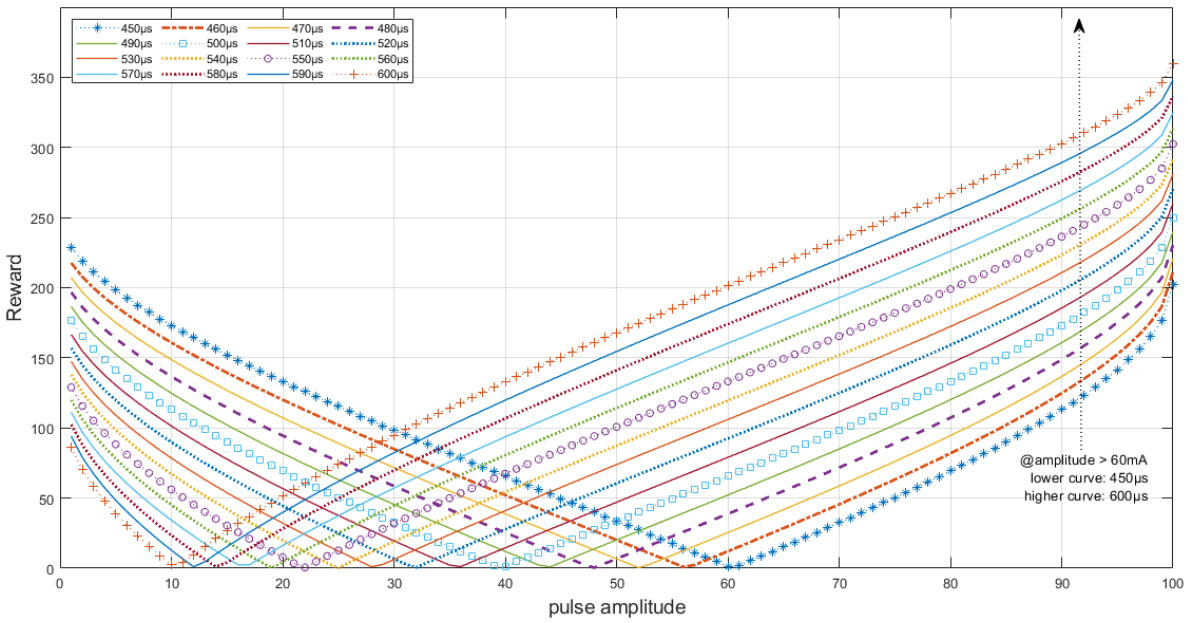

Figure 20 – Reward curves relating amplitude and pulse width prioritization.

the pulse charge (i.e. the product of pulse width, amplitude and frequency) is demonstrated in Figure 20.

Notice that there is an inversion in the numerical reward obtained for each pulse width employed to improve the stimulation cost and efficiency. At lower amplitudes, narrower pulse widths return higher rewards as it is preferable to decrease the stimulation cost; at higher amplitudes, the agent is expected to perceive greater rewards as the pulse width increases. Although a constant value for the cadence error was assumed to plot the graph, the rewards obtained are also dependent on the variable value of the cadence error (see Equation 4.1). The reward signal can be defined in different ways and, in this work, it was determined by practical observation of the algorithm performance on the track. After testing some settings and to prevent the pulse amplitude from saturating quickly, it was decided to give greater rewards for larger pulse widths when the amplitude is above half of its range to prioritize the increase of the electrical stimulation pulse charge to sustain muscle contractions longer and, below half of its range value, the rewards are greater for narrower pulse widths aiming to prioritize the stimulation cost.

4. For the agent to decide which action is best, the value of taking each action must be calculated. With the knowledge of the rewards of each chosen action, it is possible to estimate the *action values*, i.e. the expected return for using action A_t in a particular state S_t. For instance, let's define the expectation of R_t given the selection of action A_t for any of the possible actions as:

$$q(a) \doteq E[\, R_t \mid A_t = a \,] \, \forall \, a \in A \tag{4.2}$$

The sample-average method was implemented for estimating the action values as defined in Equation 4.3:

$$Q_{n_{a_c}+1} = \frac{1}{n_{a_c}} \sum_{n=1}^{n_{a_c}} R_i = Q_{n_{a_c}} + \frac{1}{n_{a_c}} [\, R_{n_{a_c}} - Q_{n_{a_c}} \,] \tag{4.3}$$

where n_{a_c} represents the counter of every action for the specific channel. Considering the RL concepts presented by Sutton and Barto (2018), we can think of these estimations as $NewEstimate \leftarrow OldEstimate + StepSize[Reward - OldEstimate]$.

5. By maintaining estimates of the action values, it is possible to determine the actions whose estimated values are the greatest (*greedy actions*). In RL algorithms, the agent is exploiting its current knowledge of the values of the actions when selecting these *greedy-actions*. If instead the agent randomly selects one of the *non-greedy* actions, it is exploring because the estimates of the non-greedy action's value can be improved. The simple *decayed-epsilon-greedy* method was implemented in the proposed algorithm to balance exploration and exploitation. This artifice is necessary since exploitation allows to maximize the expected reward in one step, but exploration can yield the greatest total reward in the long run. At every time-step, a random number is created and compared to a predefined epsilon parameter $\epsilon \in [0, 1]$, which

refers to the probability of the agent choosing to explore instead of exploiting greedy actions. Different configurations for the ϵ and decaying-rate parameters can be defined to evaluate the best configuration for the FES-*cycling* activity. It is hypothesized that a more exploratory characteristic of the agent can be beneficial for prolonged periods for the FES-assisted cycling activity, as it would learn to adapt the parameters to the real state of the muscle.

6. The algorithm predicts that the interactions between the agent and the environment are broken into sub-sequences, called episodes. This is because the baseline parameters must also be changed to find the best stimulation pattern between all channels used. At the end of each episode, the agent chooses the action that returned the greatest action-value and changes the stimulation parameters baseline for all channels. The next episode starts evaluating the agent-environment interaction from this new scenario, independent from the previous one. The user-defined parameter ϵ is also reduced at the end of each episode.

7. Finally, to track the desired pedaling cadence, the pulse amplitude of each channel is modulated simultaneously by a PI controller over the instantaneous baseline stimulation pattern which is constantly modified by the RL agent. The controller was described in Chapter 3. Thus, even though the agent is responsible for optimizing the stimulation pattern, the PI controller modulates the pulse amplitude for cadence tracking.

At this stage, it was not intended to compare between the controller performances but rather to demonstrate that the agent has the ability to learn a predefined policy and that this new approach has some potential to be applied to assisted modalities in order to: 1) overcome the time-consuming problem of stimulation pattern definition; and 2) achieve more efficiency in terms of the injected electrical charge and consequently delay muscle fatigue. Stimulation cost and reward over time, pedaling distance, average speed and power generated on pedals were evaluated.

4.2.6 Intervention Protocol

Three scenarios where considered for the controller:

i PI control without the PI algorithm enabled;

ii PI control with the PI algorithm parameters $\epsilon = 0.6$ and $dr = 0.99$ (60%@.99);

iii PI control with the PI algorithm parameters $\epsilon = 0.4$ and $dr = 0.99$ (40%@.99);

Each of these three scenarios were evaluated in two different gear ratios for the tricycle, M1 and M2, with the latter being heavier. In all 6 possible scenarios, all

stimulation channels started at parameters set to $45mA$ and $50mA$ for the right and left leg, respectively, pulse width to $500\mu s$ and frequency to $35Hz$. The range for the pulse parameters were set to $\Delta a = 10mA$ and $\Delta\omega = 100\mu s$ The parameter $P_{c,max}$ was therefore set to $600\mu s$; however, $P_{c,min}$ was set to $450\mu s$. The step size for each variable was defined as $a = 2mA$ and $\omega = 20\mu s$. The agent was supposed to interact with the environment for a predefined period of $5s$ before choosing an action once again. Each episode lasted for $45s$ before decreasing ϵ and modifying the baseline parameters with each channel's greedy action.

Before the start of each cycling session, the tricycle tires were calibrated and the same electrode placement was respected to ensure similarity between the experiments. The participant was installed on the tricycle to pedal on an official outdoor athletics track. A 3-minute passive cycling on a stationary bike stand (without stimulation) was performed before and after each session. When starting the cycling session, the experimenter only helped the pedal to come out of inertia. The session was limited to sixty minutes and, in case of exceeding that time, until completing the current lap. If the volunteer could not complete the established time and could no longer pedal, the session would last until the tricycle stopped. No human intervention was allowed during the session other than the provision of water at the volunteer's request while maintaining pedaling.

4.3 Results

An external link for the application firmware and software is available in Supplementary Materials (Section 1.5). **Algorithm 1** presents the main idea behind the implemented *decayed-epsilon-greedy* firmware strategy.

Algorithm 1 Reinforcement Learning Algorithm

Input: $\overline{e}(\dot{\theta})$, θ

```
error ←| ē(θ̇) |                                   ▷ average cadence error
counter ← counter + 1                              ▷ increment @10Hz

for c ← 0 to nChannels − 1 do                      ▷ for every enabled channel
    if counter % 50 is > 0 then                    ▷ observes the state for 5s
        if θ is within channel_c range then
            a ← action_c                           ▷ ...for the selected action
            calculate reward                       ▷ obtained from Eq. 1
        end if
    else
        if counter < maxInteractions then          ▷ choose new action after 5s
            r ← randomNumber
            if r < ϵ then
                action_c ← between 0 and 8         ▷ choose a random action
                if action_c decrements P_width when P_amp is Max then
                    action_c ← 0                   ▷ do not change parameters
                else if action_c exceeds any parameter's limit then
                    action_c ← argmax(q_c)
                end if
            else
                action_c ← argmax(q_c)             ▷ choose the greedy action
            end if
            stimultationParam_c + (action_c)       ▷ parameters altered temporally
            n_{c,a} ← n_{c,a} + 1                  ▷ action counters incremented
        else                                       ▷ Episode end: update Baseline...
            action_c ← argmax(q_c)                 ▷ ...with greedy action
            stimultationParam_c ← stimultationParam_c + action_c
            for j ← 0 to 8 do
                q_{c,j} ← 0                        ▷ estimate values are re-initiated
                n_{c,j} ← 0                        ▷ action counters are re-initiated
            end for
        end if
    end if
end for
if counter = maxIterations then    ▷ End of episode: update ϵ and reset counter
    ϵ ← ϵ · dr                                     ▷ decaying rate dr ∈ [0, 1]
    counter ← 0
end if
```

Table 1 presents the cycling results obtained from each session configuration and includes distance covered, time duration, average speed and average power. Both the proposed controller (which includes the RL algorithm) and the PI-only controller allowed the participant to perform overground cycling.

Table 1 – Performance results for 6 different control techniques, using or not the RL algorithm. For the PI+RL format, "60%;@.99" means the agent is exploring new actions 60% of the time and decaying this percentage to 99% at the end of every episode. The "40%;@.99" format, in turn, represents a 40% exploratory rate, meaning the agent may choose to exploit actions most of the time instead of exploring new actions

session	format	RL setting	gear ratio	distance (m)	duration	Avg. Vel. (km/h)	Avg. Power (W)
1	only PI	NA	M1	4676	1:04:59	4.3	10.73±1.81
2	PI + RL	60%;@.99	M1	4682	1:05:27	4.2	10.47±1.89
3	PI + RL	40%;@.99	M1	4688	1:02:22	4.5	11.53±1.87
4	only PI	NA	M2	2931	0:37:46	4.6	12.18±2.84
5	PI + RL	60%;@.99	M2	3773	0:46:35	4.8	12.90±3.02
6	PI + RL	40%;@.99	M2	3844	0:51:54	4.4	11.33±3.17

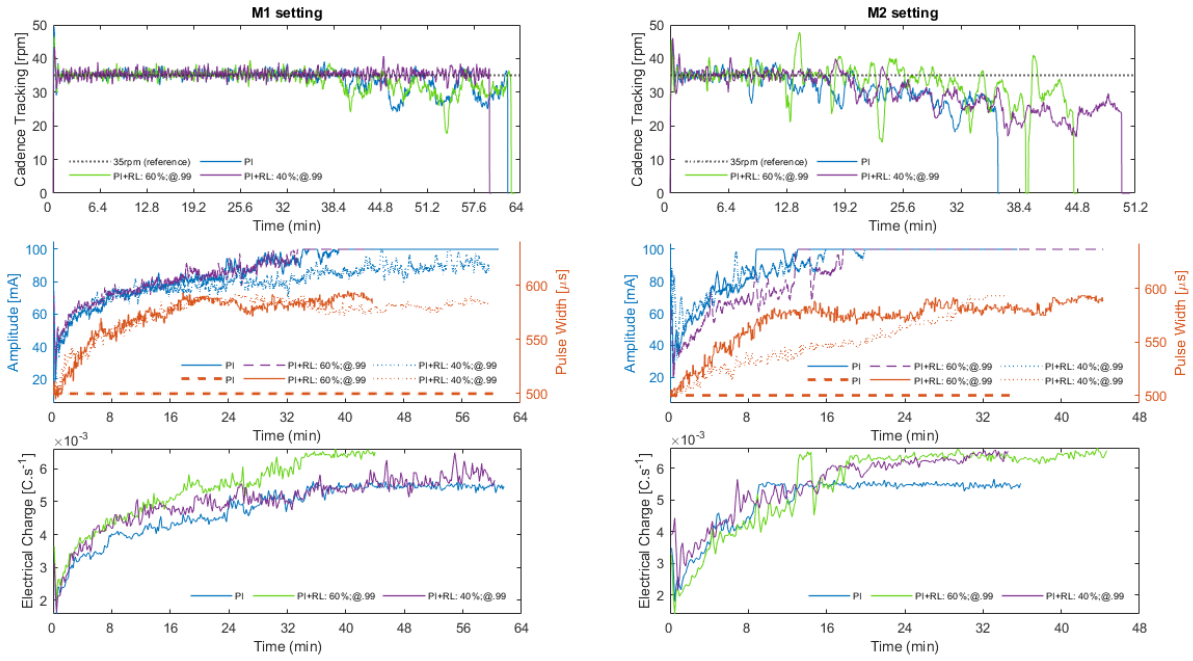

Figure 21 – Algorithm performance for M1 (left plots) and M2 (right plots) settings for PI-only, 60% exploration rate and 40% exploration rate configurations. The results presented in subplots are divided into: 1) cadence tracking; 2) modulation of amplitude and pulse width; 3) injected electrical charge. for the six cycling sessions. During the session "$M1 : P1 + RL : 60\%; @.99$" the application closed unexpectedly, however, without affecting the interpretation of the data

Figure 21 shows the algorithm performance obtained during the six different sessions, divided into M1 (left plots) and M2 (right plots) gear ratio settings. The subplots are divided into: 1) cadence tracking; 2) the sum of the instantaneous amplitude and pulse width of the six stimulation channels; 3) the sum of the injected electrical charge of the six stimulation channels.

In M1 scenario, despite the "@40%.99" curve being shorter in the plot, it presented a better average speed (4.5km/h) and managed to cover a greater distance (4688m) in

less time (1h02min22s). The "@60%.99" setting has achieved equivalent cycling results compared to the PI-only, being, respectively, $4682m - 4676m$; $1h05min27s - 1h04min59s$; $4.2km/h - 4.3km/h$; and $10.47 \pm 1.89W - 10.73 \pm 1.81W$. It will be interesting in the future to analyze the influence of cadence and gear ratio on cycling performance. So far, however, while the M2 setup is heavier for the rider, the results obtained with the RL suggest a better adaptation to the cycling scenario compared to the PI-only format.

In both M1 and M2 scenarios, the algorithm was able to keep track of the preset pedaling cadence of 35rpm at least until amplitude saturation. For the M1 setting, the best result was obtained when the algorithm was configured to a 40% exploration rate, in which the controller was able to track the setpoint cadence for the whole session. As the tracking results when the RL algorithm was enabled are very similar to the PI-only configuration for the @60%.99 setting, it can be stated that the algorithm allowed for cadence tracking as designed and the modulation of the stimulation pattern by the RL agent did not negatively impact pedaling performance. It can be also suggested that the pedaling cadence error is more affected when the exploratory rate is higher (i.e. 60%) as the agent is supposed to explore new actions more frequently.

The plot of the second line shows the variation of pulse amplitude and width during the sessions. For the PI-only setting, the pulse width was maintained constant as the controller modulated only the pulse amplitude. It can be noted that the cadence tracking starts to be affected when the amplitude saturates at $100mA$ for any of the different scenarios. However, specially for the M2 configuration, the increase of pulse width performed by the agent suggests that the time at which saturation occurred was delayed, as a consequence of the defined policy for his interaction with the cycling environment.

The plots at the bottom show the sum of the injected electrical charge over time for the M1 and M2 settings, considering all channels enabled at that moment. For better visualization, a simple moving average with window size of 100 was employed. During M2 sessions, it can be noted that the electrical charge reaches higher values more quickly because this scenario is heavier for cycling, however, due to the increase in pulse width performed by the agent, it is observed that the amplitude took longer to reach $100mA$ compared to PI-only configuration. However, the PI-only controller led to overall lower charge injection. In this work, the electrical charge employed has a direct relationship with the policy defined for the agent to learn. Therefore, as it was defined for larger pulse widths to be more rewarding when the pulse amplitude is above half of its range, then the stimulation cost will be higher for heavier cycling scenarios.

Figure 22 shows the accumulated reward over time obtained by the agent during cycling sessions based on different exploratory rates and the accumulated absolute value of cadence error over time sampled at $10Hz$. It can be seen that the agent is capable of increasing the accumulated reward received by interacting with the environment. However,

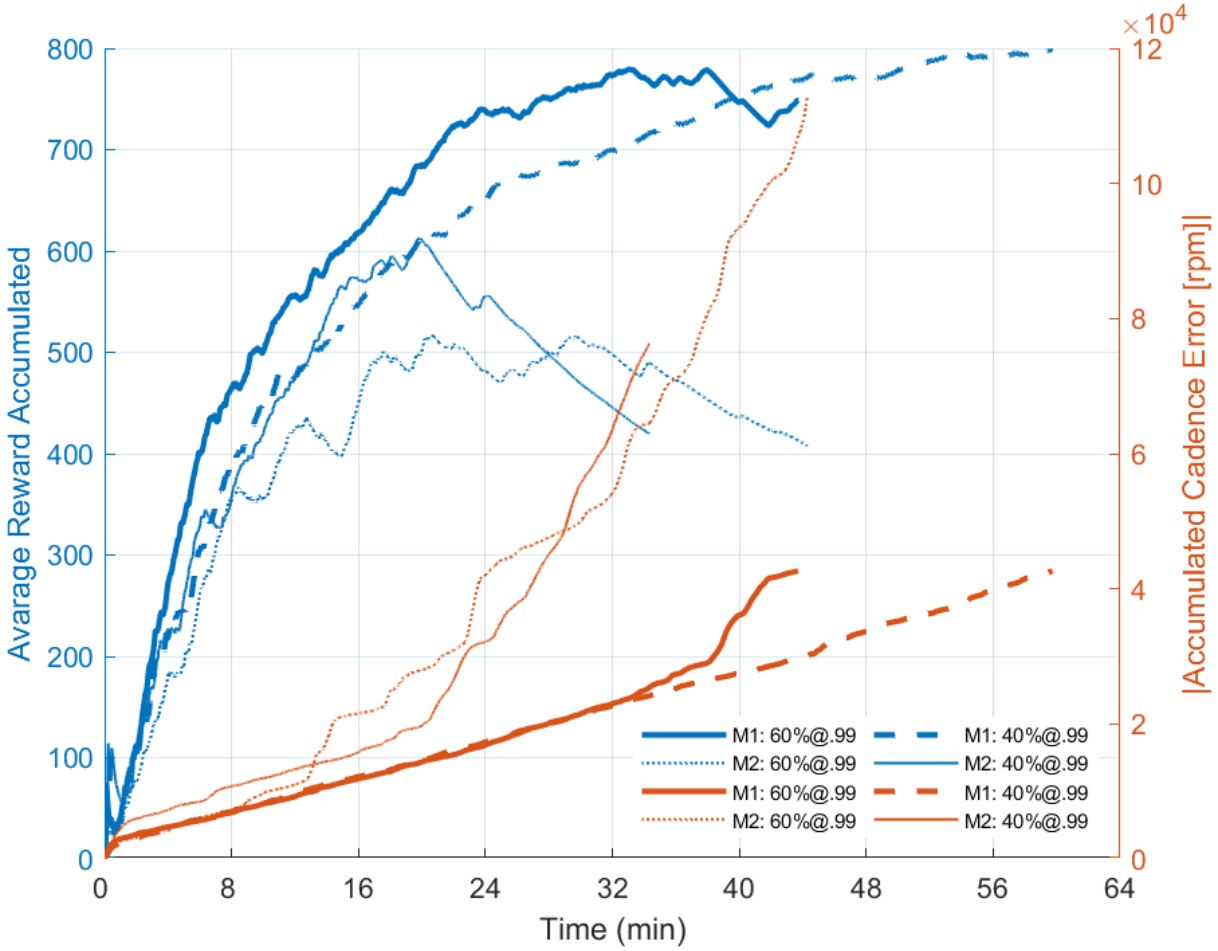

Figure 22 – Reward over time during cycling sessions and the accumulated absolute value of cadence error. The agent's ability to explore different actions over time to increase the reward received can be interpreted as its ability to learn the best action for the time-varying scenario of FES-cycling. Data obtained from the Android App with sample frequency @10Hz

when the pulse amplitude saturates and the cadence error increases as the controller cannot track the cadence efficiently, the rewards received start to decrease. At this stage, the agent is not able to identify which action is best to implement anymore. During the session "$M1 : P1 + RL : 60\%; @.99$" the application closed unexpectedly, however, without affecting the interpretation of the data. The session duration seems to be shorter compared to Table 1 due to the eventual loss of packets between the mobile and the stimulation system.

4.4 Discussion

A novel algorithm for optimizing the pulse parameters of six different channels based on Reinforcement Learning (RL) concepts was developed for simplifying the control techniques and adjustment of the stimulation parameters to the time-varying characteristics of the non-linearity and time-variability of the muscle dynamics under electric-evoked

contractions. A general controller was designed to track a reference cadence and was constituted by a PI-controller acting over a non-stationary stimulation pattern modified by a RL agent with a *decayed-epsilon-greedy* strategy. The agent was designed to interact with the cycling environment according to a predefined policy and was supposed to learn to modulate the electrical charge applied to the stimulated muscle groups in order to adjust the injected electrical charge. The performance of the proposed algorithm was evaluated during real cycling experiments.

Figure 21 presents the results for cadence tracking obtained in the six different explored configurations. For the M1 gear ratio, the controller was able to track the 35 rpm cadence longer if compared to the M2 format as it is less difficult for the rider to cycle. The policy for the agent to learn is associated with the injected electrical charge and the cadence error. When the sessions started, it was observed that the agent prioritized increasing the pulse width. Specially for the M2 setting, this feature delayed the amplitude saturation, resulting in a longer capacity of the algorithm to track the predefined cadence. Indirectly, this feature can positively affect pedaling performance by increasing the average speed and session time.

For instance, for the M2 gear ratio configuration, in which the difficulty for pedaling was greater and it was eventually expected more electrical charge to continue to evoke contractions during the sessions, the RL results suggest a better performance of covered distance and time. When the RL algorithm was enabled, the distance covered by the cyclist was 31% longer (3733m for the @60%.99 and 3844m for the @40%.99 scenarios) compared to sessions where only PI control was used (2931m). However, it cannot be stated that the PI-only configuration had a worse performance because it was performed some weeks before testing the RL+PI algorithm as a baseline reference and not for comparison purposes. The volunteer may have presented a better result due to the training. Therefore, it is essential to emphasize that the main objective was not to compare the controller performances at this stage but instead demonstrate that this new approach has some potential to be applied to FES-assisted modalities.

The experiments evidenced that the agent correctly learned how to accumulate the received reward. As the goal of the agent is to maximize this quantity over time and not the immediate reward, which justifies the exploratory feature of the algorithm, the agent was supposed to choose to explore novel actions more often when higher exploratory rates were defined. Figure 22 evidences a higher reward accumulated for the 60%- exploration rate during the sessions in the M1 scenario until he was able to track the predefined cadence. For M2, the most exploratory setting returned more reward to the agent in the long term if compared to the 40%-exploration rate as supposed. It can also be seen that, by incrementing the pulse width, , the amplitude took longer to saturate (Figure 21), supporting the hypothesis that the agent was able to learn the policy. For

session configuration "$M1 : P1 + RL : 60\%; @.99$", a loss of data transfer between the mobile application and the FES system affected the final curve plotting.

Notice that the rewards received by the agent are still related to the pedaling cadence error. In this case, when the amplitude parameters saturate, resulting in the PI controller's inability to guarantee the cadence tracking, a decay in the accumulation of the reward received over time is noticed. This characteristic can be seen in Figure 22 when the accumulated reward curves start to decrease, mainly for the M2 configuration. Also, considering that the agent takes time interacting with the environment to learn how to modify parameters, if the reward relationship favored a decrease in pulse width, it would be expected that the amplitude would be increased by the controller to continue tracking the cadence. If the amplitude parameter saturates (considering the amplitude as the stimulation control output signal), the cadence error would tend to increase since the controller would not be able to track the cadence anymore. Thus, as the rewards received by the agent are linked to the cadence error, there would be no guarantee for him to estimate the action-values correctly. Therefore, the agent would not be able to recover his capacity to modulate the stimulation pattern precisely.

When comparing the two gear ratio configurations, it can be noticed from Figure 21 that the electrical charge spent during M1 sessions is lower as the output power produced (Table 1), a characteristic consistent with the difficulty of the movement being less than in M2. In the case of lesser pedaling difficulty (scenario M1), where a lower stimulated cost is expected, the configuration with the PI controller proved to be as efficient. The M2 pedaling arrangement seemed more efficient as the pedaling performance has shown better distance covered and session-duration results.

However, the electrical charge is higher for the two gear ratio configurations when using the RL algorithm. This feat was expected and it is justified because the reward dynamics were defined here to favor greater pulse widths for greater amplitudes. From practical observation of the difficulty for our pilot to cycle on the track, it required greater pulse intensities. In this sense, an essential requirement of the algorithm is the definition of the relationship of rewards to the electrical charge used for pedaling since the agent will prioritize the rules defined for such an experiment. The rewards relationship can therefore be modified to prioritize the reduction of the accumulated electrical charge depending on the experiment to be performed. This feature opens a pathway to study new interaction-reward dynamics in the future.

For the proposed controller, it was also necessary to evaluate different parameter settings for the RL algorithm (number of interactions, episode duration, exploration rate, time evaluating rewards, step size for pulse width and amplitude, etc.) and policies for the reward-interaction dynamic between the agent and the environment, which is part of the process of tuning the algorithm. Also, in addition to the algorithm parameters, the more

actions the agent has available to evaluate, the longer it takes to learn. In this sense, the time it takes the agent to learn the policy is related to the algorithm settings and to the number of actions available for him to learn. As muscle fatigue is yet a limitation to the use of electrical stimulation to assist functional activities and consequently a limitation to the session duration, depending on how much the volunteer can pedal, the agent will not have enough time to learn. Therefore, it is necessary to balance the time to learn and the possible cycling capacity in terms of duration for the volunteer.

To overcome this drawback, a better approach would be to use mathematical models to simulate a priori different combinations of parameters, as well as the agent's exploration and exploitation characteristics to learn the policy. In (Wannawas; Subramanian; Faisal, 2021), researchers suggested the RL controller be trained to learn a defined stimulation strategy to cycle at the desired cadences in simulation before evaluating the performance in the real world. They developed a deep RL algorithm to control the stimulation of different leg muscles during FES-*cycling* sessions and demonstrated the ability of the agent to learn from its iterations with the system. They trained the agent and compared the results to other controlling methods (Proportional Integral Derivative (PID) and Fuzzy Logic Control) using a musculoskeletal model. The results suggested that the proposed method was able to compensate for muscle fatigue and track desired cadences. Unlike the work cited, in which the RL algorithm was used to track cadence, our approach employed a PI control strategy to track a predefined cadence and the RL agent was responsible to adjust the baseline stimulation pattern. The accumulation of the two functions by the agent will be studied in future works.

The researchers also conducted a simulation study in which a trained RL controller was transferred to another model with moderately different seat position. Besides potential results, the researchers found that the RL controller required some additional minutes of interaction before producing good tracking performance. Unlike this approach, however, it was demonstrated the possibilities of a control method using reinforcement learning concepts during real overground cycling sessions in being able to track desired cycling cadences. In addition to evaluating the performance of the algorithm in three different control strategies, no additional training was needed. Also, parameter adjustment could be done independently for each session, adjusting for the physiological characteristics of that moment. It was also demonstrated the agent's accumulative reward over time, which permits the understanding of his learning capacity. This feature was not demonstrated elsewhere.

In Sijobert et al. (2019), despite the positive results and the advantage of simplifying the FES-*cycling* implementation, the study evaluated pedaling using only the quadriceps muscle and for one single participant. Also, given that the researchers chose to let the participant control the intensity manually and therefore no automatic control of cadence

was implemented, the electrical charge may not have been optimally efficient during cycling sessions, which impacts on the stimulation cost, a definition of the ratio of the total charge rate to the mechanical work rate (Hunt et al., 2012). Furthermore, the researchers stated that the accuracy and precision of real-time interpretation algorithms are needed to ensure reliability and the accuracy and precision are needed to be assessed (Guillou et al., 2021), which could limit its applicability given the complexity of analysis.

In (Schmoll et al., 2021), researchers presented an algorithm to automatically detect stimulation intervals by evaluating the torque measured by a commercial crank power meter installed on an instrumented tricycle and using IMUs. In our work, it was used an incremental encoder that limited the continuous calculation of the pedaling cadence since it is a device that generates discrete data. Instead of modifying the parameters based on cadence, an approach in which the power or torque exerted on the pedals can be used to evaluate the agent seems to be more adequate. Furthermore, it was hypothesize that the use of IMUs could improve the performance of the agent as more data would be available for cadence assessment. In this sense, the time needed for the agent to learn the policy could be reduced and the evaluation of different reference cadences could be better explored.

Besides the presented method being also able to produce pedaling, it was addressed an automatic adaptation of the muscle activation pattern online during the session, a feature that would favor the modulation of parameters to the time-varying conditions of the muscle state. Another approach for this method would be inclusion of the torque evaluation exerted on pedals for the definition of the initial stimulation pattern (including the stimulation interval) that is yet to be studied in future works.

4.5 Conclusion

As stated initially, the search for methods that facilitate the definition of stimulation patterns seems to be a common objective of recent studies. The method proposed in this work presented exploratory results that suggest the possibility of using reinforcement learning methods to control and adjust the stimulation parameters in order to track a desired cadence. The maintenance of the average pedaling cadence throughout the sessions and the increase in the average distance covered by the volunteer indicate the possibility of delaying muscle fatigue using the proposed algorithm.

Three different control configurations were presented, each one being evaluated in two contexts of pedaling difficulty by a volunteer with spinal cord injury. In all cases where the RL algorithm was enabled, the participant could cycle at least equivalently than when only the PI controller was operating. According to the interaction-reward relationship established, it was possible to demonstrate that the agent can learn to increase its rewards

over time. In this study, it is suggested that such a method may favor an increase in pedaling endurance which, in turn, increases the amount of accumulated electrical charge spent during the sessions. However, if the interaction-reward relationship is altered to suit the purposes of greater electrical efficiency, the agent may also learn to reduce the stimulation cost.

In this sense, this study suggests that a RL algorithm can generate a positive impact on the efficiency of electrical stimuli during FES-assisted cycling sessions since the electrical charge spent to maintain a predefined cadence can be therefore reduced. However, different reward strategies must be evaluated together with the policies created for the agent.

5 Effects on body composition and bone mineral density during 2 years of FES-cycling: case report of a 38-year-old male with paraplegia

5.1 Introduction

This section presents a single-participant case report aiming to assess changes in Bone Mineral Density (BMD) and body composition (BC) in a 38-year-old man with complete Spinal Cord Injury (SCI) during a 2-year period of cycling sessions assisted by Functional Electrical Stimulation (FES-cycling).

Stationary and non-stationary FES-*cycling* sessions were performed on a recumbent tricycle 3 times a week concomitantly with strengthening sessions NMES twice a week until completing a period of 24 months. Two training protocols with different intensities were evaluated. BMD and body composition, including body fat percentage, fat mass and lean mass were evaluated using the Dual-Energy X-Ray Absorptiometry (DXA) test every 3 months.

The main objective was to assess the impact of two different cycling training programs on muscle atrophy, body composition and bone metabolism. The secondary objectives were to document: 1) pedaling performance in both stationary and non-stationary scenarios; 2) peak-torque during Maximal Evoked Contraction (MEC); 3) evaluation of health status, disability, quality of life; and 4) lessons learned during the research.

Although not specifically an article, this section was written following the CARE (CAse REport) guidelines for case reports (Riley et al., 2017). The contextualization for the case report was provided in Chapter 1. A detailed discussion of relevant studies is presented in this chapter, however.

5.2 Narrative

5.2.1 Patient Information

A 38-year-old male 13 years post T8 complete SCI classified as AIS grade A in the ISNCSCI, commonly referred to as the ASIA exam (Betz et al., 2019), participated in

the 2-year study. The experiments were approved by a local ethical committee (CAAE: 30989620.6.0000.5149, Approval number: 4.190.128) and began during the pandemic crises of COVID-19 on September 2020 after obtaining the written informed consent of the volunteer.

According to a medical evaluation, the volunteer did not presented potential risk of fractures during the activity ($T\text{-}score < -2,5$) or had any clinical contraindication for ES. He presented unrestricted joint movement and had no cardiovascular problems, epilepsy, or had lower limb fractures in the 12 months prior to the start of the protocol. Finally, he was not associate to other FES-assisted activities for the lower limbs outside the protocol of this research and had never used FES prior to his inclusion.

The volunteer's Bone Mass Index (BMI) was estimated at $21.8 kg/m^2$ (height 177cm and weight 68.2kg). He participated fully in the social and work activities of his daily life and used to practice regular physical activity despite being a smoker, including weight lifting at least three times a week, adapted boxing and physical therapy sessions two times a week. Cholecalciferol (vitamin D3) 7000-IU/week was prescribed to him by a medical doctor in the beginning of the program. He was also asked to follow a nutritional prescription, however, the diet was not monitored despite being necessary.

During the first FES cycling sessions, the participant reported subjective discomfort in the abdominal region and headache. At the same instant, the session was stopped. It was hypothesized that this episode could be associated with autonomic dysreflexia, which is a consequence of a dysregulation of the autonomic nervous system that can lead to a life-threatening hypertensive event when there is a noxious stimulus below the level of spinal cord injury. An episode of autonomic dysreflexia may represent mild discomfort and headache, associated with an acute increase (>20-30mmHg) in blood pressure (Allen KJ, Leslie SW, 2022). Although the volunteer was classified as T8 and autonomic dysreflexia is associated with injuries above T6 and unlikely to occur below T10, blood pressure was constantly measured to ensure that the application of FES during exercise did not pose any risk to the volunteer. He was also taken for evaluation by two physicians who found no problems to continue with the assisted cycling sessions.

Studies have already mentioned that discomfort perceived by individuals with neurological disabilities may be associated with stimulation parameters (Naaman; Stein; Thomas, 2000), although there is no consensus on the current characteristics (pulse width, frequency and amplitude) (Scheer et al., 2021; Ibitoye et al., 2016; Barss et al., 2018). Initially, the system was configured to 50Hz pulse-frequency and after the report of the volunteer, although subjective, the parameter was changed to 35Hz to minimize the perception of discomfort.

In the sixth month of the intervention protocol, the volunteer underwent surgery for testicular torsion and had to stop sessions for approximately 3 weeks. No other event

related to pain or similar to what was reported by the volunteer occurred during the training program. However, the volunteer also suffered the consequences of the COVID-19 health crisis in which, for this study specifically, the temporary closure of fitness centers and recreational spaces, as well as the distancing of family and friends, may have resulted in a physical and mental impact on him.

5.2.2 Intervention Protocol

Figure 23 illustrates the time line of the study design. The 2-year intervention protocol was based on the protocol published by Fattal et al. (2018) and was divided into a *pre-cycling* phase and two different intensity training programs. Details about each phase are described below.

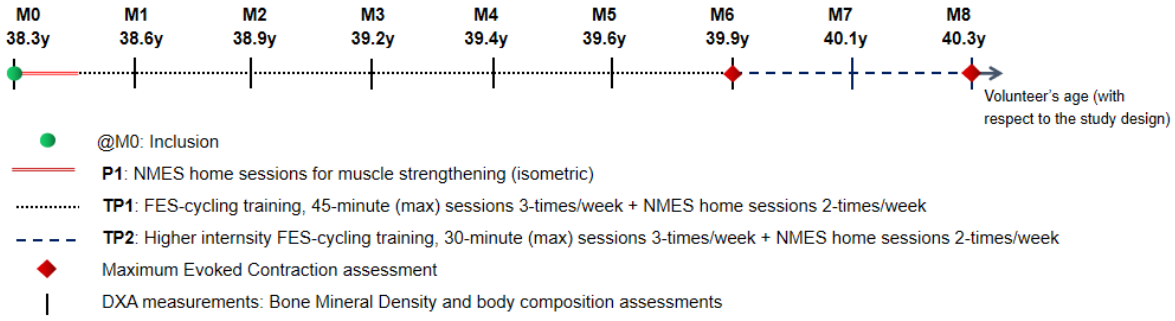

Figure 23 – Time line of the study design. P1 corresponds to the *pre-cycling* phase. **TP1** and **TP2** are the FES-*cycling* training programs. DXA Measurements M0-M8 are indicated.

Pre-cycling phase (**P1**): in the first month, the volunteer performed isometric NMES home-sessions to adapt and strengthen the lower limbs muscles prior to the FES-*cycling* intervention. Sessions lasted 30 minutes approximately and were performed 3 times a week. During each session, the volunteer remained in a sitting position and performed two 15-minute subsections to evoke contractions of the: 1) *vastus lateralis* (VL) and *rectus femoris* (RF) muscles; 2) *hamstring* (HAM) and *vastus medialis* (VM) muscles. Surface electrodes were placed as illustrated in Figure 24 respecting the configuration described in subsubsection 5.2.2.2.

An ES system with the same topology as the FES-*cycling* sessions was used. Biphasic rectangular electrical pulses were delivered at a sequence of 10s-ON/10s-OFF, alternating between the left and right sides, including a 0.5s ramping up and down in every train of pulses. The pulse parameters were set to 500μs width, 30Hz frequency and current amplitude initially adjusted to produce a muscle contraction of at least 3/5 on the quality of the evoked muscle contraction scale (Segers et al., 2014). The amplitude was automatically increased by 1mA after 5 series of pulses.

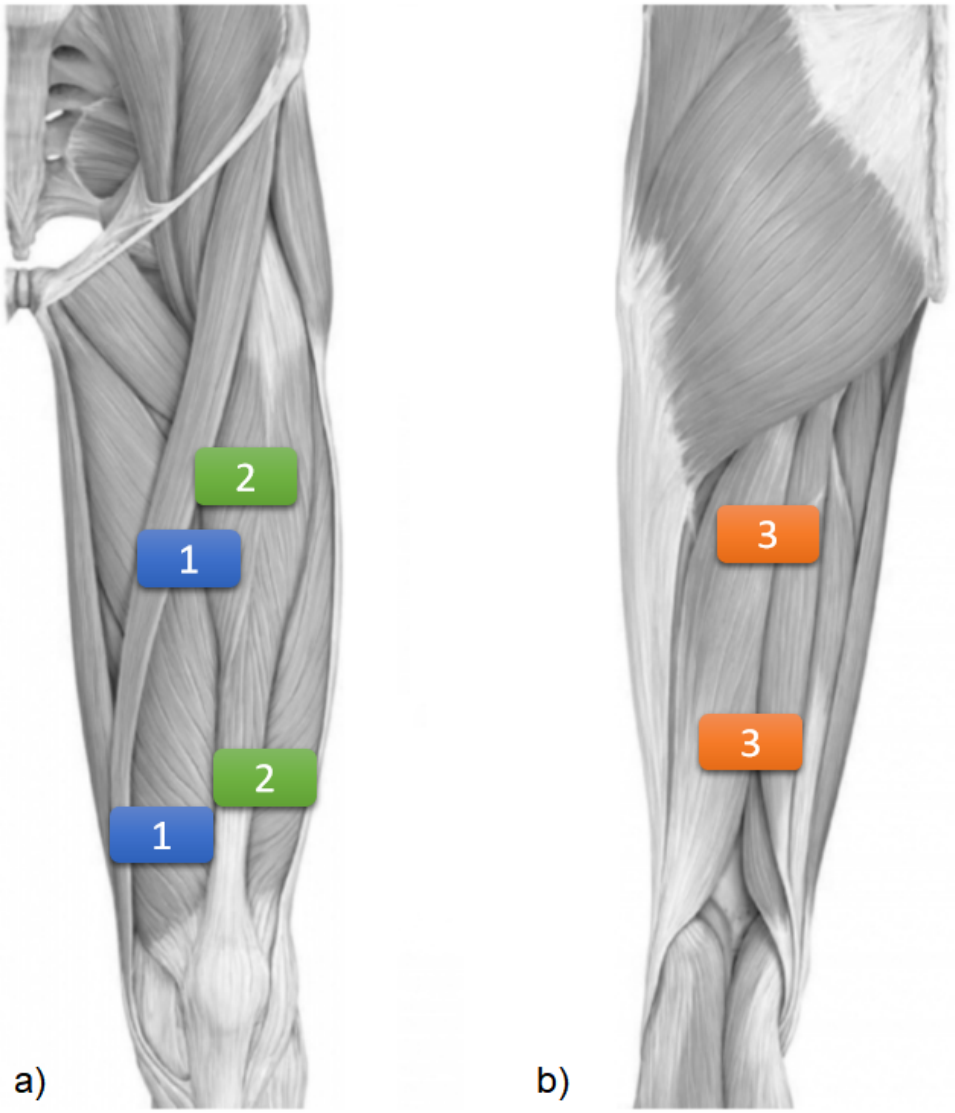

Figure 24 – Electrode Positioning over the anterior (a) and posterior (b) compartments of the thigh. Rectangular self-adhesive surface electrodes were used as indicated to evoke muscle contractions of the: 1) *vastus medialis* (VM), 2) *vastus lateralis* (VL)+*rectus femoris* (RF), and 3) *hamstring* (HAM).

FES-cycling training program (**TP**): the volunteer underwent FES-*cycling* sessions 3 times a week and maintained **P1** NMES strengthening sessions alternately twice a week. FES-*cycling* sessions were performed in two incremental intensity training programs, **TP1** and **TP2**, with maximum pedaling duration limited to 45 and 30 minutes, respectively. To increase the training intensity, the gear ratio of the tricycle and the magnetic resistance of the trainer were manually adjusted according to the expected pedaling time. In **TP2**, the pedaling difficulty was changed to require the volunteer to start the cycling session with a stimulation intensity demand corresponding to $60 - 70\%$ of the pulse amplitude necessary to reach the MEC measured (see subsubsection 5.2.2.1). As the pedaling cadence decreased due to muscle fatigue, the resistance was manually adjusted to allow the volunteer to

continue pedaling throughout the session. It was expected that different outcomes on bone mineral density and body composition could be achieved with these two different intensity protocols.

Before starting each session, the tricycle tires were calibrated and the same electrode placement was respected. A 3-minute of passive cycling (i.e., without stimulation, manually) on a stationary bike trainer stand was performed. Shortly thereafter, FES-*cycling* was initiated with the researcher just helping the pedal to come out of inertia. While maintaining pedaling, no human intervention was allowed other than the provision of water at the request of the volunteer. When fatigue interrupted pedaling, cycling was stopped and restarted after 5-10 minutes, twice more, at most. When the session finished, another 3 minutes of passive pedaling was repeated. Total distance, time, maximum and average speed were measured through a commercial speedometer (model SD-568AE, Sunding, DongGuan, China). Incremental load adjustments were made mainly by changing the bicycle's gear ratio and eventually by modifying the trainer magnetic resistance.

The reference pedaling cadence was adjusted mainly between 35 to 42rpm via the developed mobile application described in subsubsection 3.2.1.2. The stimulation parameters were also set by the same app. Pulse width was set to $500 - 600\mu s$ and frequency was adjusted to 35Hz to promote greater comfort to the volunteer. Finally, pulse amplitude was modulated by a Proportional-Integral (PI) controller and was limited to 100mA. The final stimulation pattern, the proprietary constant current topology electrical stimulation device, the mobile application interface, some mechanical aspects of the tricycle, the calf support orthoses to stabilize the volunteer's legs and the whole FES-*cycling* system were described in Chapter 3.

Most sessions were performed stationary and after the 12^{th} month, FES-*cycling* sessions were eventually held on an athletics track (non-stationary) at the Sports Training Center of the Federal University of Minas Gerais (CTE-UFMG). Since the experiments were started, pedaling time and distance were evaluated as primary functional parameters which are related to the load imposed on pedaling. Eventually, it was evaluated how long the volunteer could cycle on the track even if exceeding the session time limit. Finally, although the protocol did not aim to verify if the volunteer could meet the competition requirements of the Cybathlon 2016 (make 742m in less than 480s (Coste; Wolf, 2018)), his performance in running two laps around an athletics track (800m) was evaluated once.

5.2.2.1 Assessments

Measurements of calcified tissue in target regions of the body were established by the World Health Organization (WHO) to be performed via DXA scan tests (Varacallo M, Davis DD, Pizzutillo P, 2022), although considering it as the gold standard is still suggested as premature (Scafoglieri; Clarys, 2018). Even so, this technique is widely

adopted in the scientific literature and is recommended in the official position statement of the International Society of Clinical Densitometry (ISCD) (Morse et al., 2019).

In this work, Bone Mineral Density (BMD) and body composition (BC) measurements were assessed through the DXA scan test using the Lunar iDXA System (GE Healthcare, software: 14.10, model ME+210584) approximately every 3 months. Body composition assessed Fat Mass (FM), Lean Mass (LM) and fat mass ratio of arms, legs, trunk, android, gynoid and total body regions. BMD measurements of the Femur Total (FT), Femoral Neck (FN), pelvis and lumbar spine (LS, first to fourth lumbar vertebrae L1-L4) were evaluated. BMD was expressed as g/cm^2 and as *T-score*, which represents the Standard Deviation (SD) from the mean in a healthy, young, and compatible population. The least significant change with 95% confidence interval is $0.022 g/cm^2$ for the spine and $0.033 g/cm^2$ for the total femur. Variations below these values, in absolute terms, were not considered statistically significant. Results of previous exams were reanalyzed in order to optimize sequential densitometric monitoring.

A first evaluation was taken before the *pre-cycling* phase and corresponds to baseline values used for comparison with the subsequent assessments. A final measurement was taken after 24 months. All scans were performed by a medical doctor in accordance with the manufacturer's guidelines. Figure 25 illustrates the volunteer under the DXA test scan for the assessment of the LS region of interest.

The current amplitude of the high-intensity training program **TP2** was based on the pulse intensity required to reach the Maximal Evoked Contraction (MEC) during knee extension and flexion, which was assessed in the 18^{th} month. Isometric peak-torque for the right leg was assessed on an isokinetic dynamometer (Biodex System 4 Pro, Biodex Medical Systems, NY, United States) under stimulation parameters at frequency of 30Hz and pulse width of $500\mu s$; pulse trains of 10s and followed by a rest interval of 10s; similar to the **P1** NMES sessions. The amplitude was increased in 10mA steps, from 50mA to 100mA. The volunteer was positioned on the Biodex backrest inclined at 85^o and the equipment belts were used for stabilization. The dynamometer axis of rotation was aligned with the lateral femoral condyle, indicating the anatomical joint axis of the knee of the leg under evaluation. The fixation of the lower limbs to the active arm of the dynamometer was performed 3cm above the lateral malleolus as illustrated in Figure 26. Knee extension and flexion were assessed individually. For the first, *rectus femoris* (RF), *vastus lateralis* (VL) and *vastus medialis* (VM) muscles were electrically evoked; for the later, *hamstring* (HAM) was stimulated. The stimulation programs were applied and peak torques were measured at a 90^o position (0^o corresponds to full extension) for both (extension and flexion) tests. ES electrodes were positioned following the same configuration adopted in the training protocol (see subsubsection 5.2.2.2). The procedure was repeated in the 24^{th} month to evaluate any peak-evoked torque changes.

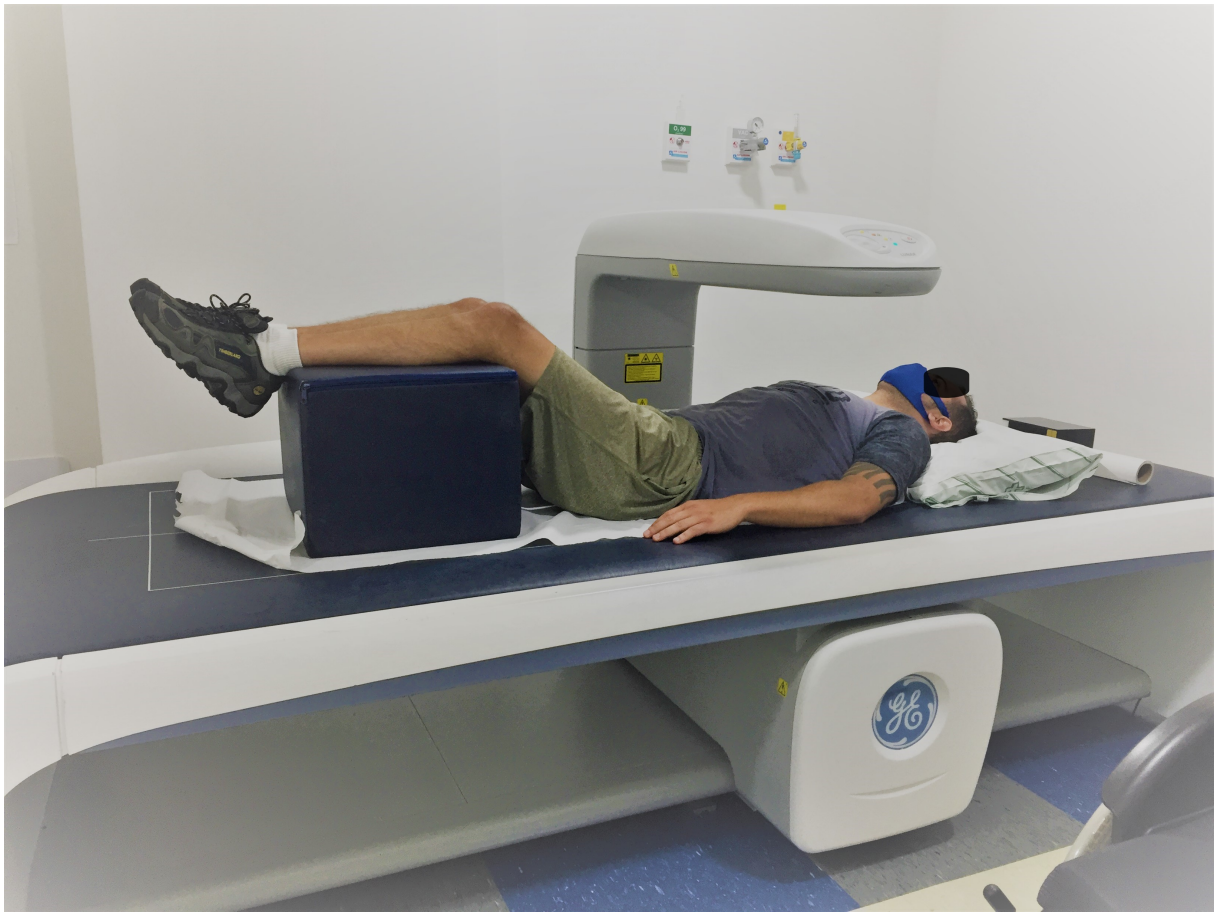

Figure 25 – Dual-Energy X-Ray Absorptiometry (DXA) scan test for the Lumbar Spine (LS) BMD assessment.

5.2.2.2 Electrode Positioning

For all protocol phases (**P1**, **TP1** and **TP2**) and for MEC evaluation, rectangular self-adhesive surface electrodes (9x5cm, Arktus®, Santa Tereza do Oeste, Brazil) were placed as illustrated in Figure 24 and are described as follows:

- *vastus medialis* (VM): one electrode 3cm above the upper edge of the patella on the distal motor point and another electrode on the proximal motor point of the same muscle;
- *vastus lateralis* (VL) + *rectus femoris* (RF): a electrode positioned 3cm above the upper edge of the patella on the distal motor point of the VL muscle and another electrode on the proximal motor point of the RF muscle;
- *hamstring* (HAM): one electrode placed 5cm above the popliteal fossa and the other 15-20cm above the popliteal fossa.

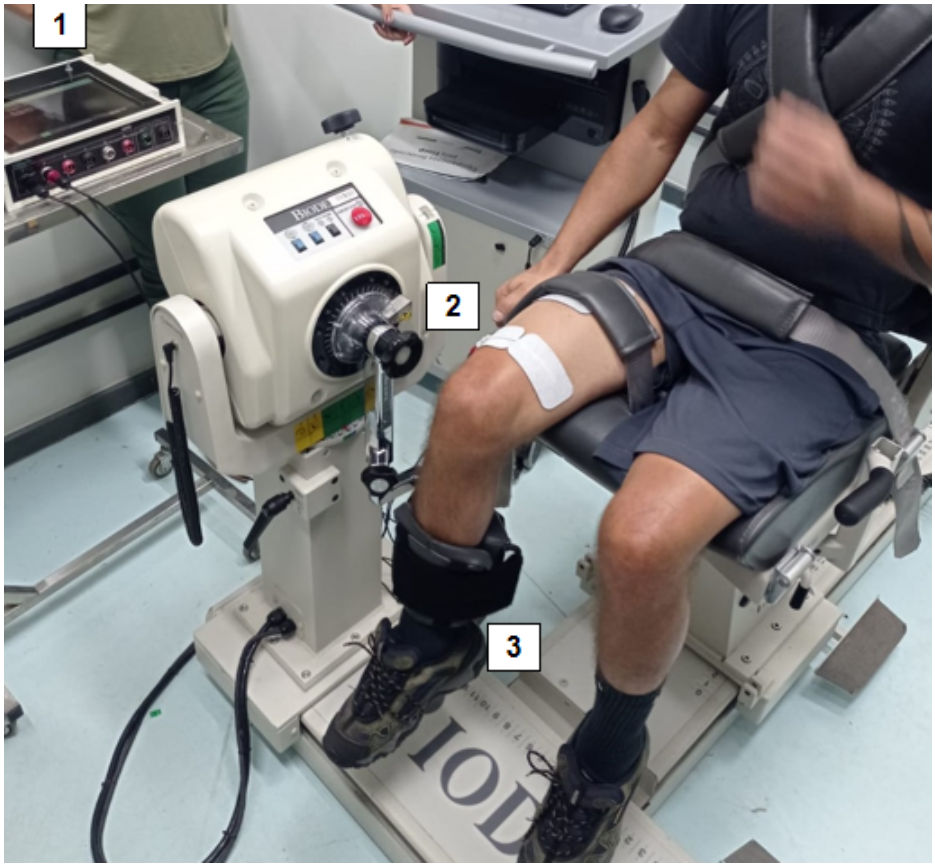

Figure 26 – Volunteer positioned on the Biodex during the MEC extension evaluation. 1) ES system; 2) electrode positioning; 3) lower limb fixation

5.3 Clinical Findings

A complete data assessment regarding changes in BMD obtained during the program intervention is presented in Table 2.

Table 2 – Changes in Bone Mineral Density.

			M0	M1	M2	M3	M4	M5	M6	M7	M8
			38.3y	38.5y	38.9y	39.2y	39.4y	39.6y	39.9y	40.1y	40.3y
Bone Mineral Density (g/cm²)	Total Body		1054	1050	1043	1040	1042	1049	1039	1038	1033
	Lumbar spine	L1	1299	1397	1363	1353	1452	1444	1396	1350	1416
		L2	1452	1524	1470	1539	1508	1455	1491	1477	1442
		L3	1486	1593	1521	1575	1574	1502	1528	1503	1526
		L4	1360	1408	1385	1383	1406	1343	1370	1328	1362
		L1-L4	1400	1480	1436	1463	1477	1432	1445	1412	1435
	Pelvis		0.788	0.783	0.791	0.764	0.797	0.788	0.790	0.781	0.738
	Femur Total	R	0.751	0.770	0.748	0.742	0.758	0.731	0.727	0.724	0.697
	Femoral Neck	R	0.727	0.728	0.713	0.699	0.706	0.694	0.679	0.685	0.662
	Legs		0.877	0.878	0.862	0.858	0.860	0.848	0.847	0.845	0.838
T-score	Total Body		-1.4	-1.5	-1.6	-1.6	-1.6	-1.5	-1.6	-1.6	-1.7
	Femoral Neck	R	-2.5	-2.3	-2.5	-2.5	-2.4	-2.6	-2.6	-2.7	-2.9
	Femur total	R	-2.6	-2.6	-2.7	-2.8	-2.7	-2.8	-2.9	-2.9	-3.0
	Lumbar Spine	L1-L4	1.5	2.2	1.8	2.0	2.1	1.8	1.9	1.6	1.8

BMD decreased in all regions of interest, with the exception of the lumbar spine.

An increase of $0.035g/cm^2$ (or 2.5%) was observed in the L1-L4 BMD and T-score progressed from +1.5 to +1.8 if compared to the baseline reference values. However, the maximum variation registered during the intervention was $+0.080g/cm^2$ and maximum T-score registerd was +2.2. Conversely, BMD decreased $0.039g/cm^2$ (-4.44%), $0.065g/cm^2$ (-8.9%), $0.054g/cm^2$ (-7.2%) and $0.050g/cm^2$ (-6.34%) in the legs, total femur, femoral neck and pelvis, respectively. T-score changed from -2.5 to -2.9 in the femoral neck and from -2.6 to -3.0 in the total femur. The total body BMD decreased by $0.021g/cm^2$ and T-score changed from -1.4 to -1.7 over the whole period.

Regarding body composition, in the first 18 months (**P1**+**TP1**), the volunteer lost 17.08%, 24.44%, 21.79% and 18.66% of fat and the fat mass ratio decrease by 4.1%, 4.8%, 5.00%, 3.3% in legs, android, gynoid and total body regions, respectively. In absolute terms, the volunteer lost 1013g, 391g, 570g and 3443g of fat in the same regions. This scenario was accompanied by a slightly increase in lean mass in legs (249g) and gynoid (32g) regions. Total body lean mass decreased by 1704g mainly because of the arms (-920g).

From the 18^{th} to the 24^{th} month (**TP2**), lean mass in legs, android, gynoid and total body regions increased by 1072g, 204g, 251g and 2368g respectively. It was also observed an overall increase of 387g, 490g, 291g and 2914g of fat mass in the same regions. Over the 24-month–study, there was a 9.78% increase lean mass and a 10.57% decrease in legs fat mass. Figure 27 highlights the body composition trend in a nutshell.

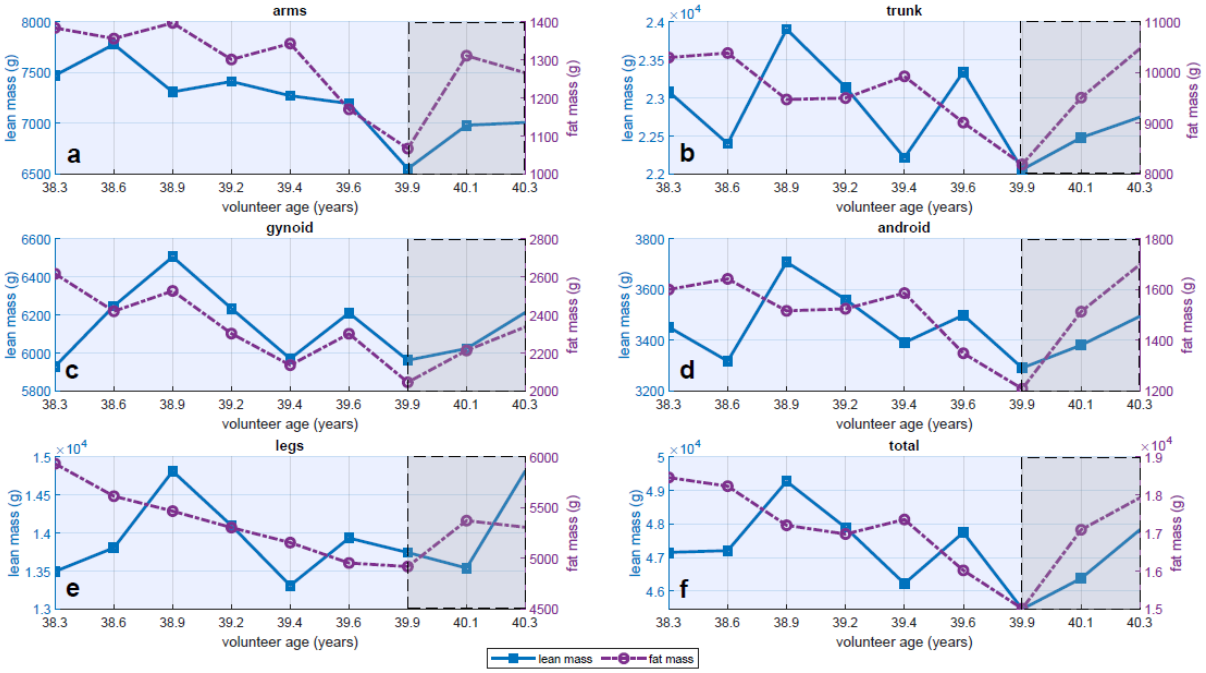

Figure 27 – Measurements of lean mass and fat mass for arms (a), trunk (b), gynoid (c), android (d), legs (e) and total body (f) regions during the 2-year protocol. The highlighted area corresponds to the **TP2** protocol phase.

A complete data assessment regarding changes in BMD and body composition

during the 2-year intervention program and other results including health, disability and quality of life reports can be assessed in Appendix C for documentation purposes.

MEC was achieved at 90mA for both extension and flexion and did not change significantly at 100mA. Extension peak torque increased from 41.3N.m to 55.7N.m $(34,9\%)$ between the 18th and 24th months but flexion slightly decreased from 19.5N.m to 18.6N.m $(4,6\%)$.

Regarding the performance results, maximum pedaling duration increased dramatically from the 2nd to the 7^{th} months, being for each month respectively (in minutes): 0.71 ± 0.18; 1.17 ± 1.57; 8.00 ± 6.21; 6.38 ± 2.29 (volunteer surgery); 39.13 ± 8.30; and 45.00 ± 0.33. In this period, the volunteer covered on the training stand a distance of 5349m at an average speed of 7.1 km/h and a maximum speed of 8.0 km/h in his best result. On the athletics track, the volunteer manage to complete 11 laps (approx. 4688m) at an average speed of 4.5km/h in 62 minutes (in the 23^{th} month). He also completed the distance requirements for the Cybathlon FES Bike Race in 495s even though the trike was not optimized for competition (weight and tyres), had not started ramp laps and had not trained for this activity. The mark reached suggests the possibility of a positive result in the competition.

5.4 Discussion

The main objective of this single-participant case report was to assess changes in BC and BMD in a 38-year-old man with complete SCI (AIS A, T8) during a 24-month period of FES-cycling. The main physiological variables were periodically evaluated via Dual-Energy X-Ray Absorptiometry (DXA) scan test, which provides a practical means to quantify both whole-body and regional changes in body composition associated with SCI (Morse et al., 2019). In this work, additional measurements including the ultrasound assessment of lower limb muscle mass and VO_2 could not be performed due to the restricted access to the UFMG laboratories during the COVID-19 pandemic.

As FES-assisted activities imply the use of electrical pulses to evoke muscle contraction, tension is exerted on the bones and adaptive bone remodeling is expected to be stimulated. Previous work has found a positive effect on bone parameters in the distal femur with active loading after a 12-month training period on a FES-assisted bicycle (Frotzler et al., 2008), although some studies have found no statistically significant change in BMD (Fattal et al., 2018) or if they reported improvement in BMD, it was not detailed in relation to body segments (Dolbow et al., 2014).

In this study, the decrease found in total femur BMD exceeded the least significant change, indicating a high risk of fracture and suggesting the initiation of recovery treatment. According to a medical evaluation, however, the volunteer could continue performing cycling

activities as the risks of fractures and joint sprains were minimized by the use of calf support orthoses described in Chapter 3. Although the assessment of increments in lumbar spine BMD is considered less relevant in the field of SCI and despite being within the normal range for a reference population composed of healthy, age-adjusted individuals (Morse et al., 2019), the findings suggest a relevant outcome in this region which was not reported previously.

Even though mineral density gains have been suggested in the literature, the results obtained during the 2-year intervention program indicated that FES-*cycling* alone may not be sufficient to improve BMD or to replace mechanical and/or vibrational loading therapies for the lower limbs. Therapies like mechanical loading are suggested to support reversing the osteoporotic process induced by SCI in long bones of the lower extremity as the stress imposed generates changes in bone size, shape and density, which stimulates the bone modeling by formation and resorption (Akkawi; Zmerly, 2018; Frost, 2003).

Individuals with SCI are also at high risk of obesity as a result of low levels of physical activity and the imbalance between energy expenditure and diet (Raguindin et al., 2021). The first 18-month results suggested that longer training sessions have a significant impact on fat loss, especially in the lower limbs. A considerable fat mass ratio decrease in all corporal regions was observed, supporting the results presented by Dolbow et al. (2014). In the 6-month **TP2** phase, there was an increase in the fat ratio differently from Fattal et al. (2021), in which sessions were also limited to 30min. However, the results of both studies may have been influenced by the absence of a controlled nutritional diet.

Although other physiological variables such VO_2 and ultrasound of the lower limbs would complement the study, the findings obtained from this case report suggested a strong possibility to be compared with other literature studies. It is important to highlighted that unlike the aforementioned studies which performed one DXA scan before and another after the end of the intervention protocol, this study assessed BMD and body composition periodically, which allowed a consistent analysis of the results obtained from different intensity training programs.

It is therefore suggested that more frequent assessments may better indicate the impact of FES-*cycling* on body composition. For example, the gain in muscle mass in the legs throughout the period was consistent with the case studies cited, but the periodic evaluation evidenced an oscillation not previously reported and allowed to observe the effect of the different proposed training. Finally, the results regarding BMD support that areal measurements by DXA in persons with a traumatic SCI at the distal femur, but not the lumbar spine, are substantially lower than that of the general population of similar age and gender (Morse et al., 2019).

5.5 Conclusion

It is concluded that 2 years of FES-*cycling* in a SCI volunteer increased BMD in the lumbar spine, but not in the femur region of interest. The BMD decrease in the femur zone suggests caution in the hypotheses that FES-*cycling* can improve the BMD of lower limbs in this population. However, body composition findings support that FES-*cycling* can restore muscle mass, improve evoked force and decrease fat mass if associated with adequate training and reinforced by a controlled nutrition program.

5.6 Patient Perspective

The volunteer had expectations to try new assistive technologies and participate in a study in an institution of the grandeur of the Federal University of Minas Gerais (UFMG), which were all met. He reported having had no difficulties in participating in the study, except for the period of isolation to which he was submitted due to the COVID-19 pandemic. He also mentioned that the results obtained had a positive impact on his health and that he would participate again in similar studies. He highlights the gain in muscle lean mass and improvement in his quality of life as being positive, with no negative points. In general, he is grateful for the opportunity to have participated as a volunteer, that he thought the project was sensational, and that he tried to do his best believing that it would motivate other people with disabilities. Finally, he thinks that having participated in the project can somehow immortalize him, because other future generations will study this subject and will also feel inspired to help people with reduced mobility.

5.7 Lessons Learned from the Author

Based on a better view after 2 years of a intervention protocol following a volunteer with complete SCI and based on the experience I have acquired during the research, despite several limitations imposed by the COVID-19 pandemic, I would have included in the project the analysis of: 1) the quadriceps tendon using Magnetic Resonance Imaging (MRI) to minimize the risk of joint sprains; 2) ultrasound of the lower limbs for a more frequent analysis of the muscle response to the training program; 3) a chest strap heart-rate monitor to measure and document the heart rate of during cycling sessions. I would also have included a controlled nutritional diet accompanied by a questionnaire to assess the volunteer's adherence to the proposed diet in order to reduce the biased results brought by inadequate food intake.

There was a great learning experience in having to work without the support of a multidisciplinary team (in large part due to the study having started during the critical period of the pandemic), however, the contributions of professionals from other areas

(nutrition, physiotherapy, physical education) could have greatly enriched the research. Furthermore, with the assistance of other researchers and professionals, more volunteers could have participated in the study.

Anyway, from a personal point of view, the results obtained during this research were very enriching, in several aspects. Figure 28 illustrates the author and the volunteer in one of the non-stationary sessions being performed at CTE-UFMG.

Figure 28 – This picture needs no caption.

6 Summary and Research Perspectives

Although Functional Electrical Stimulation (FES) assisted exercises have great potential to improve the functional level of individuals with Spinal Cord Injury and increase their quality of life, numerous challenges are still observed, such as the complexity of implementation or even the inaccessibility to FES-assisted technologies.

The present D.Sc. dissertation discussed all aspects necessary to implement an adaptive FES-cycling system and opened the design of an High-Capacity Functional Electrical Stimulation (HCFES) system to the entire scientific community. Firmware, hardware and software are available for download and different Functional Electrical Stimulation strategies can be implemented in the clinic or for research purposes using this project.

In addition to evaluate the HCFES electrical stimulation capabilities, it was demonstrated the system's high computational capacity as it was able to embed relatively-complex machine learning algorithms to improve the definition of stimulation parameters for the FES-cycling exercise modality. The feature introduced by this D.Sc. dissertation has a potential to overcome the complexity and time-consuming process of defining the stimulation parameters that discourage the use of FES-assisted exercices for clinical or research purposes.

The method proposed in this work also demonstrated the possibility of using reinforcement learning methods to control and adjust the stimulation parameters in order to track desired cadences. It was also suggested that the proposed algorithm can generate a positive impact on the efficiency of electrical stimuli during FES-cycling sessions since the electrical charge spent to maintain a predefined cadence can be reduced. This feature opens a pathway to study the use of machine learning algoithms in FES-assisted modalities in the future.

Future work will address the use of RL methods in the development of novel control strategies to improve the pedaling endurance by reducing the onset muscle fatigue occurrence. It is of interest to evaluate how a more efficient stimulation cost as consequence of the dynamic change of the baseline stimulation pattern can delay the muscle fatigue and increase the cycling performance.

The High-Capacity Functional Electrical Stimulation (HCFES) system's applicability was also validated with a volunteer with complete paraplegia and an intervention program of two years was performed. Body composition and BMD were accessed frequently and the obtained findings support that FES-cycling can restore muscle mass, improve evoked force and decrease fat mass if associated with adequate training and reinforced by

a controlled nutrition program.

Further randomized controlled studies should investigate if there is causality relationship between FES-*cycling* training, increase in BMD and controlled nutritional diet.

References

Ahuja, C. S.; Wilson, J. R.; Nori, S.; Kotter, M. R. N.; Druschel, C.; Curt, A.; Fehlings, M. G. Traumatic spinal cord injury. **Nature Reviews Disease Primers**, v. 3, n. 1, p. 17018, Apr 2017. ISSN 2056-676X. https://doi.org/10.1038/nrdp.2017.18.

Akkawi, I.; Zmerly, H. Osteoporosis: Current Concepts. **Joints**, v. 6, n. 2, p. 122–127, jun. 2018.

Alizadeh, A.; Dyck, S. M.; Karimi-Abdolrezaee, S. Traumatic Spinal Cord Injury: An Overview of Pathophysiology, Models and Acute Injury Mechanisms. **Frontiers in Neurology**, v. 10, 2019. ISSN 1664-2295. https://www.frontiersin.org/articles/10.3389/fneur.2019.00282.

Allen KJ, Leslie SW. **AUTONOMIC DYSREFLEXIA. [UPDATED 2022 MAY 27]**. In: StatPearls [Internet]. Treasure Island (FL): StatPearls Publishing, 2022. https://www.ncbi.nlm.nih.gov/books/NBK482434/.

Barss, T. S.; Ainsley, E. N.; Claveria-Gonzalez, F. C.; Luu, M. J.; Miller, D. J.; Wiest, M. J.; Collins, D. F. Utilizing physiological principles of motor unit recruitment to reduce fatigability of electrically-evoked contractions: A narrative review. **Arch. Phys. Med. Rehabil.**, Elsevier BV, v. 99, n. 4, p. 779–791, abr. 2018.

Bear, M. F.; Connors, B. W.; Paradiso, M. A. **Neuroscience**. 4. ed. Philadelphia, PA: Lippincott Williams and Wilkins, 2015.

Bellman, M. J.; Cheng, T.-H.; Downey, R. J.; Hass, C. J.; Dixon, W. E. Switched control of cadence during stationary cycling induced by functional electrical stimulation. **IEEE Transactions on Neural Systems and Rehabilitation Engineering**, Institute of Electrical and Electronics Engineers (IEEE), v. 24, n. 12, p. 1373–1383, dez. 2016. https://doi.org/10.1109/tnsre.2015.2500180.

Bellman, M. J.; Downey, R. J.; Parikh, A.; Dixon, W. E. Automatic control of cycling induced by functional electrical stimulation with electric motor assistance. **IEEE Transactions on Automation Science and Engineering**, v. 14, n. 2, p. 1225–1234, 2017.

Bennett J, M Das J, Emmady PD. **Spinal Cord Injuries. [Updated 2022 May 11]**. In: StatPearls [Internet]. Treasure Island (FL): StatPearls Publishing, 2022. https://www.ncbi.nlm.nih.gov/books/NBK560721/?report=classic.

Betz, R.; Biering-Sørensen, F.; Burns, S. P.; Donovan, W.; Graves, D. E.; Guest, J.; Jones, L.; Kirshblum, S.; Krassioukov, A.; Mulcahey, M. J.; Read, M. S.; Rodriguez, G. M.; Rupp, R.; Schuld, C.; Tansey, K.; Walden, K.; ASIA; Committee, I. I. S. The 2019 revision of the international standards for neurological classification of spinal cord injury (isncsci)—what's new? **Spinal Cord**, v. 57, n. 10, p. 815–817, Oct 2019. ISSN 1476-5624. https://doi.org/10.1038/s41393-019-0350-9.

Blazevich, A. J.; Collins, D. F.; Millet, G. Y.; Vaz, M. A.; Maffiuletti, N. A. Enhancing adaptations to neuromuscular electrical stimulation training interventions. **Exercise and**

Sport Sciences Reviews, Ovid Technologies (Wolters Kluwer Health), v. 49, n. 4, p. 244–252, jun. 2021. https://doi.org/10.1249/jes.0000000000000264.

Bo, A. P.; Fonseca, L. O. da; Guimaraes, J. A.; Fachin-Martins, E.; Paredes, M. E.; Brindeiro, G. A.; Sousa, A. C. C. de; Dorado, M. C.; Ramos, F. M. Cycling with spinal cord injury: A novel system for cycling using electrical stimulation for individuals with paraplegia, and preparation for cybathlon 2016. **IEEE Robotics Automation Magazine**, v. 24, n. 4, p. 58–65, 2017.

Boncompagni, S. Severe muscle atrophy due to spinal cord injury can be reversed in complete absence of peripheral nerves. **European Journal of Translational Myology**, v. 22, n. 4, p. 161–200, Dec. 2012. https://www.pagepressjournals.org/index.php/bam/article/view/bam.2012.4.161.

Botelho, R. V.; Albuquerque, L. D. G.; Junior, R. B.; Júnior, A. A. A. **Epidemiology of traumatic spinal injuries in Brazil: systematic review**. **Arquivos Brasileiros de Neurocirurgia: Brazilian Neurosurgery**, Georg Thieme Verlag KG, v. 33, n. 02, p. 100–106, jun. 2014. https://doi.org/10.1055/s-0038-1626255.

Bristow, D.; Tharayil, M.; Alleyne, A. A survey of iterative learning control. **IEEE Control Systems Magazine**, v. 26, n. 3, p. 96–114, 2006.

Champs, A. P. S.; Maia, G. A. G.; Oliveira, F. G.; Melo, G. C. N. de; Soares, M. M. S. Osteoporosis-related fractures after spinal cord injury: a retrospective study from brazil. **Spinal Cord**, Springer Science and Business Media LLC, v. 58, n. 4, p. 484–489, nov. 2019. https://doi.org/10.1038/s41393-019-0387-9.

Coelho-Magalhães, T.; Vilaça-Martins, A. F.; Araújo, P. A.; Resende-Martins, H. Programmable Multichannel Neuromuscular Electrostimulation System: A Universal Platform for Functional Electrical Stimulation. In: Bastos-Filho, T. F.; Caldeira, E. M. de O.; Frizera-Neto, A. (Ed.). **XXVII Brazilian Congress on Biomedical Engineering**. Cham: Springer International Publishing, 2022. p. 1371–1377. ISBN 978-3-030-70601-2.

Coelho-Magalhães, T.; Amaral, G. M.; Silva, P. E.; Resende-Martins, H. Effects on Bone Mineral Density and Body Composition During 24 months of FES-assisted Cycling: Case Report of a 38-year-old Male with Paraplegia. **Case Report Submitted**, 2022.

Coelho-Magalhães, T.; Coste, C. A.; Resende-Martins, H. A Novel Functional Electrical Stimulation-Induced Cycling Controller Using Reinforcement Learning to Optimize Online Muscle Activation Pattern. **Sensors**, v. 22, n. 23, 2022. ISSN 1424-8220. https://www.mdpi.com/1424-8220/22/23/9126.

Coelho-Magalhães, T.; Fachin-Martins, E.; Silva, A.; Coste, C. A.; Resende-Martins, H. Development of a High-Power Capacity Open Source Electrical Stimulation System to Enhance Research into FES-Assisted Devices: Validation of FES Cycling. **Sensors**, v. 22, n. 2, 2022. ISSN 1424-8220. https://www.mdpi.com/1424-8220/22/2/531.

Coelho-Magalhães, Tiago. **Sistema de Eletroestimulação Neuromuscular Multicanais Programável para o Auxílio da Marcha de Pacientes Portadores de Deficiência Motora**. Programa de Pós-graduação em Engenharia Elétrica da UFMG, 2018. https://www.ppgee.ufmg.br/defesas/1581M.PDF.

Coste, C. A.; Wolf, P. FES-cycling at cybathlon 2016: Overview on teams and results. **Artif. Organs**, v. 42, n. 3, p. 336–341, mar. 2018.

Cousin, C.; Duenas, V.; Dixon, W. Fes cycling and closed-loop feedback control for rehabilitative human–robot interaction. **Robotics**, v. 10, n. 2, 2021. ISSN 2218-6581. https://www.mdpi.com/2218-6581/10/2/61.

Doheny, E. P.; Caulfield, B. M.; Minogue, C. M.; Lowery, M. M. Effect of subcutaneous fat thickness and surface electrode configuration during neuromuscular electrical stimulation. **Medical Engineering Physics**, v. 32, n. 5, p. 468–474, 2010. ISSN 1350-4533. https://www.sciencedirect.com/science/article/pii/S135045331000055X.

Dolbow, D. R.; Gorgey, A. S.; Gater, D. R.; Moore, J. R. Body composition changes after 12 months of FES cycling: case report of a 60-year-old female with paraplegia. **Spinal Cord**, Springer Science and Business Media LLC, v. 52, n. S1, p. S3–S4, jun. 2014. https://doi.org/10.1038/sc.2014.40.

Duenas, V. H.; Cousin, C. A.; Ghanbari, V.; Fox, E. J.; Dixon, W. E. Torque and cadence tracking in functional electrical stimulation induced cycling using passivity-based spatial repetitive learning control. **Automatica**, v. 115, p. 108852, 2020. ISSN 0005-1098. https://www.sciencedirect.com/science/article/pii/S0005109820300509.

Duenas, V. H.; Cousin, C. A.; Parikh, A.; Dixon, W. E. Functional electrical stimulation induced cycling using repetitive learning control. In: **2016 IEEE 55th Conference on Decision and Control (CDC)**. 2016. p. 2190–2195.

Duenas, V. H.; Cousin, C. A.; Rouse, C.; Fox, E. J.; Dixon, W. E. Distributed repetitive learning control for cooperative cadence tracking in functional electrical stimulation cycling. **IEEE Transactions on Cybernetics**, Institute of Electrical and Electronics Engineers (IEEE), v. 50, n. 3, p. 1084–1095, mar. 2020. https://doi.org/10.1109/tcyb.2018.2882755.

Fattal, C.; Schmoll, M.; Guillou, R. L.; Raoult, B.; Frey, A.; Carlier, R.; Azevedo-Coste, C. Benefits of 1-yr home training with functional electrical stimulation cycling in paraplegia during covid-19 crisis. **American Journal of Physical Medicine & Rehabilitation**, v. 100, n. 12, 2021. ISSN 0894-9115. https://journals.lww.com/ajpmr/Fulltext/2021/12000/Benefits_of_1_Yr_Home_Training_With_Functional.6.aspx.

Fattal, C.; Sijobert, B.; Daubigney, A.; Lucas, B.; Azevedo-Coste, C. The feasibility of training with fes-assisted cycling: Psychological, physical and physiological consideration. **Annals of Physical and Rehabilitation Medicine**, v. 60, p. e15, 2017. ISSN 1877-0657. 32nd Annual Congress of the French Society of Physical and Rehabilitation Medicine. https://www.sciencedirect.com/science/article/pii/S187706571730324X.

Fattal, C.; Sijobert, B.; Daubigney, A.; Fachin-Martins, E.; Lucas, B.; Casillas, J.-M.; Azevedo, C. Training with FES-assisted cycling in a subject with spinal cord injury: Psychological, physical and physiological considerations. **The Journal of Spinal Cord Medicine**, Informa UK Limited, v. 43, n. 3, p. 402–413, jul. 2018. https://doi.org/10.1080/10790268.2018.1490098.

Fonseca, L. O. da; Bó, A. P.; Guimarães, J. A.; Gutierrez, M. E.; Fachin-Martins, E. Cadence tracking and disturbance rejection in functional electrical stimulation cycling for paraplegic subjects: A case study. **Artificial Organs**, Wiley, v. 41, n. 11, p. E185–E195, nov. 2017. https://doi.org/10.1111/aor.13055.

Frost, H. M. Bone's mechanostat: A 2003 update. **The Anatomical Record Part A: Discoveries in Molecular, Cellular, and Evolutionary Biology**, v. 275A, n. 2, p. 1081–1101, 2003. https://anatomypubs.onlinelibrary.wiley.com/doi/abs/10.1002/ar.a.10119.

Frotzler, A.; Coupaud, S.; Perret, C.; Kakebeeke, T. H.; Hunt, K. J.; Donaldson, N. de N.; Eser, P. High-volume FES-cycling partially reverses bone loss in people with chronic spinal cord injury. **Bone**, Elsevier BV, v. 43, n. 1, p. 169–176, jul. 2008. https://doi.org/10.1016/j.bone.2008.03.004.

Galea, M. P.; Dunlop, S. A.; Davis, G. M.; Nunn, A.; Geraghty, T.; Hsueh, Y. seng; Churilov, L. Intensive exercise program after spinal cord injury ("full-on"): study protocol for a randomized controlled trial. **Trials**, Springer Science and Business Media LLC, v. 14, n. 1, p. 291, 2013. https://doi.org/10.1186/1745-6215-14-291.

Gibbons, R. S.; Beaupre, G. S.; Kazakia, G. J. FES-rowing attenuates bone loss following spinal cord injury as assessed by HR-pQCT. **Spinal Cord Series and Cases**, Springer Science and Business Media LLC, v. 2, n. 1, abr. 2016. https://doi.org/10.1038/scsandc.2015.41.

Gorgey, A. S.; Dolbow, D. R.; Dolbow, J. D.; Khalil, R. K.; Castillo, C.; Gater, D. R. **Effects of spinal cord injury on body composition and metabolic profile – Part I, journal = The Journal of Spinal Cord Medicine**. Informa UK Limited, v. 37, n. 6, p. 693–702, jul. 2014. https://doi.org/10.1179/2045772314y.0000000245.

Gregory, C. M.; Bickel, C. S. Recruitment Patterns in Human Skeletal Muscle During Electrical Stimulation. **Physical Therapy**, v. 85, n. 4, p. 358–364, 04 2005. ISSN 0031-9023. https://doi.org/10.1093/ptj/85.4.358.

Guillou, R. L.; Schmoll, M.; Sijobert, B.; Borges, D. L.; Fachin-Martins, E.; Resende, H.; Pissard-Gibollet, R.; Fattal, C.; Coste, C. A. A novel framework for quantifying accuracy and precision of event detection algorithms in fes-cycling. **Sensors**, v. 21, n. 13, 2021. ISSN 1424-8220. https://www.mdpi.com/1424-8220/21/13/4571.

Guimarães, J. A.; Fonseca, L. O. da; Santos-Couto-Paz, C. C. D.; Bó, A. P. L.; Fattal, C.; Azevedo-Coste, C.; Fachin-Martins, E. Towards parameters and protocols to recommend FES-cycling in cases of paraplegia: A preliminary report. **Eur. J. Transl. Myol.**, v. 26, n. 3, p. 6085, jun. 2016.

Hall, P. J. E. **Guyton and Hall Textbook of Medical Physiology**. 2015. ISBN 9781455770052.

Hamid, S.; Hayek, R. Role of electrical stimulation for rehabilitation and regeneration after spinal cord injury: an overview. **European Spine Journal**, Springer Science and Business Media LLC, v. 17, n. 9, p. 1256–1269, ago. 2008. https://doi.org/10.1007/s00586-008-0729-3.

Ho, C. H.; Triolo, R. J.; Elias, A. L.; Kilgore, K. L.; DiMarco, A. F.; Bogie, K.; Vette, A. H.; Audu, M. L.; Kobetic, R.; Chang, S. R.; Chan, K. M.; Dukelow, S.; Bourbeau, D. J.; Brose, S. W.; Gustafson, K. J.; Kiss, Z. H. T.; Mushahwar, V. K. Functional electrical stimulation and spinal cord injury. **Phys. Med. Rehabil. Clin. N. Am.**, v. 25, n. 3, p. 631–54, ix, ago. 2014.

Hunt, K.; Fang, J.; Saengsuwan, J.; Grob, M.; Laubacher, M. On the efficiency of FES cycling: A framework and systematic review. **Technology and Health Care**, IOS Press, v. 20, n. 5, p. 395–422, set. 2012. https://doi.org/10.3233/thc-2012-0689.

Ibitoye, M. O.; Hamzaid, N. A.; Hasnan, N.; Wahab, A. K. A.; Davis, G. M. Strategies for rapid muscle fatigue reduction during FES exercise in individuals with spinal cord injury: A systematic review. **PLOS ONE**, Public Library of Science (PLoS), v. 11, n. 2, p. e0149024, fev. 2016. https://doi.org/10.1371/journal.pone.0149024.

Jubeau, M.; Gondin, J.; Martin, A.; Sartorio, A.; Maffiuletti, N. Random motor unit activation by electrostimulation. **International Journal of Sports Medicine**, Georg Thieme Verlag KG, v. 28, n. 11, p. 901–904, nov. 2007. https://doi.org/10.1055/s-2007-965075.

Maffiuletti, N. A. Physiological and methodological considerations for the use of neuromuscular electrical stimulation. **European Journal of Applied Physiology**, Springer Science and Business Media LLC, v. 110, n. 2, p. 223–234, maio 2010. https://doi.org/10.1007/s00421-010-1502-y.

Magee, D. J.; Zachazewski, J. E.; Quillen, W. S. **Scientific Foundations and Principles of Practice in Musculoskeletal Rehabilitation**. 2007. ISBN 1416002502.

Mata, A. S.; Torras, A. B.; Carrillo, J. A. C.; Juanco, F. E.; Fernández, A. J. G.; Martínez, F. N.; Fernández, A. O. **Fundamentals of Machine Theory and Mechanisms**. Springer International Publishing, 2016. https://doi.org/10.1007/978-3-319-31970-4.

Melo, P.; Silva, M.; Martins, J.; Newman, D. Technical developments of functional electrical stimulation to correct drop foot: Sensing, actuation and control strategies. **Clinical Biomechanics**, Elsevier BV, v. 30, n. 2, p. 101–113, fev. 2015. https://doi.org/10.1016/j.clinbiomech.2014.11.007.

Mendell, L. M. The size principle: a rule describing the recruitment of motoneurons. **Journal of Neurophysiology**, v. 93, n. 6, p. 3024–3026, 2005. PMID: 15914463. https://doi.org/10.1152/classicessays.00025.2005.

Metani, A.; Popović-Maneski, L.; Mateo, S.; Lemahieu, L.; Bergeron, V. Functional electrical stimulation cycling strategies tested during preparation for the first cybathlon competition – a practical report from team ens de lyon. **European Journal of Translational Myology**, v. 27, n. 4, Dec. 2017. https://www.pagepressjournals.org/index.php/bam/article/view/7110.

Moon, J.-Y.; Hwang, T.-S.; Sim, S.-J.; Chun, S.-I.; Kim, M. Surface mapping of motor points in biceps brachii muscle. **Ann. Rehabil. Med.**, Korean Academy of Rehabilitation Medicine, v. 36, n. 2, p. 187–196, abr. 2012.

Morse, L. R.; Biering-Soerensen, F.; Carbone, L. D.; Cervinka, T.; Cirnigliaro, C. M.; Johnston, T. E.; Liu, N.; Troy, K. L.; Weaver, F. M.; Shuhart, C.; Craven, B. C. Bone mineral density testing in spinal cord injury: 2019 ISCD official position. **Journal of Clinical Densitometry**, Elsevier BV, v. 22, n. 4, p. 554–566, out. 2019. https://doi.org/10.1016/j.jocd.2019.07.012.

Naaman, S. C.; Stein, R. B.; Thomas, C. Minimizing discomfort with surface neuromuscular stimulation. **Neurorehabilitation and Neural Repair**, SAGE Publications, v. 14, n. 3, p. 223–228, set. 2000. https://doi.org/10.1177/154596830001400308.

Nas, K. **Rehabilitation of spinal cord injuries**. **World Journal of Orthopedics**, Baishideng Publishing Group Inc., v. 6, n. 1, p. 8, 2015. https://doi.org/10.5312/wjo.v6.i1.8.

Nascimento, T. L. do; Rogério, L. P. W.; Reis, M. M. dos; Almeida, L. P. de; Finger, G.; GREGGIANIN, G. F.; Nascimento, T. L. do; Cecchini, A. M. de L.; Cecchini, F. M. de L.; Sfreddo, E. Thoracolumbar spinal arthrodesis - epidemiology and costs. **Coluna/Columna**, FapUNIFESP (SciELO), v. 16, n. 1, p. 52–55, jan. 2017. https://doi.org/10.1590/s1808-185120171601162774.

Peckham, P. H.; Knutson, J. S. Functional electrical stimulation for neuromuscular applications. **Annual Review of Biomedical Engineering**, Annual Reviews, v. 7, n. 1, p. 327–360, ago. 2005. https://doi.org/10.1146/annurev.bioeng.6.040803.140103.

Rabello, R.; Fröhlich, M.; Maffiuletti, N. A.; Vaz, M. A. Influence of pulse waveform and frequency on evoked torque, stimulation efficiency, and discomfort in healthy subjects. **American Journal of Physical Medicine &amp Rehabilitation**, Ovid Technologies (Wolters Kluwer Health), v. 100, n. 2, p. 161–167, jul. 2020. https://doi.org/10.1097/phm.0000000000001541.

Ragnarsson, K. T. Functional electrical stimulation after spinal cord injury: current use, therapeutic effects and future directions. **Spinal Cord**, v. 46, n. 4, p. 255–274, Apr 2008. ISSN 1476-5624. https://doi.org/10.1038/sj.sc.3102091.

Ragnarsson, K. T.; Szecsi, J.; Straube, A.; Fornusek, C. Functional electrical stimulation after spinal cord injury: current use, therapeutic effects and future directions. **Spinal Cord**, v. 46, n. 4, p. 255–274, Apr 2008. ISSN 1476-5624. https://doi.org/10.1038/sj.sc.31020TY-JOUR.

Raguindin, P. F.; Bertolo, A.; Zeh, R. M.; Fränkl, G.; Itodo, O. A.; Capossela, S.; Bally, L.; Minder, B.; Brach, M.; Eriks-Hoogland, I.; Stoyanov, J.; Muka, T.; Glisic, M. Body composition according to spinal cord injury level: A systematic review and meta-analysis. **Journal of Clinical Medicine**, MDPI AG, v. 10, n. 17, p. 3911, ago. 2021. https://doi.org/10.3390/jcm10173911.

Riley, D. S.; Barber, M. S.; Kienle, G. S.; Aronson, J. K.; von Schoen-Angerer, T.; Tugwell, P.; Kiene, H.; Helfand, M.; Altman, D. G.; Sox, H.; Werthmann, P. G.; Moher, D.; Rison, R. A.; Shamseer, L.; Koch, C. A.; Sun, G. H.; Hanaway, P.; Sudak, N. L.; Kaszkin-Bettag, M.; Carpenter, J. E.; Gagnier, J. J. Care guidelines for case reports: explanation and elaboration document. **Journal of Clinical Epidemiology**, v. 89, p. 218–235, 2017. ISSN 0895-4356. https://www.sciencedirect.com/science/article/pii/S0895435617300379.

Roberts, T. T.; Leonard, G. R.; Cepela, D. J. **Classifications In Brief: American Spinal Injury Association (ASIA) Impairment Scale**, journal = Clinical Orthopaedics &amp Related Research. Ovid Technologies (Wolters Kluwer Health), v. 475, n. 5, p. 1499–1504, maio 2017. https://doi.org/10.1007/s11999-016-5133-4.

Robinson, A.; Robinson, A.; Snyder-Mackler, L. **Clinical Electrophysiology: Electrotherapy and Electrophysiologic Testing**. Wolters Kluwer Health/Lippincott Williams & Wilkins, 2008. (Point (Lippincott Williams and Wilkins) Series). ISBN 9780781744843. https://books.google.com.br/books?id=C2-9bcIjPBsC.

Rouhani, H.; Same, M.; Masani, K.; Li, Y. Q.; Popovic, M. R. PID controller design for FES applied to ankle muscles in neuroprosthesis for standing balance. **Frontiers in Neuroscience**, Frontiers Media SA, v. 11, jun. 2017. https://doi.org/10.3389/fnins.2017.00347.

Scafoglieri, A.; Clarys, J. P. Dual energy x-ray absorptiometry: gold standard for muscle mass? **J. Cachexia Sarcopenia Muscle**, v. 9, n. 4, p. 786–787, ago. 2018.

Schauer, T. Sensing motion and muscle activity for feedback control of functional electrical stimulation: Ten years of experience in berlin. **Annual Reviews in Control**, v. 44, p. 355–374, 2017. ISSN 1367-5788. https://www.sciencedirect.com/science/article/pii/S1367578817301141.

Scheer, J. W. van der; Goosey-Tolfrey, V. L.; Valentino, S. E.; Davis, G. M.; Ho, C. H. Functional electrical stimulation cycling exercise after spinal cord injury: a systematic review of health and fitness-related outcomes. **Journal of NeuroEngineering and Rehabilitation**, v. 18, n. 1, p. 99, Jun 2021. ISSN 1743-0003. https://doi.org/10.1186/s12984-021-00882-8.

Schmoll, M.; Guillou, R. L.; Borges, D. L.; Fattal, C.; Fachin-Martins, E.; Coste, C. A. Standardizing fatigue-resistance testing during electrical stimulation of paralysed human quadriceps muscles, a practical approach. **Journal of NeuroEngineering and Rehabilitation**, Springer Science and Business Media LLC, v. 18, n. 1, jan. 2021. https://doi.org/10.1186/s12984-021-00805-7.

Segers, J.; Hermans, G.; Bruyninckx, F.; Meyfroidt, G.; Langer, D.; Gosselink, R. Feasibility of neuromuscular electrical stimulation in critically ill patients. **J. Crit. Care**, Elsevier BV, v. 29, n. 6, p. 1082–1088, dez. 2014.

Sezer, N. Chronic complications of spinal cord injury. **World Journal of Orthopedics**, Baishideng Publishing Group Inc., v. 6, n. 1, p. 24, 2015. https://doi.org/10.5312/wjo.v6.i1.24.

Siddiqui, A. M.; Khazaei, M.; Fehlings, M. G. Translating mechanisms of neuroprotection, regeneration, and repair to treatment of spinal cord injury. In: **Sensorimotor Rehabilitation - At the Crossroads of Basic and Clinical Sciences**. Elsevier, 2015. p. 15–54. https://doi.org/10.1016/bs.pbr.2014.12.007.

Sijobert, B.; Le Guillou, R.; Fattal, C.; Azevedo Coste, C. FES-Induced Cycling in Complete SCI: A Simpler Control Method Based on Inertial Sensors. **Sensors**, v. 19, n. 19, 2019. ISSN 1424-8220. doi:10.3390/s19194268.

Sutton, R. S.; Barto, A. G. **Reinforcement Learning**. 2. ed. Cambridge, MA: Bradford Books, 2018. (Adaptive Computation and Machine Learning series).

Varacallo M, Davis DD, Pizzutillo P. **Osteoporosis in Spinal Cord Injuries. [Updated 2022 Feb 12]**. In: StatPearls [Internet]. Treasure Island (FL): StatPearls Publishing, 2022. https://www.ncbi.nlm.nih.gov/books/NBK526109/.

Varma, A. K.; Das, A.; Wallace, G.; Barry, J.; Vertegel, A. A.; Ray, S. K.; Banik, N. L. Spinal cord injury: A review of current therapy, future treatments, and basic science frontiers. **Neurochemical Research**, Springer Science and Business Media LLC, v. 38, n. 5, p. 895–905, mar. 2013. https://doi.org/10.1007/s11064-013-0991-6.

Wannawas, N.; Subramanian, M.; Faisal, A. A. Neuromechanics-based deep reinforcement learning of neurostimulation control in fes cycling. In: **2021 10th International IEEE/EMBS Conference on Neural Engineering (NER)**. 2021. p. 381–384.

APPENDIX A – Tricycle Vector Diagram

First of all, in the case of a four-bar linkage system, the Grashof condition must be respected. It states that the sum of the shortest and longest link of a planar quadrilateral link must be less than or equal to the sum of the two remaining links so that the shorter link can rotate completely with respect to a neighboring link. Therefore, from Figure 29:

$$r_1 + r_2 < r_3 + r_4 \tag{A.1}$$

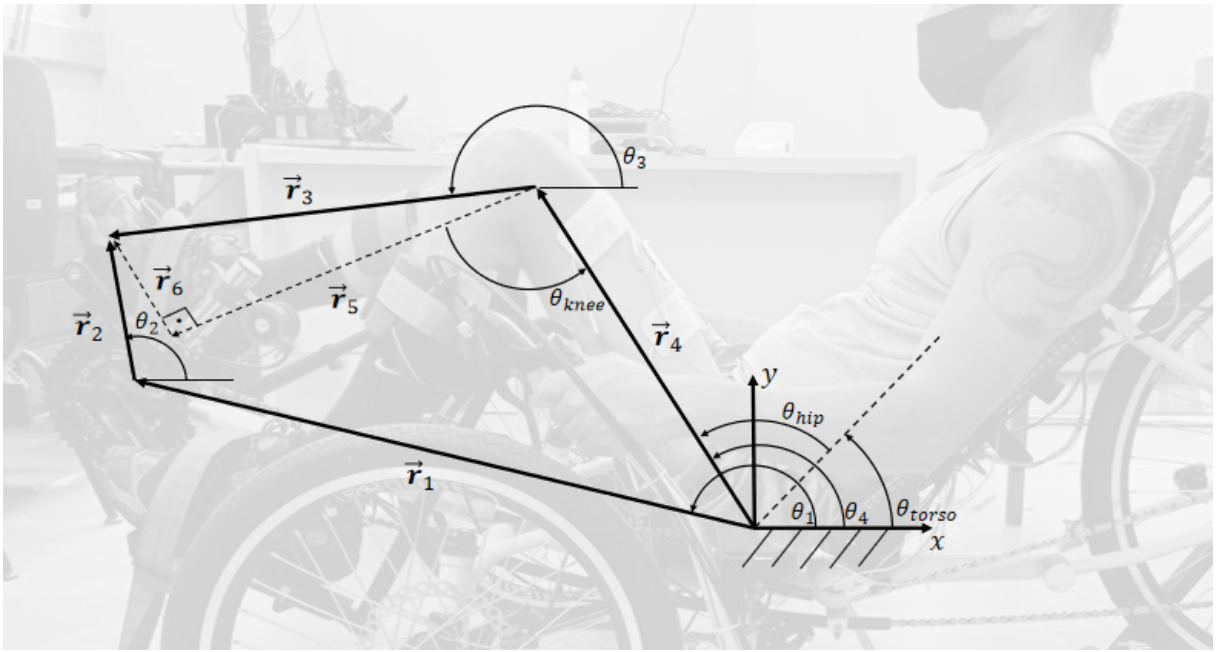

Figure 29 – Vector diagram of the trike with reference to the right leg.

The analysis of the mechanism position is given by the vector equation of the system by Raven's method:

$$\vec{r_1} + \vec{r_2} - \vec{r_3} - \vec{r_4} = 0 \tag{A.2}$$

$$r_1{}^{i\theta_1} + r_2{}^{i\theta_2} - r_3{}^{i\theta_3} - r_4{}^{i\theta_4} = 0 \tag{A.3}$$

Converting the equation to trigonometric form and isolating $r_3{}^{i\theta_3}$:

$$\begin{aligned} r_1(\cos\theta_1 + i\sin\theta_1) + r_2(\cos\theta_2 + i\sin\theta_2) - r_4(\cos\theta_4 + i\sin\theta_4) \\ = r_3(\cos\theta_3 + i\sin\theta_3) \end{aligned} \tag{A.4}$$

Building the system and equations into real and imaginary parts and applying Freudenstein's method, we obtain:

$$\begin{cases} r_1\cos\theta_1 + r_2\cos\theta_2 - r_4\cos\theta_4 = r_3\cos\theta_3 \\ r_1\sin\theta_1 + r_2\sin\theta_2 - r_4\sin\theta_4 = r_3\sin\theta_3 \end{cases} \tag{A.5}$$

Raising the two equations to the second power and adding the terms:

$$\begin{aligned} {r_3}^2 = {r_1}^2 + {r_2}^2 + {r_4}^2 + 2r_1 r_2 \cos(\theta_2 - \theta_1) \\ -2r_1 r_4(\cos\theta_1 \cos\theta_4 + \sin\theta_1 \sin\theta_4) - 2r_2 r_4(\cos\theta_2 \cos\theta_4 + \sin\theta_2 \sin\theta_4) \end{aligned} \tag{A.6}$$

Dividing by $2r_2r_4$, we get:

$$\begin{aligned} 0 = \frac{{r_1}^2 + {r_2}^2 - {r_3}^2 + {r_4}^2}{2r_2 r_4} + \frac{r_1}{r_4}\cos(\theta_2 - \theta_1) \\ -\frac{r_1}{r_2}(\cos\theta_1 \cos\theta_4 + \sin\theta_1 \sin\theta_4) - (\cos\theta_2 \cos\theta_4 + \sin\theta_2 \sin\theta_4) \end{aligned} \tag{A.7}$$

Simply put, the following terms will be used:

$$\begin{cases} k_1 = \frac{r_1}{r_2} \\ k_2 = \frac{r_1}{r_4} \\ k_3 = \frac{{r_1}^2 + {r_2}^2 - {r_3}^2 + {r_4}^2}{2r_2 r_4} \end{cases} \tag{A.8}$$

From A.8, we simplify equation A.7:

$$\begin{aligned} 0 = k_3 + k_2 \cos(\theta_2 - \theta_1) \\ -k_1(\cos\theta_1 \cos\theta_4 + \sin\theta_1 \sin\theta_4) - (\cos\theta_2 \cos\theta_4 + \sin\theta_2 \sin\theta_4) \end{aligned} \tag{A.9}$$

We replace $\cos\theta_4$ and $\sin\theta_4$ by its expressions in terms of the tangent of half an angle in A.9:

$$\begin{aligned} 0 = k_3 + k_2 \cos(\theta_2 - \theta_1) - k_1(\cos\theta_1 \frac{1 - \tan^2\frac{\theta_4}{2}}{1 + \tan^2\frac{\theta_4}{2}} + \sin\theta_1 \frac{2\tan\frac{\theta_4}{2}}{1 + \tan^2\frac{\theta_4}{2}}) \\ -(\cos\theta_2 \frac{1 - \tan^2\frac{\theta_4}{2}}{1 + \tan^2\frac{\theta_4}{2}} + \sin\theta_2 \frac{2\tan\frac{\theta_4}{2}}{1 + \tan^2\frac{\theta_4}{2}}) \end{aligned} \tag{A.10}$$

Then the denominators are removed and the terms are grouped together:

$$\begin{aligned} 0 = (k_3 + k_2\cos(\theta_2 - \theta_1) + k_1\cos\theta_1 + \cos\theta_2)\tan^2\frac{\theta_4}{2} \\ -(2\sin\theta_2 + 2k_1\sin\theta_1)\tan\frac{\theta_4}{2} + (k_3 + k_2\cos(\theta_2 - \theta_1) - k_1\cos\theta_1 - \cos\theta_2) \end{aligned} \tag{A.11}$$

The coefficients are again renamed:

$$\begin{cases} A = k_3 + k_2\cos(\theta_2 - \theta_1) + k_1\cos\theta_1 + \cos\theta_2 \\ B = -2\sin\theta_2 - 2k_1\sin\theta_1 \\ C = k_3 + k_2\cos(\theta_2 - \theta_1) - k_1\cos\theta_1 - \cos\theta_2 \end{cases} \tag{A.12}$$

Equation A.11 can be rewritten as:

$$A\tan^2\frac{\theta_4}{2} + B\tan\frac{\theta_4}{2} + C = 0 \tag{A.13}$$

Which allows us to find the value of θ_4:

$$\theta_4 = 2\tan^{-1}\frac{-B \pm \sqrt{B^2 - 4AC}}{2A} \tag{A.14}$$

to determine the hip angle θ_{hip}:

$$\theta_{hip} = \theta_4 - \theta_{torso} \tag{A.15}$$

where θ_{torso} corresponds to the inclination of the subject's trunk on the tricycle. In the same way, but isolating θ_4 in the equation A.5, we relate:

$$\begin{cases} k_4 = \frac{r_1}{r_2} \\ k_5 = \frac{r_1}{r_3} \\ k_6 = \frac{{r_1}^2 + {r_2}^2 + {r_3}^2 - {r_4}^2}{2r_2r_3} \end{cases} \tag{A.16}$$

We determine the coefficients:

$$\begin{cases} D = k_6 + k_5\cos(\theta_2 - \theta_1) + k_4\cos\theta_1 + \cos\theta_2 \\ E = -2\sin\theta_2 - 2k_4\sin\theta_1 \\ F = k_6 + k_5\cos(\theta_2 - \theta_1) - k_4\cos\theta_1 - \cos\theta_2 \end{cases} \tag{A.17}$$

Which allows us to find the value of θ_3:

$$\theta_3 = 2\tan^{-1}\frac{-E \pm \sqrt{E^2 - 4DF}}{2D} \tag{A.18}$$

And finally determine θ_{knee}:

$$\theta_{knee} = 180 + \theta_4 - \theta_3 - \tan^{-1}\frac{r_5}{r_6} \tag{A.19}$$

The MATLAB application developed to evaluate the joint angles and its relationship to the distance between the crank and the rider is illustrated in Figure 30.

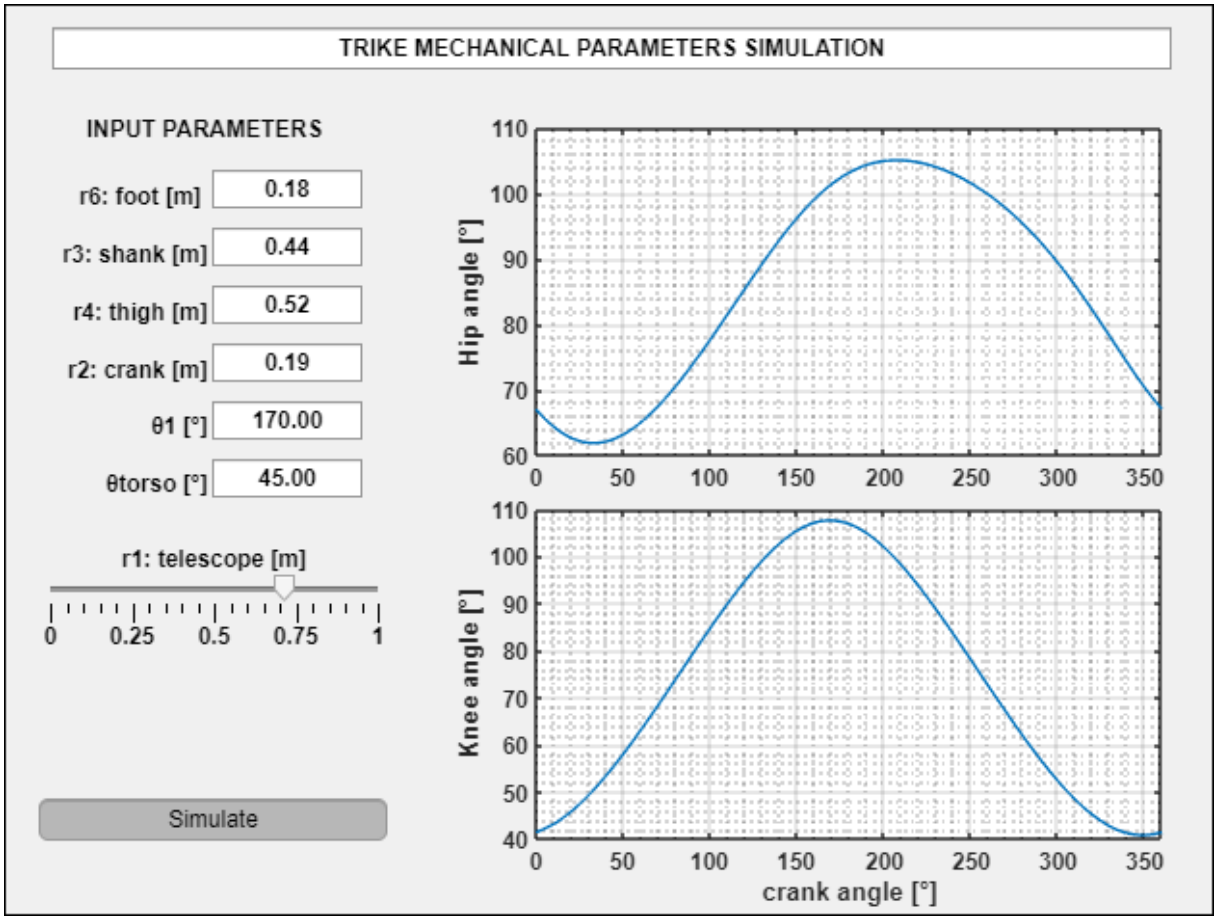

Figure 30 – MATLAB Application developed for the evaluation of tricycle configurations in relation to the volunteer's biomechanics. See Supplementary Materials (Section 1.5)

APPENDIX B – HCFES Schematics

The HCFES project can be downloaded at: https://osf.io/pf3ru/. Schematics are presented in sequence.

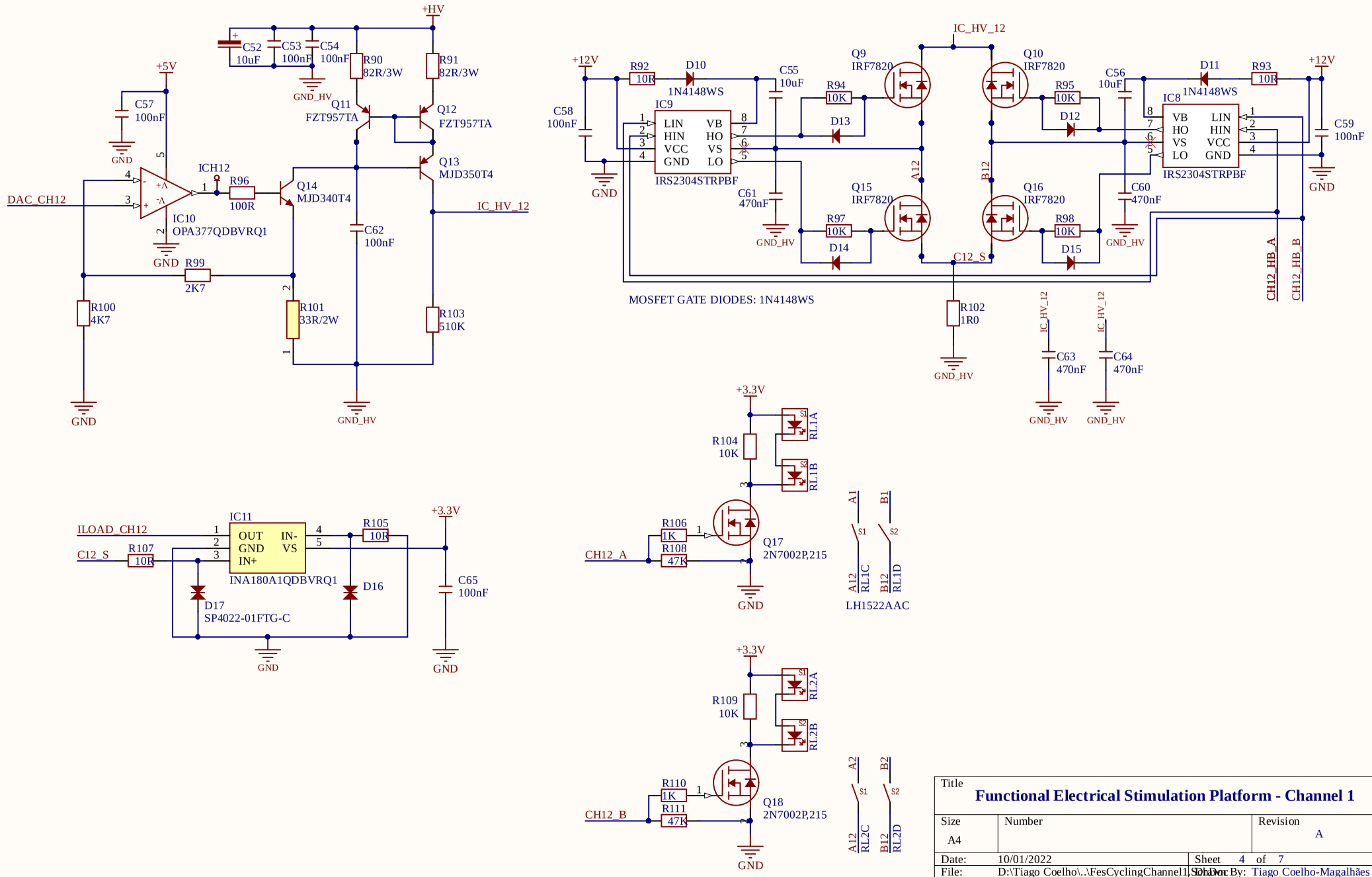

Title	**Functional Electrical Stimulation Platform - Channel 1**	
Size: A4	Number	Revision: A
Date: 10/01/2022	Sheet 4 of 7	
File: D:\Tiago Coelho\..\FesCyclingChannel1.SchDoc	Drawn By: Tiago Coelho-Magalhães	

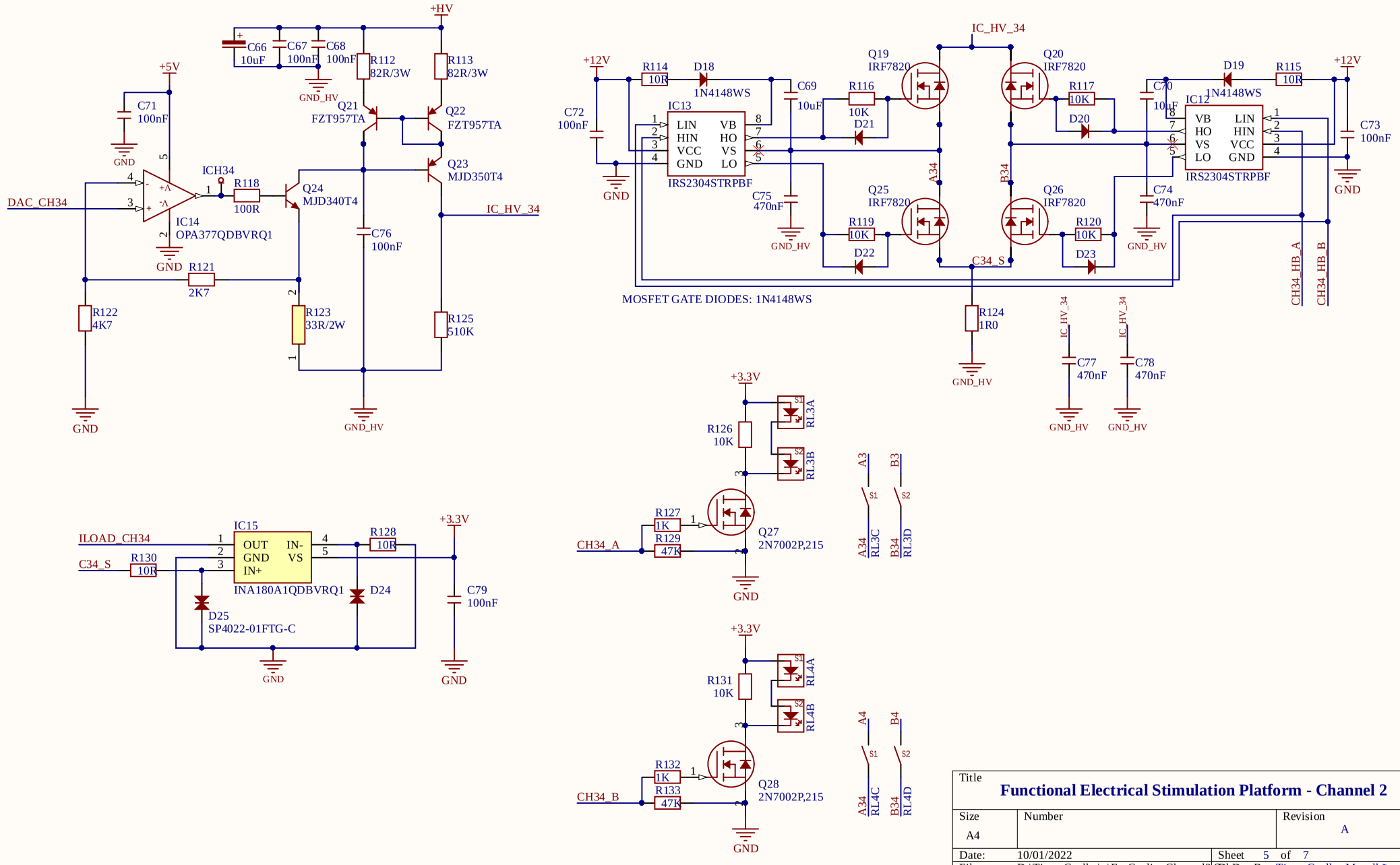

Title	**Functional Electrical Stimulation Platform - Channel 2**	
Size A4	Number	Revision A
Date: 10/01/2022		Sheet 5 of 7
File: D:\Tiago Coelho\..\FesCyclingChannel2.SchDoc		Drawn By: Tiago Coelho-Magalhães

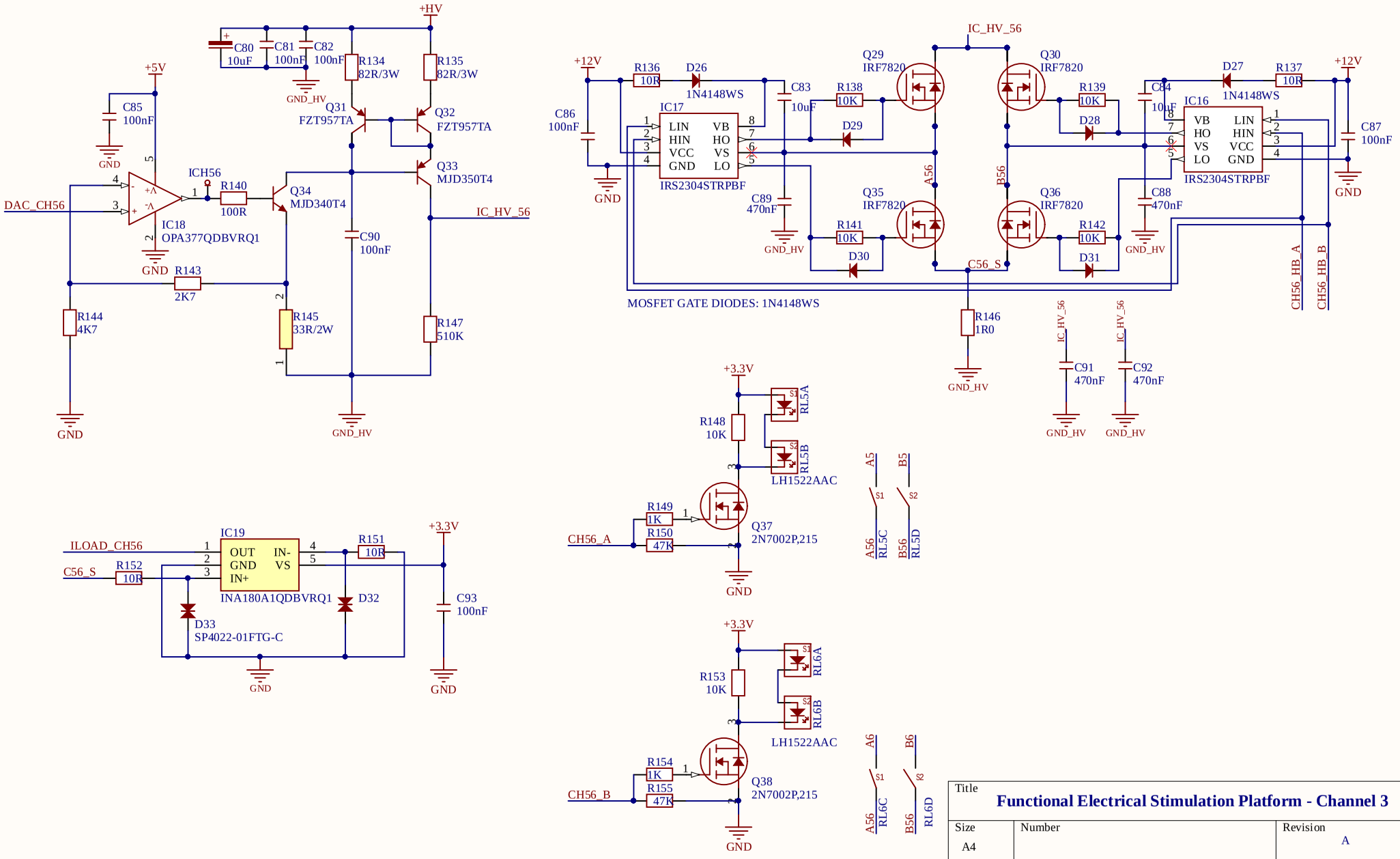

Title	**Functional Electrical Stimulation Platform - Channel 3**	
Size A4	Number	Revision A
Date: 10/01/2022		Sheet 6 of 7
File: D:\Tiago Coelho\..\FesCyclingChannel3.SchDoc		Drawn By: Tiago Coelho-Magalhães

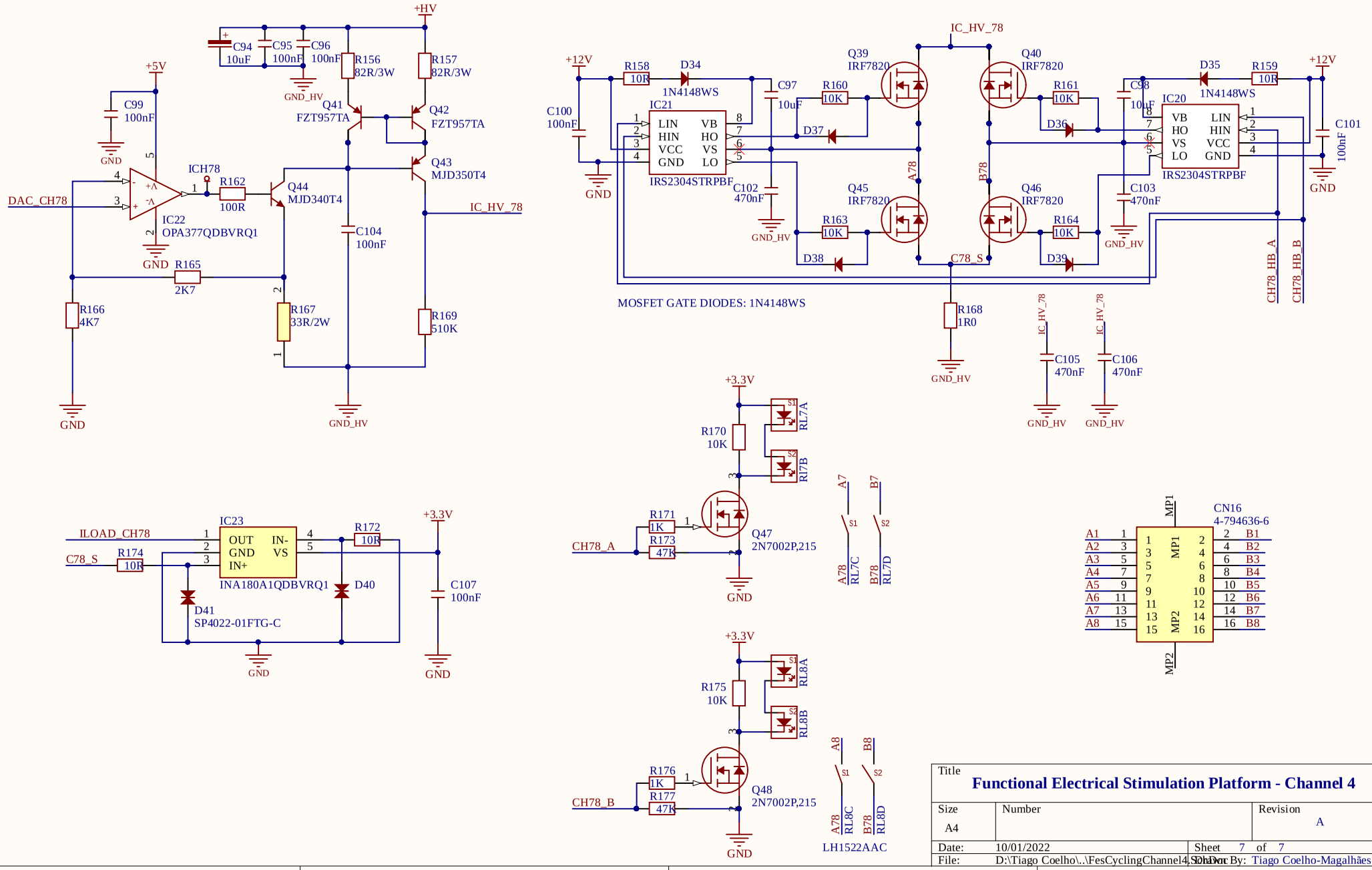

Title	**Functional Electrical Stimulation Platform - Channel 4**	
Size: A4	Number	Revision: A
Date: 10/01/2022	Sheet 7 of 7	
File: D:\Tiago Coelho\..\FesCyclingChannel4.SchDoc	Drawn By: Tiago Coelho-Magalhães	

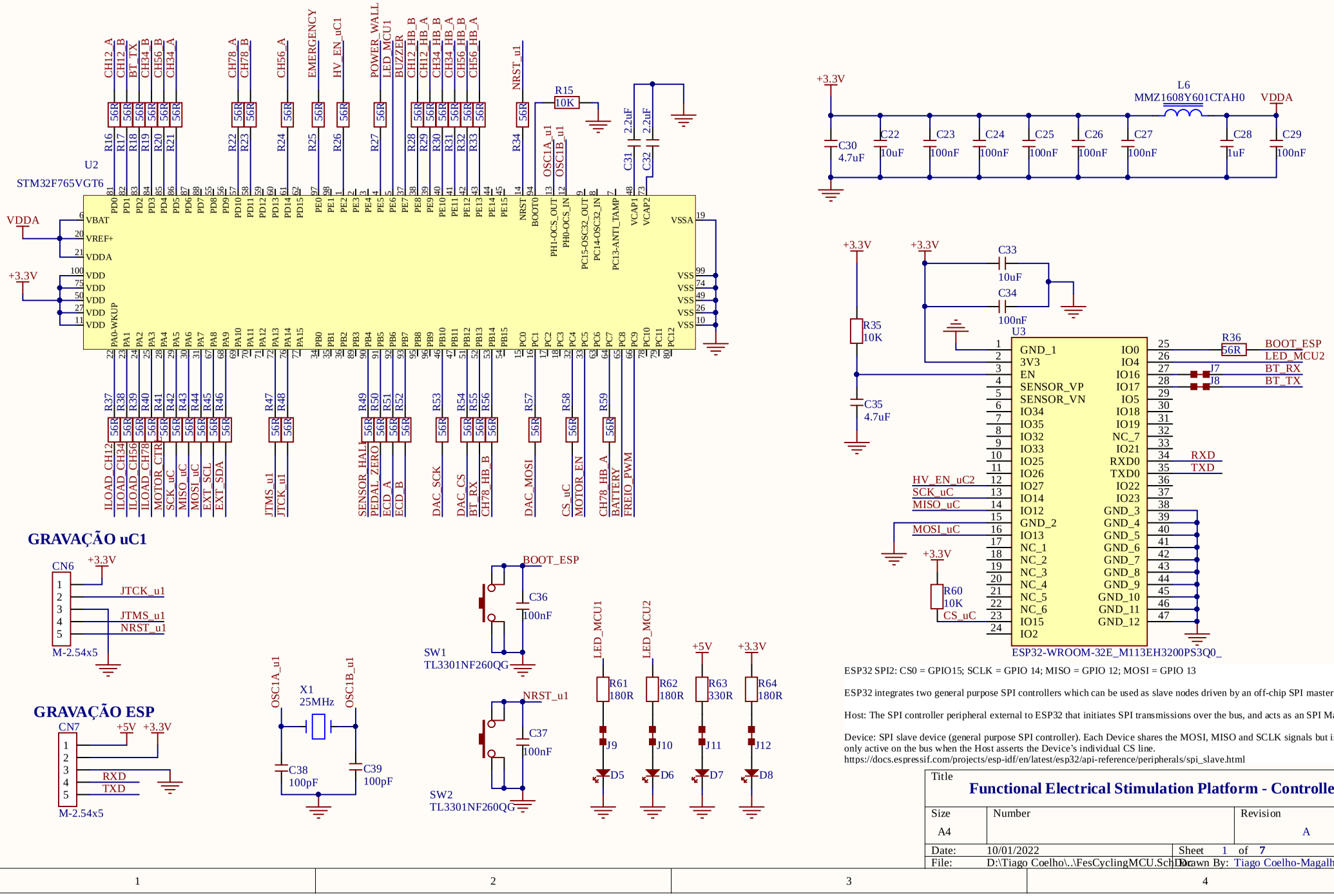

ESP32 SPI2: CS0 = GPIO15; SCLK = GPIO 14; MISO = GPIO 12; MOSI = GPIO 13

ESP32 integrates two general purpose SPI controllers which can be used as slave nodes driven by an off-chip SPI master

Host: The SPI controller peripheral external to ESP32 that initiates SPI transmissions over the bus, and acts as an SPI Master.

Device: SPI slave device (general purpose SPI controller). Each Device shares the MOSI, MISO and SCLK signals but is only active on the bus when the Host asserts the Device's individual CS line.
https://docs.espressif.com/projects/esp-idf/en/latest/esp32/api-reference/peripherals/spi_slave.html

Title: **Functional Electrical Stimulation Platform - Controller**		
Size: A4	Number:	Revision: A
Date: 10/01/2022	Sheet 1 of 7	
File: D:\Tiago Coelho\..\FesCyclingMCU.SchDoc	Drawn By: Tiago Coelho-Magalhães	

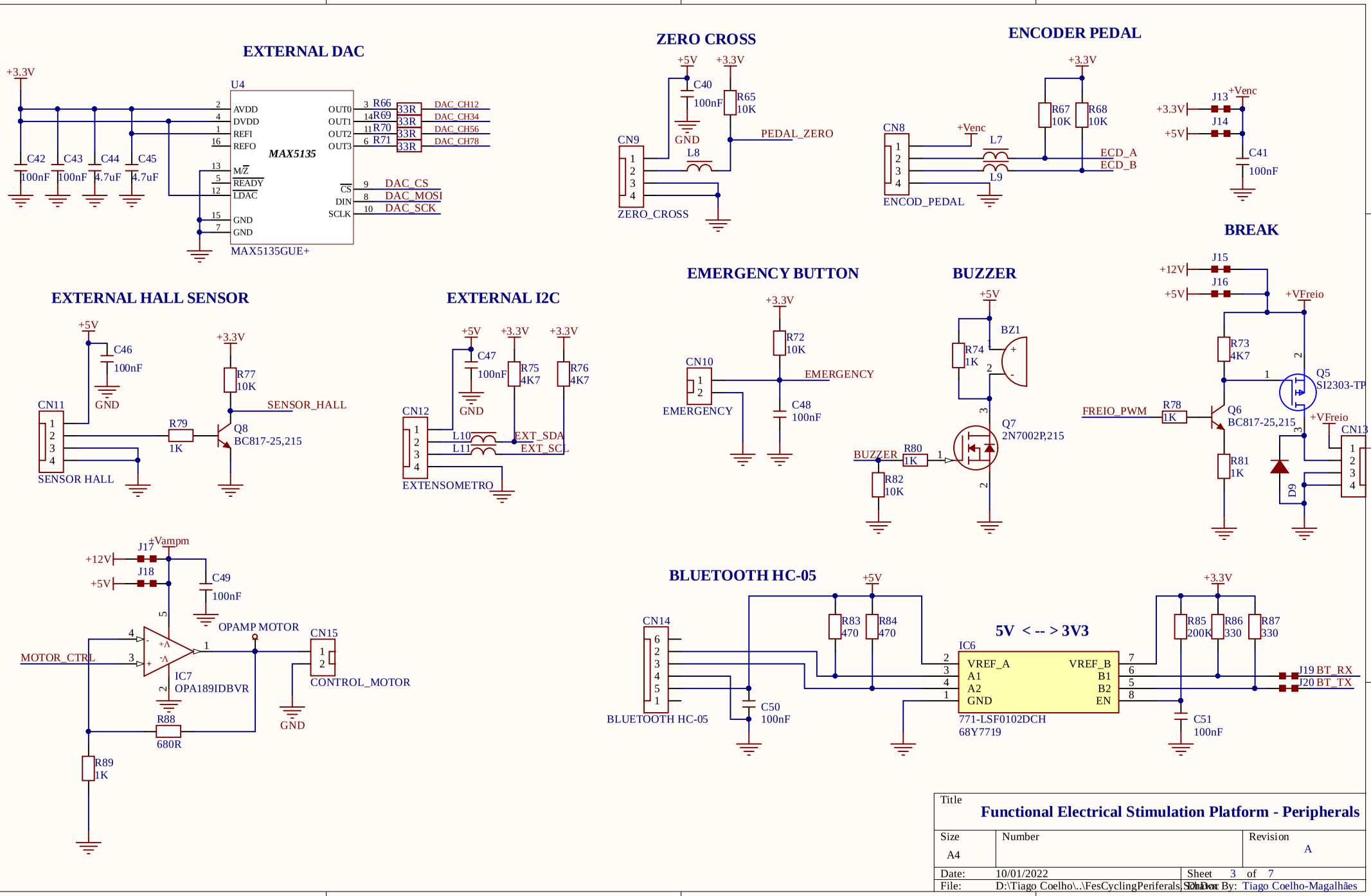
EXTERNAL DAC
+3.3V
U4
AVDD
DVDD
REFI
REFO
M/Z
READY
LDAC
GND
GND
MAX5135
OUT0
OUT1
OUT2
OUT3
CS
DIN
SCLK
MAX5135GUE+
C42 100nF
C43 100nF
C44 4.7uF
C45 4.7uF
R66 33R
R69 33R
R70 33R
R71 33R
DAC_CH12
DAC_CH34
DAC_CH56
DAC_CH78
DAC_CS
DAC_MOSI
DAC_SCK
ZERO CROSS
+5V
+3.3V
C40 100nF
R65 10K
CN9
GND
L8
PEDAL_ZERO
ZERO_CROSS
ENCODER PEDAL
+3.3V
R67 10K
R68 10K
CN8
+Venc
L7
L9
ECD_A
ECD_B
ENCOD_PEDAL
J13
J14
+Venc
C41 100nF
EXTERNAL HALL SENSOR
+5V
C46 100nF
GND
+3.3V
R77 10K
SENSOR_HALL
CN11
R79 1K
Q8 BC817-25,215
SENSOR HALL
EXTERNAL I2C
+5V
+3.3V
+3.3V
C47 100nF
R75 4K7
R76 4K7
GND
CN12
L10
L11
EXT_SDA
EXT_SCL
EXTENSOMETRO
EMERGENCY BUTTON
+3.3V
R72 10K
CN10
EMERGENCY
C48 100nF
BUZZER
+5V
BZ1
R74 1K
Q7 2N7002P,215
BUZZER
R80 1K
R82 10K
BREAK
J15
J16
+12V
+5V
+VFreio
R73 4K7
Q5 SI2303-TP
FREIO_PWM
R78 1K
Q6 BC817-25,215
+VFreio
R81 1K
D9
CN13
J17
J18
±Vampm
+12V
+5V
C49 100nF
OPAMP MOTOR
CN15
MOTOR_CTRL
IC7
OPA189IDBVR
CONTROL_MOTOR
GND
R88 680R
R89 1K
BLUETOOTH HC-05
+5V
+3.3V
CN14
R83 470
R84 470
5V < -- > 3V3
IC6
VREF_A
A1
A2
GND
VREF_B
B1
B2
EN
771-LSF0102DCH
68Y7719
R85 200K
R86 330
R87 330
J19 BT_RX
J20 BT_TX
BLUETOOTH HC-05
C50 100nF
C51 100nF
Title
Functional Electrical Stimulation Platform - Peripherals
Size
A4
Number
Revision
A
Date: 10/01/2022
Sheet 3 of 7
File: D:\Tiago Coelho\..\FesCyclingPeriferals.SchDoc
Drawn By: Tiago Coelho-Magalhães

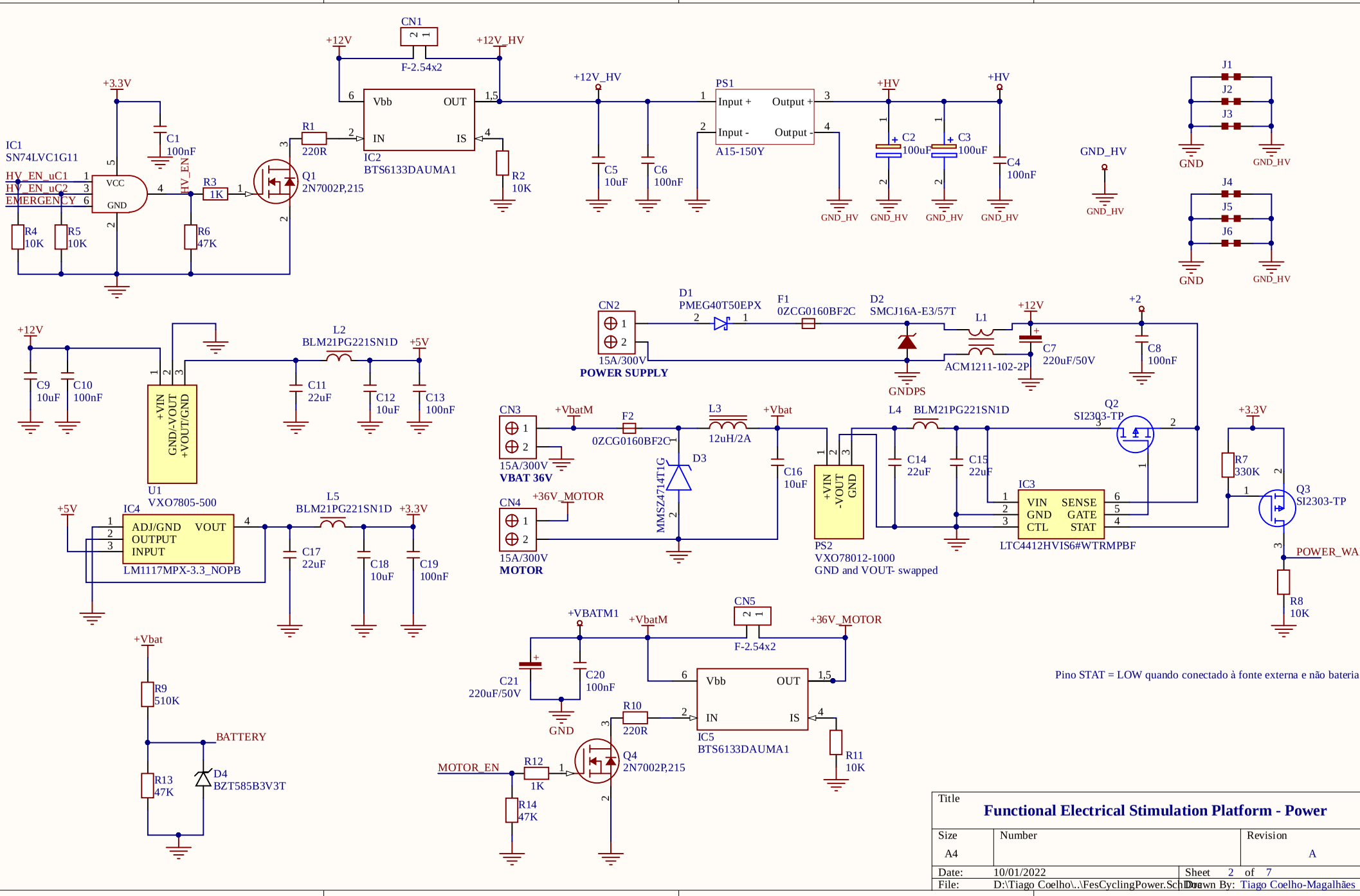
IC1
SN74LVC1G11
HV_EN_uC1
HV_EN_uC2
EMERGENCY
VCC
GND
HV_EN
C1
100nF
R1
220R
R2
10K
R3
1K
R4
10K
R5
10K
R6
47K
Q1
2N7002P,215
CN1
F-2.54x2
+12V
+12V_HV
IC2
BTS6133DAUMA1
Vbb
OUT
IN
IS
C5
10uF
C6
100nF
PS1
A15-150Y
Input +
Input -
Output +
Output -
C2
100uF
C3
100uF
C4
100nF
+HV
GND_HV
GND
J1
J2
J3
J4
J5
J6
CN2
15A/300V
POWER SUPPLY
D1
PMEG40T50EPX
F1
0ZCG0160BF2C
D2
SMCJ16A-E3/57T
GNDPS
L1
ACM1211-102-2P
C7
220uF/50V
C8
100nF
+2
C9
10uF
C10
100nF
U1
VXO7805-500
+VIN
GND-VOUT
+VOUT/GND
L2
BLM21PG221SN1D
+5V
C11
22uF
C12
10uF
C13
100nF
CN3
15A/300V
VBAT 36V
+VbatM
F2
0ZCG0160BF2C
L3
12uH/2A
+Vbat
D3
MMSZ4714T1G
C16
10uF
CN4
15A/300V
MOTOR
+36V_MOTOR
PS2
VXO78012-1000
GND and VOUT- swapped
+VIN
-VOUT
GND
L4
BLM21PG221SN1D
C14
22uF
C15
22uF
Q2
SI2303-TP
IC3
LTC4412HVIS6#WTRMPBF
VIN
GND
CTL
SENSE
GATE
STAT
+3.3V
R7
330K
Q3
SI2303-TP
POWER_WALL
R8
10K
IC4
LM1117MPX-3.3_NOPB
ADJ/GND
OUTPUT
INPUT
VOUT
L5
BLM21PG221SN1D
C17
22uF
C18
10uF
C19
100nF
+Vbat
R9
510K
BATTERY
R13
47K
D4
BZT585B3V3T
+VBATM1
CN5
F-2.54x2
C21
220uF/50V
C20
100nF
R10
220R
IC5
BTS6133DAUMA1
R11
10K
MOTOR_EN
R12
1K
Q4
2N7002P,215
R14
47K
Pino STAT = LOW quando conectado à fonte externa e não bateria
Title
Functional Electrical Stimulation Platform - Power
Size
A4
Number
Revision
A
Date:
10/01/2022
Sheet
2
of
7
File:
D:\Tiago Coelho\..\FesCyclingPower.SchDoc
Drawn By:
Tiago Coelho-Magalhães

APPENDIX C – DXA Measurements

BMD and BC data can be assessed at: https://osf.io/95xbs/. Optimized data is presented below:

Table 3 – Body composition: Fat mass ratio (%)

age	38.3y	38.6y	38.9y	39.2y	39.4y	39.6y	39.9y	40.1y	40.3y
total	28.1	27.9	25.9	26.2	27.3	25.1	24.8	26.9	27.3
amrs	15.6	14.8	16.0	14.9	15.6	14.0	14.0	15.8	15.3
total legs	30.5	28.9	26.9	27.3	27.9	26.2	26.4	28.4	26.4
leg left	30.5	29.3	27.4	28.3	28.0	26.6	27.2	28.4	27.5
leg right	30.6	28.5	26.5	26.3	27.8	25.9	25.4	28.4	25.2
android	31.7	33.1	29.0	30.0	31.9	27.8	26.9	30.9	32.7
gynoid	30.6	27.9	28.0	27.0	26.4	27.0	25.6	26.9	27.3

Table 4 – Body composition: Fat mass (g)

age	38.3y	38.6y	38.9y	39.2y	39.4y	39.6y	39.9y	40.1y	40.3y
total	18456	18229	17201	16971	17353	16017	15013	17084	17927
amrs	1384	1356	1397	1301	1343	1170	1067	1311	1266
total legs	5932	5612	5465	5303	5155	4954	4919	5370	5305
leg left	2997	2878	2791	2765	2572	2607	2600	2675	2778
leg right	2935	2734	2674	2538	2583	2347	2319	2696	2528
android	1600	1642	1516	1524	1586	1349	1209	1513	1699
gynoid	2616	2419	2526	2302	2136	2301	2046	2213	2337

Table 5 – Body composition: Lean mass (g)

age	38.3y	38.6y	38.9y	39.2y	39.4y	39.6y	39.9y	40.1y	40.3y
total	47169	47206	49267	47893	46226	47746	45465	46380	47833
amrs	7474	7785	7310	7412	7272	7194	6554	6982	7008
total legs	13495	13797	14811	14098	13310	13933	13744	13539	14815
leg left	6843	6930	7398	6994	6605	7206	6946	6742	7308
leg right	6652	6866	7413	7103	6705	6727	6797	6797	7507
android	3452	3318	3708	3561	3391	3499	3291	3381	3495
gynoid	5930	6247	6505	6234	5970	6210	5962	6023	6213

Table 6 – Body composition: Total mass (Kg)

age	38.3y	38.6y	38.9y	39.2y	39.4y	39.6y	39.9y	40.1y	40.3y
total	68.2	68.0	69.0	67.4	66.2	66.3	63.0	66.0	68.3
amrs	9.3	9.6	9.2	9.2	9.1	8.8	8.0	8.7	8.7
total legs	20.2	20.2	21.0	20.1	19.2	19.6	19.4	19.6	20.8
leg left	10.2	10.1	10.6	10.1	9.5	10.2	9.9	9.8	10.4
leg right	9.9	10.1	10.4	10.0	9.6	9.4	9.5	9.8	10.4
android	5.1	5.0	5.3	5.2	5.1	4.9	4.6	5.0	5.3
gynoid	8.8	8.9	9.3	8.7	8.3	8.7	8.2	8.4	8.7

Table 7 – Bone Mineral Density (g/cm^2)

		M0	M1	M2	M3	M4	M5	M6	M7	M8
		38.3y	38.6y	38.9y	39.2y	39.4y	39.6y	39.9y	40.1y	40.3y
Total body		1054	1050	1043	1040	1042	1049	1039	1038	1033
	L1	1299	1397	1363	1353	1452	1444	1396	1350	1416
	L2	1452	1524	1470	1539	1508	1455	1491	1477	1442
Lumbar spine	L3	1486	1593	1521	1575	1574	1502	1528	1503	1526
	L4	1360	1408	1385	1383	1406	1343	1370	1328	1362
	L1-L4	1400	1480	1436	1463	1477	1432	1445	1412	1435
Pelvis		0.788	0.783	0.791	0.764	0.797	0.788	0.790	0.781	0.738
Femoral neck	R	0.751	0.770	0.748	0.742	0.758	0.731	0.727	0.724	0.697
Femur (total)	R	0.727	0.728	0.713	0.699	0.706	0.694	0.679	0.685	0.662
Legs		0.877	0.878	0.862	0.858	0.860	0.848	0.847	0.845	0.838

Biography

Tiago Coelho Magalhães received the B.S. degree in Electrical Engineering from National Institute of Telecommunications (INATEL), Brazil, in 2012, and received the M.Sc. degree in Electrical Engineering from Federal University of Minas Gerais (UFMG), Brazil, in 2018. He is currently associated with the Biomedical Engineering Laboratory at UFMG. His research is focused on the development of assistive technologies by means of biomedical instrumentation and embedded electronic systems for applications involving functional electrical stimulation, specifically those involving rehabilitation and mobility of the lower limbs.

From January 2023, he will be associated to the CAMIN team at the *Institut National de Recherche en Informatique et en Automatique* (INRIA), France, for a postdoctoral fellowship focused on the design and development of neuroprosthetic solutions for sensorimotor deficiencies aiming to improve the functional capacity and quality of life of of individuals with neurological disabilities.

e-mail: tiagocoelhom@ufmg.br

LinkedIn: linkedin.com/in/tiagocoelhom

Research Gate: researchgate.net/profile/Tiago-Magalhaes-18